Work performance evaluation of heavy-duty mobile machines (HDMMs)

For the academic degree of

DOCTOR OF ENGINEERING (Dr.-Ing.)

by the Faculty of Mechanical Engineering
of the Karlsruhe Institute of Technology (KIT)

accepted
Dissertation

by

M.Sc. Amirmasoud Molaei

Date of the oral examination:	July 3, 2025
First expert examiner:	Prof. Dr.-Ing. Marcus Geimer
Second expert examiner:	Prof. Dr.-Ing. Rania Rayyes

Work performance evaluation of heavy-duty mobile machines (HDMMs)

Zur Erlangung des akademischen Grades eines

Doktors der Ingenieurwissenschaften (Dr.-Ing.)

von der KIT-Fakultät für Maschinenbau
des Karlsruher Instituts für Technologie (KIT)

angenommene

Dissertation

von

M.Sc. Amirmasoud Molaei

Tag der mündlichen Prüfung:	03. Juli 2025
Erster Gutachter:	Prof. Dr.-Ing. Marcus Geimer
Zweiter Gutachter:	Prof. Dr. Rania Rayye

Abstract

Work performance evaluation of heavy-duty mobile machines (HDMMs)

The construction industry is crucial for economic growth, but its productivity has not improved much despite its importance. Heavy-duty mobile machines (HDMMs), particularly excavators, play a central role in construction projects, with their productivity directly impacting projects' productivity and costs. This dissertation aims to tackle several challenges regarding the automatic productivity estimation of an excavator in earth-moving operations, such as loading, trenching, and grading.

In the beginning, the significance of the construction industry and the critical role of HDMMs within it are discussed. It highlights the challenges faced by the industry, including low productivity growth and outdated practices, emphasizing the need for automated productivity estimation and progress monitoring. Then, an excavator is introduced as the main application in the research study. In the next phase, existing research studies for the productivity estimation of HDMMs are thoroughly explored to identify research gaps and to design multiple research questions that drive the dissertation's focus.

Capturing motion information using inertial measurement units (IMUs) holds promise for recognizing activities and automatically estimating cycle time and productivity. Also, the importance of analysis of working conditions and estimating theoretical cycle time and productivity is stated. In addition, 3D sensors and building information modeling (BIM) can be integrated to enhance the productivity estimation and progress monitoring of an excavator in quality-centered tasks, such as grading and trenching operations.

First, an activity recognition method is proposed to identify the excavator working cycle using supervised classification methods and motion information, such as angular velocities and joint angles, obtained from four IMUs attached to moving parts of an excavator, including the swing body, boom, arm, and bucket. Human operators perform tasks using a medium-rated excavator under different working conditions, such as different types of material, swing angle, digging depth, and weather conditions to collect a dataset. The proposed method can effectively recognize the working cycles of an excavator. Task recognition can aid management teams in monitoring productivity and progress, optimizing resource allocation, and scheduling. Using the results of the task recognition algorithm, productivity can be calculated based on task-specific metrics.

Next, an approach is designed to automatically determine the productivity and operational effectiveness of an excavator in the loading operation. Firstly, an algorithm is proposed to recognize the excavator's sub-tasks using supervised learning and motion data obtained

from IMUs. Then, a method is presented to estimate the actual cycle time based on the sequence of activities detected using the trained classification model. The actual cycle time cannot solely reveal the machine's performance since operating conditions can significantly influence the cycle time. Therefore, a reference is required to analyze the actual cycle time. Secondly, the theoretical cycle time of an excavator is automatically estimated based on the operating conditions, such as swing angle and digging depth. Thirdly, the relative cycle time is obtained by dividing the theoretical cycle time by the actual cycle time. The relative cycle time index can effectively monitor the performance of an excavator in loading operations and can be useful for worksite managers to monitor the performance of each machine in worksites.

In the next step, a technique is proposed to estimate the excavator's actual productivity in trenching and grading operations. In these tasks, the quantity of material moved is not significant; precision within specified tolerances is the key focus. The productivity definitions for trenching and grading operations are the trench's length per unit of time and graded area per unit of time, respectively. In the method, a height map from working areas is constructed. Also, BIM is utilized to acquire information regarding the target model and required accuracy. The productivity is estimated using the map comparison between the working areas and the desired model. The method can effectively estimate productivity and monitor the progress of these operations. The obtained information can guide managers to track the productivity of each individual machine and modify planning and time-scheduling.

This dissertation employs advanced technologies, such as IMUs, machine learning techniques, elevation terrain mapping algorithms, and BIM. It aims to streamline productivity estimation and progress monitoring for excavators, ultimately contributing to more efficient and successful construction projects. It underscores the potential for future research to enhance these methodologies, expand their applicability to other HDMMs and tasks, and address remaining challenges to propel the construction industry towards greater productivity and sustainability.

***Keywords*:** Excavator, Productivity Estimation, Progress Monitoring, Loading Operation, Grading Operation, Trenching Operation, Activity Recognition, Actual Cycle Time Estimation, Theoretical Cycle Time, Relative Cycle Time Index, Swing Angle, Digging Depth, Building Information Modeling (BIM), Elevation Terrain Mapping

Kurzfassung

Arbeits leistungsbewertung von hochleistungs-mobilmaschinen (HDMMs)

Die Bauindustrie ist entscheidend für das Wirtschaftswachstum, doch trotz ihrer Bedeutung hat sich die Produktivität nicht wesentlich verbessert. Schwere mobile Maschinen (HDMMs), insbesondere Bagger, spielen eine zentrale Rolle in Bauprojekten, wobei ihre Produktivität die Produktivität und Kosten der Projekte direkt beeinflusst. Diese Dissertation zielt darauf ab, mehrere Herausforderungen bei der automatischen Produktivitätsschätzung eines Baggers bei Erdbewegungsarbeiten wie Laden, Graben und Planieren zu bewältigen.

Zunächst wird die Bedeutung der Bauindustrie und die kritische Rolle der HDMMs innerhalb dieser Branche erörtert. Es werden die Herausforderungen hervorgehoben, mit denen die Branche konfrontiert ist, einschließlich des geringen Produktivitätswachstums und veralteter Praktiken, und der Bedarf an automatischer Produktivitätsschätzung und Fortschrittsüberwachung wird betont. Anschließend wird der Bagger als Hauptanwendungsobjekt der Forschungsarbeit vorgestellt. In der nächsten Phase werden bestehende Forschungsstudien zur Produktivitätsschätzung von HDMMs gründlich untersucht, um Forschungslücken zu identifizieren und mehrere Forschungsfragen zu formulieren, die den Fokus der Dissertation lenken.

Die Erfassung von Bewegungsinformationen mithilfe von Inertial Measurement Units (IMUs) verspricht, Aktivitäten zu erkennen und automatisch die Zykluszeit und Produktivität zu schätzen. Außerdem wird die Bedeutung der Analyse von Arbeitsbedingungen und der Schätzung theoretischer Zykluszeiten und Produktivitäten betont. Darüber hinaus können 3D-Sensoren und Building Information Modeling (BIM) integriert werden, um die Produktivitätsschätzung und Fortschrittsüberwachung eines Baggers bei qualitätsorientierten Aufgaben wie Planieren und Graben zu verbessern.

Zunächst wird eine datengetriebene Methode zur Erkennung von Arbeitszyklen unter Verwendung von überwachten Klassifikationsmethoden und Bewegungsinformationen, wie Winkelgeschwindigkeiten und Gelenkwinkel, die von vier an beweglichen Teilen eines Baggers angebrachten IMUs erfasst werden, vorgeschlagen. Menschliche Bediener führen Aufgaben mit einem mittelgroßen Bagger unter verschiedenen Arbeitsbedingungen, wie unterschiedlichen Materialtypen, Schwenkwinkel, Grabtiefe und Wetterbedingungen, aus, um einen Datensatz zu sammeln. Die vorgeschlagene Methode kann die Arbeitszyklen eines Baggers effektiv erkennen. Die Aufgabenerkennung kann Managementteams dabei helfen, die Produktivität und den Fortschritt zu überwachen, Ressourcen

optimal zuzuweisen und Zeitpläne zu erstellen. Mithilfe der Ergebnisse des Aufgabenerkennungsalgorithmus kann die Produktivität basierend auf aufgabenspezifischen Metriken berechnet werden.

Als nächstes wird ein Ansatz entwickelt, um die Produktivität und betriebliche Effizienz eines Baggers beim Ladevorgang automatisch zu bestimmen. Zunächst wird ein überwachter Lernalgorithmus vorgeschlagen, um die Unteraufgaben des Baggers anhand von Bewegungsdaten, die von IMUs erfasst wurden, zu erkennen. Anschließend wird eine Methode vorgestellt, um die tatsächliche Zykluszeit basierend auf der Sequenz der erkannten Aktivitäten unter Verwendung des trainierten Klassifikationsmodells zu schätzen. Die tatsächliche Zykluszeit allein kann die Leistung der Maschine nicht vollständig widerspiegeln, da die Betriebsbedingungen die Zykluszeit erheblich beeinflussen können. Daher ist eine Referenz erforderlich, um die tatsächliche Zykluszeit zu analysieren. Zweitens wird die theoretische Zykluszeit eines Baggers basierend auf den Betriebsbedingungen, wie Schwenkwinkel und Grabtiefe, automatisch geschätzt. Drittens wird die relative Zykluszeit durch Division der theoretischen Zykluszeit durch die tatsächliche Zykluszeit ermittelt. Der Index der relativen Zykluszeit kann die Leistung eines Baggers bei Ladeoperationen effektiv überwachen und für Baustellenmanager nützlich sein, um die Leistung jeder Maschine auf Baustellen zu überwachen.

Im nächsten Schritt wird eine Technik vorgeschlagen, um die tatsächliche Produktivität eines Baggers bei Graben- und Planierarbeiten zu schätzen. Bei diesen Aufgaben ist die Menge des bewegten Materials nicht entscheidend; die Präzision innerhalb festgelegter Toleranzen steht im Mittelpunkt. Die Produktivitätsdefinitionen für Graben- und Planierarbeiten sind die Grabenlänge pro Zeiteinheit bzw. die planierte Fläche pro Zeiteinheit. In der Methode wird eine Höhenkarte der Arbeitsbereiche erstellt. Außerdem wird BIM genutzt, um Informationen zum Zielmodell und den erforderlichen Genauigkeiten zu erhalten. Die Produktivität wird durch den Vergleich der Karte der Arbeitsbereiche mit dem gewünschten Modell geschätzt. Die Methode kann die Produktivität effektiv schätzen und den Fortschritt dieser Operationen überwachen. Die erhaltenen Informationen können Managern helfen, die Produktivität jeder einzelnen Maschine zu verfolgen und die Planung und Zeitplanung anzupassen.

Diese Dissertation verwendet fortschrittliche Technologien wie IMUs, maschinelle Lerntechniken, Höhenkarten-Algorithmen und BIM. Sie zielt darauf ab, die Produktivitätsschätzung und Fortschrittsüberwachung für Bagger zu rationalisieren und letztlich zu effizienteren und erfolgreicheren Bauprojekten beizutragen. Es wird betont, dass zukünftige Forschung diese Methoden verbessern, ihre Anwendbarkeit auf andere HDMMs und Aufgaben erweitern und verbleibende Herausforderungen angehen könnte, um die Bauindustrie zu größerer Produktivität und Nachhaltigkeit zu führen.

***Schlagworte*:** Bagger, Produktivitätsschätzung, Fortschrittsüberwachung, Ladevorgang, Planierarbeit, Grabarbeit, Aufgabenerkennung, Schätzung der tatsächlichen Zykluszeit, Theoretische Zykluszeit, Index der relativen Zykluszeit, Schwenkwinkel, Grabtiefe, Building Information Modeling (BIM), Höhenkarten-Erstellung

Acknowledgement

Embarking on my PhD journey on March 15th, 2021, under the esteemed guidance of Prof. Dr.-Ing. Marcus Geimer at the Institutsteil Mobile Arbeitsmaschinen (Mobima) at the Karlsruher Institut für Technologie (KIT) was a defining moment in my academic pursuit. Prof. Dr.-Ing. Geimer's mentorship, wisdom, and unwavering support have been instrumental in shaping my scholarly path, for which I am profoundly grateful. I extend my heartfelt thanks to Dr.-Ing. Jan Siebert and M.Sc. Simon Becker at KIT for their invaluable assistance and encouragement during this formative period.

In mid-September 2021, I embarked on a new chapter in Pirkkala, Finland, continuing my research journey at Novatron Oy under the mentorship of Mr. Antti Kolu. My tenure at Novatron was characterized by collaborative synergy and a nurturing environment, facilitated by the camaraderie and expertise of my esteemed colleagues: Janne Koivumäki, Paolo Forte, Jari Valtonen, Kalle Lahtinen, Niko Haaraniemi, Johanna Ylisaari, and Teemu Mononen. Their unwavering support and collective wisdom significantly enriched my research experience. I extend my deepest gratitude to Novatron for providing exceptional facilities and a robust research infrastructure that fueled my academic pursuits.

Following two enriching years at Novatron Oy, I embarked on a transformative six-month secondment at Liebherr-Werk Bischofshofen GmbH in Bischofshofen, Austria, under the mentorship of Dr.-Ing. Manuel Bös. I am immensely grateful to Dr.-Ing. Bös and my colleague Daniel Errikson for their invaluable guidance and support during this pivotal phase of my research, which broadened my perspective and honed my skills.

I extend my profound gratitude to the European Commission for funding the MORE-ITN project, which served as the cornerstone of my academic journey. This research endeavor was made possible through the generous support of the European Union's Horizon 2020 Research and Innovation Programme under the Marie Skłodowska-Curie grant agreement No. 858101. I am especially thankful to Prof. Reza Ghabcheloo and Mrs. Salla Kotakorva for their exceptional organizational skills and unwavering support throughout the project.

Beyond the confines of academia, I am humbled to have contributed to the scholarly discourse through the publication of several scientific papers and active participation in numerous scientific conferences and industrial events. These platforms not only enriched my knowledge but also fostered invaluable collaborations and insights that propelled my research forward.

Amidst my academic pursuits and professional endeavors, I am acutely aware of the unwavering support and sacrifices made by my beloved wife, Leila. Her boundless encour-

agement, patience, and understanding have been my anchor through the ebb and flow of academic challenges. To her, I owe a debt of gratitude beyond words.

Equally deserving of my deepest appreciation are my parents, Zahra and Alireza. Their enduring love, guidance, and unwavering belief in my potential have been the bedrock of my journey. Their sacrifices and support have instilled in me the resilience and determination to pursue my dreams relentlessly.

To each individual mentioned and countless others who have touched my life in profound ways, I extend my heartfelt thanks. Your contributions, whether big or small, have left an indelible mark on my journey, shaping the scholar and person I am today.

Karlsruhe, November 2024 *M.Sc. Amirmasoud Molaei*

Contents

Abbreviations and Symbols

Symbols

$accuracy_{CT}$	Accuracy of cycle time estimation	–
t_{actual}	Actual cycle time	s
ω	Angular velocity	rad/s
a	Area of graded surface	m^2
h_d	Digging depth	m
f_{depth}	Digging depth factor	–
fps	Frames per second	Hz
V_{CECE}	Heaped bucket capacity according the CECE standard	m^3
V_{SAE}	Heaped bucket capacity according the SAE standard	m^3
h	Hour	3600 s
l	Length of trench	m
$tonne$	Metric ton	1000 kg
min	Minute	60 s
θ	Pitch (rotation around y-axis)	rad
$Q_{grading}$	Productivity of grading operation	m^2/s
$Q_{trenching}$	Productivity of trenching operation	m/s
$t_{relative}$	Relative cycle time	–
ϕ	Roll (rotation around x-axis)	rad
f_s	Sampling frequency	Hz
θ_{sw}	Swing angle	$^\circ$
f_{swing}	Swing angle factor	–
$t_{theoretical}$	Theoretical cycle time	s
t	Time	s
ψ	Yaw (rotation around z-axis)	rad

Abbreviations

AHRS	Attitude and Heading Reference System
AI	Artificial Intelligence
ALS	Aerial Laser Scanning
AMC	Automated Machine Control
AMG	Automated Machine Guidance
ANN	Artificial Neural Network

BiLSTM	Bidirectional Long Short-Term Memory
BIM	Building Information Modeling
BoF	Bags-of-Features
BPNN	Back Propagation Neural Network
CAD	Computer-Aided Design
CAN	Controller Area Network
CECE	Committee for European Construction Equipment
CNN	Convolutional Neural Network
CSK	Circulant Structure of tracking-by-detection with Kernels
CV	Computer Vision
DCF	Dual Correlation Filter
DES	Discrete Event Simulation
DNN	Deep Neural Network
DT	Decision Tree
DTW	Dynamic Time Warping
EKF	Extended Kalman Filter
Faster R-CNN	Faster Region-based Convolutional Neural Network
FOV	Field-Of-View
GIS	Geographic Information System
GMM	Gaussian Mixture Model
GNSS	Global Navigation Satellite System
GPS	Global Positioning System
HDMM	Heavy-Duty Mobile Machine
HOF	Histogram of Optical Flow
HOG	Histogram of Oriented Gradients
HSV	Hue-Saturation-Value
IBL	Instance-Based Learning
IMU	Inertial Measurement Unit
KLT	Kanade and Lucas Tracker
KNN	K-Nearest Neighbor
LiDAR	Light Detection and Ranging
LMMS	Laser Mobile Mapping System
LR	Logistic Regression
LSTM	Long Short-Term Memory
MBH	Motion Boundary Histogram
MLP	Multi-Layer Perceptron
MRMR	Minimum Redundancy Maximum Relevance
NB	Naive Bayes
PPR	Production Performance Ratio

RADAR	Radio Detection and Ranging
ResNet	Residual (Neural) Network
RFID	Radio-Frequency Identification
RNN	Recurrent Neural Network
ROI	Region Of Interest
ROS	Robot Operating System
RTLS	Real-Time Location System
SAE	Society of Automotive Engineers
SMO	Sequential Minimal Optimization
SORT	Simple Online and Real-Time
SSD	Single Shot Detector
STFT	Short-Time Fourier Transform
SVM	Support Vector Machine
TLD	Tracking-Learning-Detection
TLS	Terrestrial Laser Scanning
UWB	Ultra-Wideband
YOLO	You Only Look Once

1 Introduction

The construction industry is one of the most crucial and critical industries for economic growth. In most countries, it contributes to the economy by 8–10% on average [1] and acts as a bridge connecting the economy to other industries. The construction sector is the engine of growth and generates a flow of services and goods with other industries. Increasing construction productivity allows businesses to earn more money while also reducing costs per capita [1].

In the construction industry, a project undergoes various stages in its life cycle, including design, planning, scheduling, execution, monitoring, control, and demolition. Effectively monitoring and controlling play a pivotal role in reducing time and cost overruns in construction projects [2]. It has long been a recurring topic that the construction industry needs to perform better. The industry has a bad reputation for using ineffective practices, and its productivity has increased by just 1% in over 20 years [164]. Moreover, the construction industry faces significant challenges, including a lack of skillful human operators, harsh environmental conditions, and safety [3].

Heavy-duty mobile machines (HDMMs), such as excavators and wheel loaders, play a key role in various construction projects. The total cost of a construction project is greatly impacted by the costs of HDMMs. Studies show that equipment costs can make up as much as 40% of direct costs in highway construction projects and as much as 5% to 10% of direct costs in building construction projects [4]. Evaluating and improving the productivity of construction machinery contributes to enhancing overall construction productivity and subsequently can bring about significant savings in total project expenses [2].

The well-known saying, "If you cannot measure it, you cannot improve it" [5], holds significant relevance for enhancing the performance of HDMMs and subsequently the construction industry. Within construction project management, productivity estimation and progress monitoring serve as pivotal elements, forming the basis for effective management and decision-making [6]. Monitoring the productivity of HDMMs is integral to fostering more cost-effective and successful construction projects and marking a critical step toward semi or fully autonomous worksites. Productivity estimation of HDMMs enables worksite managers to anticipate potential issues, pinpoint areas for enhancement, optimize resource allocation, refine planning and operating parameters, accurately budget for upcoming projects, and enhance overall management and financial conditions. Additionally, human operators can enhance their skills by taking advantage of the provided productivity feedback [174]. Traditional techniques for performance evaluation of HDMMs are labor-intensive, costly, and prone to human error because they rely on manual data collection and on-site observations [7]. Therefore, automated approaches are highly

required to precisely track the productivity of HDMMs in construction projects under different operating conditions.

1.1 Applications

There are various kinds of HDMMs, and the hydraulic excavator is one of the most significant pieces of equipment in the construction industry since different types of excavation work are required for almost all construction projects, including industrial and residential buildings, highways, and airports [175]. An excavator, which is a human-operated machine primarily driven by a hydraulic system, can perform various earth-moving activities, such as digging, trenching, and grading. Human operators use their senses and reasoning-based knowledge to control and monitor operations. Figure 1.1 depicts a typical hydraulic excavator. An excavator consists of three main parts, the front digging manipulator, the

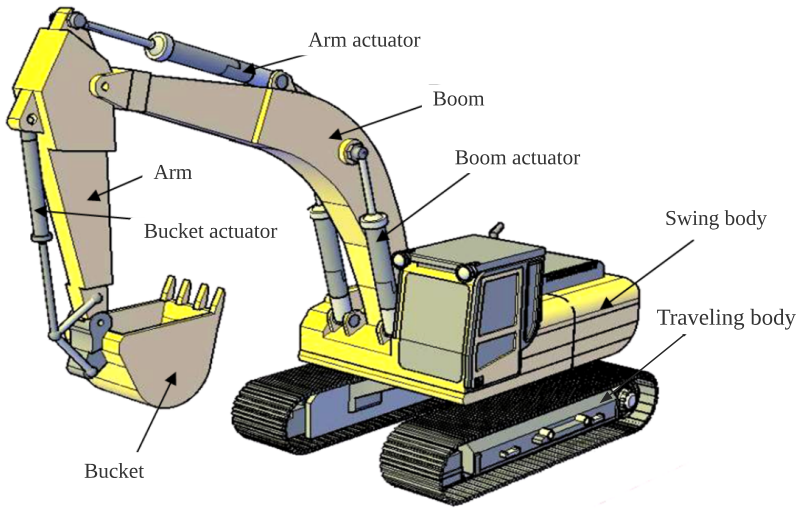

Figure 1.1: A typical hydraulic excavator [176].

swing body, and the traveling body. The boom, arm, and bucket comprise the machine's front digging manipulator. Three revolute joints connect the swing body, boom, arm, and bucket of an excavator [176].

According to a survey of research in this field, three of the most frequent duty cycles carried out by an excavator are loading (or dig & dump), trenching, and grading [8]–[10]. The simple schematics of these tasks are demonstrated in Figure 1.2. Loading operation is one of the most essential tasks in mining and construction projects. In this operation, materials are picked up and moved from one place to another using the excavator's manipulator. This can involve loading materials onto trucks for transportation or digging materials from the ground in order to prepare the site for construction [174]. Also, the loading operation can be subdivided into two categories based on the swing angle: 90° and 180° loading cycles. During a 90° loading cycle, an excavator undergoes acceleration of approximately 60° and deceleration of roughly 30° throughout the swing motion. Conversely, within a

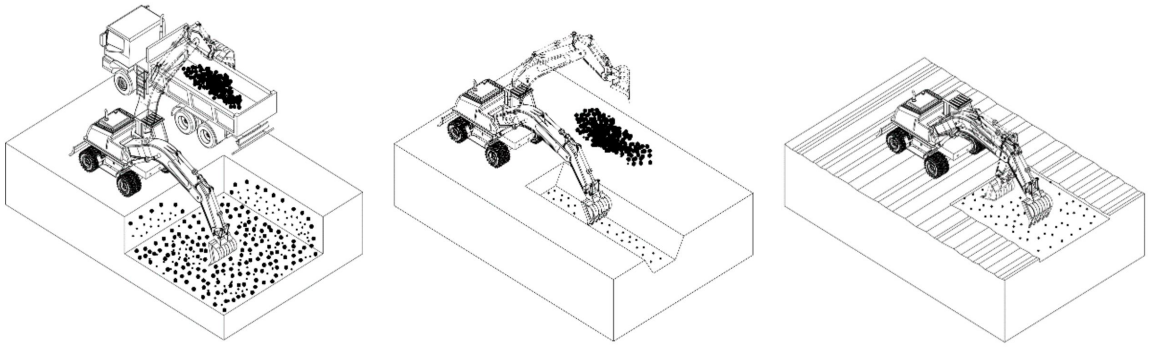

(a) Loading (b) Trenching (c) Grading

Figure 1.2: Typical excavator duty cycles [10].

180° loading cycle, both acceleration and deceleration phases span around 90° [11]. The second important duty cycle of an excavator is the trenching. In the trenching operation, an excavator is used to dig ground trenches for the installation of underground utilities, such as sewage and water pipes. The human operator digs a trench corresponding to the desired size and depth. Another important and challenging task that an excavator can perform is the grading operation. In the grading operation, an excavator is used to level and smooth the surface of the ground. This is frequently performed to create a level surface for paving or to prepare a site for construction, landscaping, or building purposes. To create a level surface, the excavator moves and distributes the material using its bucket [175], [165].

1.2 Research Hypothesis

This dissertation aims to define and estimate the actual or absolute productivity of an excavator in different earth-moving tasks, including loading, trenching, and grading operations. The next goal is to automatically evaluate the theoretical productivity or maximum capability of an excavator in these operations based on ongoing working conditions. Finally, the relative productivity or performance level of an excavator in these operations can be obtained using actual and theoretical productivity. At the core of our investigation lies the research hypothesis that the relative productivity of an excavator can be estimated in earth-moving tasks.

1.3 Thesis Outline

Chapter 1 presented the introduction and motivation of the dissertation. A short overview of the research hypothesis is discussed as well. Chapter 2 describes proposed methods for activity recognition and productivity estimation methods for different HDMMs in various earth-moving tasks. Chapter 3 outlines the proposed research framework and existing

research gaps and presents the research questions. Chapter 4 proposes a data-driven method to recognize the tasks of an excavator in earth-moving operations using motion information obtained from different moving parts of an excavator. Chapter 5 presents a method for sub-task recognition of an excavator in the loading operation. Then, the actual cycle time is estimated using the proposed sub-task recognition algorithm. Also, the working conditions, such as swing angle and digging depth, are estimated using the detected activities. Then, the theoretical cycle time of an excavator in the loading operation is estimated based on the ongoing working conditions. Finally, the performance level or operational effectiveness is evaluated. Chapter 6 describes two automatic methods to monitor the operation progress and calculate the productivity of an excavator in the trenching and grading operations. Firstly, the elevation terrain mapping algorithm is explained. Then, the productivity is estimated using a comparison of the actual map with the target model obtained from building information modeling (BIM). Lastly, chapter 7 concludes the dissertation with a summary and an outlook.

2 State of Research

Efficiently monitoring the productivity of HDMMs is essential for enhancing overall construction productivity and cost control. Nevertheless, traditional methods for equipment productivity monitoring still heavily rely on labor-intensive manual observations and record-keeping, which prove time-consuming, expensive, and prone to errors. To address these limitations, numerous research studies have been conducted on integrating information technology to automatically collect productivity-related data and monitor the productivity of construction equipment [3]. This chapter provides an in-depth exploration of the latest developments in this field.

Over the past few years, various information technologies, including machine learning [12], [13] and real-time location systems (RTLS) [14], [15], have been utilized in earth-moving equipment productivity monitoring and analyzing the influencing factors of equipment productivity. These methods can be classified into two groups based on the type of collected data: computer vision (CV)-based techniques and sensor-based techniques. Figure 2.1 illustrates the conceptual process of these methods. Some research studies [17], [18]

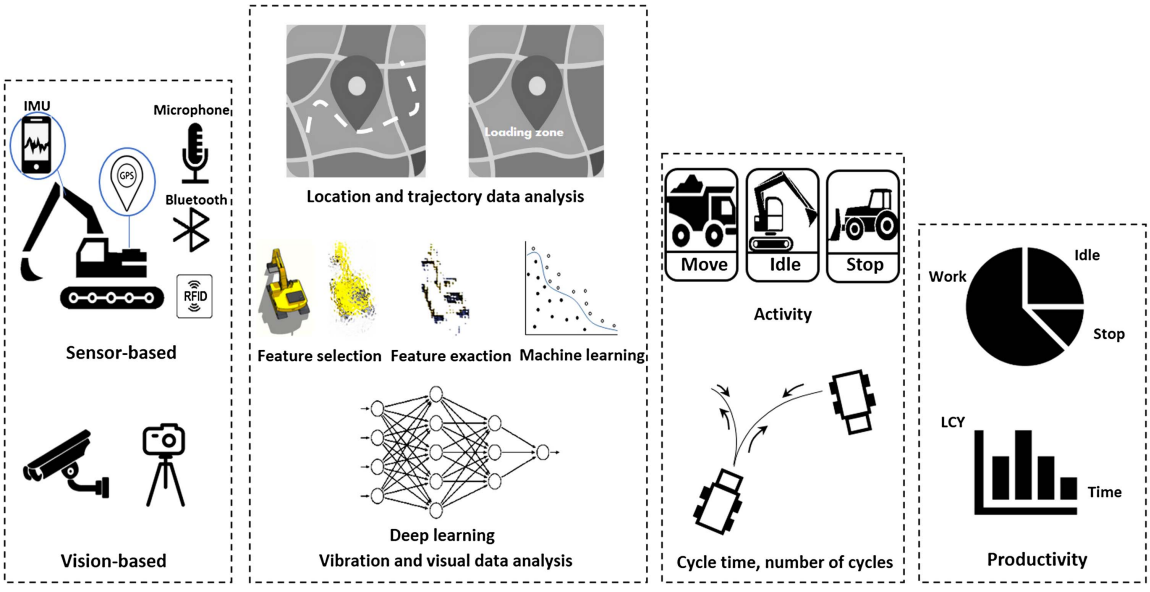

Figure 2.1: The conceptual process for equipment productivity monitoring: (a) data collection; (b) data processing; (c) operation monitoring; and (d) productivity analysis [16].

focused on evaluating the productivity of HDMMs through either CV-based or sensor-based techniques, while others [12], [19] emphasized the monitoring of factors that impact

productivity. CV-based approaches acquire operational data from surveillance cameras on construction sites. On the other hand, sensor-based methods involve the deployment of various sensors or tags, such as radio-frequency identification (RFID), global positioning system (GPS), ultra-wideband (UWB), inertial measurement unit (IMU), light detection and ranging (LiDAR), etc., on both the equipment and the construction site to capture position and pose information. Analysis of data from cameras or sensors enables the identification of work states or activities of the equipment. For instance, the location and trajectory data of a dump truck obtained from sensors can be directly utilized for identifying activities. Visual data is typically processed using CV-based techniques, such as deep learning, to recognize equipment activities. Finally, based on this activity information, the equipment productivity can be estimated in the form of the operation time, cycle time, operation quality, or soil quantity [16].

2.1 CV-Based Productivity Monitoring

The utilization of CV-based technologies for equipment productivity monitoring has become popular in recent years due to advancements in object detection and tracking algorithms within computer science. A typical CV-based productivity monitoring method comprises several key steps. Initially, equipment detection is employed to identify a specific type of equipment within image or video frames. Secondly, continuous tracking of different pieces of equipment is implemented across all video frames. The detection and tracking methods provide spatial position and movement information of the equipment. Consequently, activity recognition and pose estimation are performed to analyze the work states of the equipment, which is necessary for productivity analysis [16].

2.1.1 Detection Methods

The implementation of CV-based methods in equipment productivity monitoring begins with equipment detection methods. These methods typically initiate the process by extracting features that represent the visual characteristics of the equipment. In the next step, classifiers are trained to recognize the equipment by categorizing vectors generated from the features. The histogram of oriented gradients (HOG) serves as a widely used feature descriptor in equipment detection methods. In [12], [20], the HOG feature alongside a support vector machine (SVM) classifier is utilized for dump truck detection in videos. In [21], HOG with color features is combined with hue-saturation-values (HSV) to identify workers, excavators, and trucks in video frames employing an SVM classifier. In [22], HOG features and an SVM classifier are utilized to recognize five types of equipment (backhoe, dozer, excavator, loader, and roller) in images. In [23], a part-based model focusing on the boom is introduced to detect excavators, achieving fewer misclassifications compared to general HOG-based methods.

Several approaches identified moving equipment by subtracting it from the background. In [24], color space values are employed to recognize the excavator in images with snow

and soil backgrounds. In [25], the Gaussian mixture model (GMM) algorithm is utilized to segment regions of moving objects from the image. Secondly, two classifiers, including the Bayes classifier and a four-layer neural network, are utilized to categorize the segmented parts into workers, backhoes, and loaders. In [26]–[28], GMM and Bayes networks are used to recognize excavators and trucks in video frames. However, the background subtraction method is constrained to detecting moving and idling objects, which may not be sufficient for identifying other activities of the equipment. Earlier approaches faced a challenge in distinguishing specific equipment within a fleet. To address this limitation, in [29], a marker-based recognition method is designed to identify individual excavators and trucks in videos. This approach involves the attachment of markers onto the equipment, enabling their detection through marker recognition.

The developments of deep learning methods employing a convolutional neural network (CNN) have significantly impacted equipment detection algorithms. A fundamental distinction between feature-based methods and CNN lies in their approaches to learning the features of objects. While CNNs can automatically learn representative features from images in the dataset, feature-based methods rely on manually designed features, which is challenging in the complex construction environment [30]. Numerous CNNs have been employed for different equipment detection tasks, demonstrating superior performance compared to feature-based methods [31], [32]. In [33], a faster region-based CNN (Faster R–CNN) is utilized for excavator detection. In [30], the residual neural network (ResNet)-50 is trained using 2,920 images to recognize four pieces of equipment, including a loader, excavator, dump truck, and concrete mixer truck. In [34], Faster R-CNN [33], single shot detector (SSD) [35], and You Only Look Once (YOLO) [36] models are trained using the same dataset to recognize excavator, truck, forklift, and loader.

In [13], [37], without training a classifier for the recognition of a particular type of equipment, a tracking-based approach known as tracking-learning-detection (TLD) [38] is designed to detect the target equipment in video frames. This method initially chooses the target equipment for identification using a bounding box. Then, a tracker and a detector are trained online to locate the target in the next video frame based on trajectory, spatial information, gray-value variance, and pixel variance.

2.1.2 Tracking Methods

The tracking methods focus on associating and capturing the trajectory of each piece of equipment across all video frames. Different techniques have been employed for equipment tracking, including mean-shift tracking [39], a Kanade and Lucas tracker (KLT) [12], contour-based and point-based algorithms [40], kernel covariance [41], and Kalman filtering [26], [42].

In [40], three widely used tracking methods, including the contour-based, kernel-based, and point-based methods, are assessed to track workers, equipment, and materials in construction sites. It has been highlighted that the kernel-based method proves more suitable for tracking construction-related resources considering occlusion, illumination,

and scale variation conditions. In [43], the accuracy and robustness of 15 visual tracking methods across 20 distinct construction scenarios are evaluated. There have been challenges in tracking excavators due to self-occlusion, and only the dual correlation filter (DCF) [44] and circulant structure of tracking-by-detection with kernels (CSK) [45] methods could effectively track under heavy occlusions. In [46], a particle-based tracking system is introduced that is capable of continuous tracking of workers and equipment, including rollers, trucks, and dozers, even during extended periods of collisions. The target objects are represented using a set of particles, and offline training is not needed. In [47], the point tracking method [48] is enhanced by incorporating a failure-checking technique for tracking excavators. Initially, the optical flow images of an excavator are generated, and then key points are tracked under the assumption that the target's image brightness is constant between two consecutive frames. In [13], hybrid methods, including the median-flow algorithm [49] and the pyramidal Lucas-Kanade algorithm [50], are integrated to estimate object motions across consecutive frames, enabling the tracking of excavators in long videos. Hybrid tracking methods are also used to solve challenges regarding long-term occlusion and interclass variations. In [32], a deep simple online and real-time (SORT) tracker [51] is utilized, which combines a CNN and Kalman filter to track excavators and trucks.

2.1.3 Activity Recognition Methods

Numerous research studies moved toward developing more practical approaches to monitor operation and equipment productivity utilizing equipment detection and tracking methods. Activity recognition stands out as a key aspect of equipment monitoring since it has a direct relationship with productivity analysis. There are three primary methods in CV-based activity recognition: (1) feature-based methods, (2) rule-based analysis, and (3) spatial-temporal CNN methods (refer to Fig. 2.2).

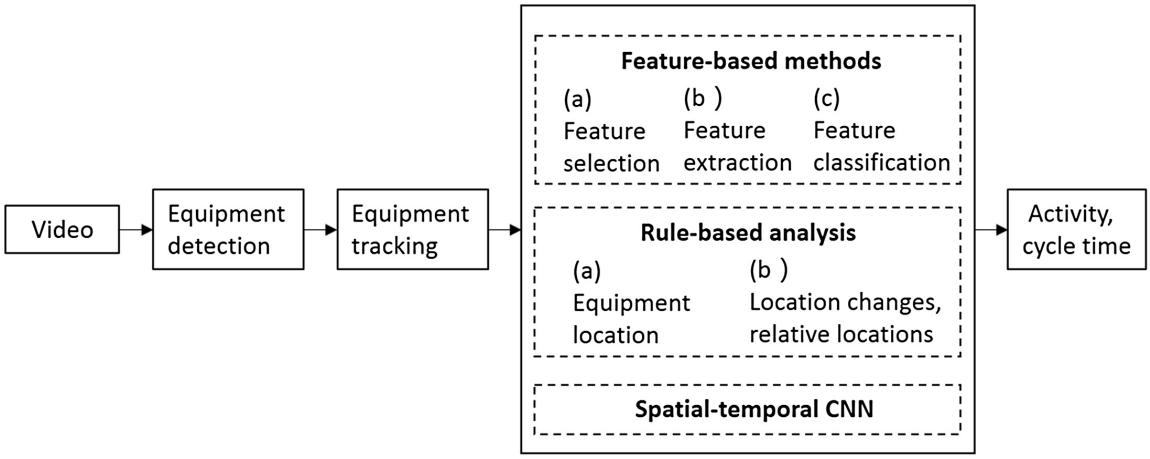

Figure 2.2: Workflow for equipment productivity analysis using CV-based methods [16].

Feature-based activity recognition methods share similarities with feature-based equipment detection approaches. Once spatial features are gathered in each video frame, these features in consecutive video frames are transformed into a vector or matrix for activity recognition. In [52], a three-dimensional (3D)-Harris corner detector is employed for identifying interest points. The HOG and histogram of optical flow (HOF) descriptors are utilized to characterize interest points in consecutive frames. Subsequently, a Bayesian neural network [53] is trained to classify different types of backhoe activities, including relocating, excavating, and swinging. The results demonstrate that the HOG feature outperforms HOF. In [17], 3D HOG as spatio-temporal features and an SVM as a classifier are utilized to identify excavator activities, including digging, hauling, dumping, and swinging, and truck activities, including filling, dumping, and moving. In [31], neural networks are employed to obtain the bounding boxes for excavators and trucks in frames of a video filmed at ground level. In the next step, the HOG, HOF, and motion boundary histograms (MBH) features of excavators and trucks are extracted every 20 frames. Finally, an SVM classifier is used to categorize the activities of an excavator (idling, swinging, loading, moving, and dumping) and a truck (idle, moving, filling, and hauling).

Rule-based methods find extensive applications in productivity analysis. These approaches identify activities by relying on the outcomes of detection and tracking steps. Initially, pixel coordinates of equipment in video frames are extracted from the detection and tracking results. Then, activities are detected by investigating the changes in coordinates within video frames or relative distances between different pieces of equipment. In [24], a color features detector based on HSV color space and a centroid tracker are utilized to acquire the excavator coordinates in video frames. The distinction between the idling and stopping activities of an excavator is established by comparing the changes in centroid coordinates across consecutive video frames. The percentage of working time in the total operation time is determined as productivity. In [12], HOG-based detectors are employed to obtain the coordinates of excavators and trucks. In the next step, utilizing vectors derived from the distances between the base point of the excavator and the four corners of the dump truck, an SVM classifier is trained to recognize loading activities. The cycle time is determined as the duration between two loading activities. In [54], a CV-based method is proposed for the identification of excavator activities, such as swinging, digging, dumping, idling, and moving, using highly varying long-sequence videos obtained from fixed cameras. In [27], [28], a construction site is partitioned into multiple interest regions. Then, the feature-based method, proposed in [17], is employed to distinguish between static and moving activities of excavators and trucks. Activity is classified as filling if both excavator and truck are detected within the earth-moving region and their distance falls below a defined threshold. Utilizing information on the excavator's bucket volume and hourly bucket numbers, the productivity as the volume of excavated soil is computed. In [55], five types of equipment (bulldozer, excavator, truck, grader, and roller) are identified using the HOG-based classifier. Then, a Bayesian network is employed to compute the probability of activities based on the other contents detected in the same frame. In [56], based on the assumption that the excavator and truck are within a certain distance during the loading phase, the loading activity is detected by comparing the changes in distance between the two pieces of equipment against predefined thresholds. In [57], a

vision-based technique is proposed to detect excavator activities (working, traveling, and idling) using TLD and bags-of-features (BoF). In [37], activities are identified by tracking changes in centroid coordinates across consecutive video frames. The interaction between excavators and trucks is analyzed to enhance accuracy. For example, if an excavator is in operation while the nearest truck is stationary, the activity of that truck is labeled as working. The presented method consists of four key steps: (1) equipment detection and tracking, (2) action recognition of individual equipment, (3) interaction analysis, and (4) post-processing.

The techniques can identify consecutive activities in long video sequences based on detection and tracking outcomes and can estimate the duration of each activity for equipment productivity calculation. Nonetheless, these methods still exhibit certain limitations. They rely on two-dimensional (2D)-pixel distance for proximity estimation instead of utilizing the more accurate 3D real distance. Since the cameras on construction sites are typically installed at inclined angles, the 2D-pixel distance fails to accurately represent the actual spatial relationships among different pieces of equipment in a real construction site. Additionally, these methods require adjusting the thresholds with changes in camera positions, which is very inconvenient [16].

Spatial-temporal neural networks are also utilized for the direct identification of equipment activities. In [58], a CNN and a long short-term memory (LSTM) network are integrated to identify excavator activities such as digging, hauling, dumping, and swinging. The approach is based on the assumption that excavators typically follow the sequence of digging, hauling, dumping, and swinging during operation [59]. Consequently, a hybrid neural network comprising a 10-layer CNN for visual features and a two-layer LSTM for sequential features is developed. However, due to the gradient descent issue of LSTM, this method faces challenges in achieving high accuracy in long videos. In [60], a 3D CNN is proposed to recognize the excavator activities using temporal and spatial information. In [61], a deep learning-based method is presented to recognize the activities of excavators and dump trucks from video frame sequences. In the method, image and temporal features are extracted using CNN and LSTM, respectively. In [32], a 101-layer 3D ResNet is employed to capture spatial-temporal features of activities within every set of 16 consecutive video frames. The model successfully identifies the digging, swinging, and loading activities of an excavator with an accuracy of 87.6%. Also, the activity durations and productivity are estimated. However, a notable limitation of this method is its requirement for a large dataset for effective training of the 3D ResNet. In [62], a deep learning-based excavator activity analysis and a safety monitoring system are proposed that can detect the activities, recognize the surrounding environment, and determine poses. In [63], a method is presented to recognize the activities of an excavator. First, the sequential patterns of visual features are extracted from the video frames using a pre-trained CNN model. Then, the activities are recognized using a bidirectional LSTM (BiLSTM) and the output of the pre-trained CNN. In [64], a vision-based method is described for automatically analyzing equipment productivity in earth-moving tasks by adopting zero-shot learning for activity recognition. The proposed method can identify activities of general construction machines (e.g., excavators and loaders) without pre-training or fine-tuning.

2.1.4 Productivity Analysis Methods

The majority of current studies computed productivity by identifying the equipment activities. Some studies determined productivity by assessing the ratio of working or idling times within the entire operation time. For instance, in [24], it has been investigated that the excavator was 3,590 *s* idling within 10,800 *s* operation time, resulting in a working rate of 66.8%. In [12], it has been determined that the excavator is involved in loading activities for 95 *min* within an excavation video with a length of 147 *min*. Certain studies focused on identifying the number of work cycles performed by excavators or trucks. Using the provided bucket volume data, the volume of excavated soil is computed. In [27], [28], by incorporating information about the duration of loading activities, the excavator bucket volume, and the number of buckets per hour, the volume of excavated soil is computed as productivity. In [56], utilizing this activity information, a technique for simulating processes is developed to estimate the cycle number of trucks and to determine the productivity of earth-moving operations. In [32], the work cycle number of an excavator is determined by analyzing the sequential relationship of identified activities. Then, the productivity is computed using bucket volume.

Rather than relying on activity recognition for productivity analysis, certain research studies employed other information to calculate productivity. In [65], a region-based fully convolutional network (R-FCN) [66] is utilized for the identification of license plate numbers on dump trucks as they enter and exit the construction site gate. It allows the calculation of truck cycles and the total volume of earth-moving by measuring the time intervals for each truck's arrival and departure. In [67], a productivity monitoring approach utilizing multiple cameras is introduced. In this method, two cameras are placed at different locations, one at the entry and the other at the loading zone. Through queueing discipline analysis, dump trucks captured by both cameras are matched, and then, cycle time and total number of cycles are determined.

Multiple CV-based methods have been proposed for the activity recognition and productivity monitoring of HDMMs, particularly excavators. Even though recorded videos can be utilized as trustworthy documentation [68], these approaches have significant limitations and practical challenges in real-world construction scenarios. These methods are highly sensitive to illumination conditions (i.e., too bright or too dark) and environmental conditions, including dust, snow, rain, fog, and wind, since they can cause the blurring of images or shaking of cameras. The length of daylight in autumn and winter in several countries, such as Finland, Sweden, and Norway, is very short, which can cause challenges [39], [69]. The methods face significant challenges in crowded and congested worksites with a lot of noise, such as background movements [70], [71]. It is highly challenging to keep a direct line of sight to resources. A network of cameras is required to cover large worksites [72]. Moreover, huge storage spaces are required to save images and video data. Also, the methods need comparatively more computing power than alternative methods [73]. Another challenge is the shortage of training datasets, which can significantly reduce the performance of the methods. The methods might not be possible to be used in some worksites due to privacy reasons. Furthermore, CV-based methods are relatively expensive since

the expenses of cameras in small-sized worksites are within the range [$1,000–$10,000] and in medium-sized worksites are within the range [$10,000–$100,000] [174], [16], [74]. Because of these challenges, CV-based methods cannot be considered as a robust and realistic solution in various construction sites.

2.2 Sensor-Based Productivity Monitoring

Sensor-based techniques involve attaching various sensors to equipment for localization and movement tracking. Through the analysis of position and pose data obtained from these sensors using classification or simulation methods, it becomes possible to estimate the equipment productivity. In this section, proposed sensor-based methods are divided into four categories based on the type of sensors: (1) RTLS sensors capable of identifying the positions and trajectories of the equipment; (2) vibration and orientation sensors that capture movement and pose information of the equipment; (3) audio sensors which can record sounds during operations; and (4) hybrid sensors that employ multiple types of sensors for equipment productivity monitoring. Ambient weather sensors are also utilized to observe the impact of weather conditions, such as temperature, humidity, and wind, on productivity [16], [75]–[77].

2.2.1 RTLS Sensors

GPS, RFID, and UWB are commonly utilized RTLS sensors capable of providing location and trajectory information of the equipment. GPS, as a satellite-based navigation system, acquires the longitude, latitude, and altitude data of the equipment. In [14], [78], [79], GPS sensors are employed to gather the trajectories of trucks and to determine the durations of the activities, such as load, travel, return, etc., through the analysis of the trajectories on the map. In [80], GPS is similarly utilized to acquire the trajectories of trucks on the map, aiming to estimate transportation costs. Certain GPS-based approaches divide the construction site into various work zones, such as excavation and loading areas. The activities or cycle time can be estimated using the analysis of the equipment's location in specific work zones. In [81], GPS sensors are attached to trucks to calculate loading and travel times by analyzing the locations of trucks on construction sites. In [82], the site is divided into work and non-work zones to determine the operational time of trucks. In [83], excavators and skid steer loaders are equipped with GPS, and the construction site is divided into gravel and excavation zones. The durations for excavation and loading activities are determined based on the equipment's locations. In [15], [76], the construction site is divided into excavation and dump zones to recognize the trucks' activities, such as entry, exit, and load.

UWB is a radio frequency positioning system employing a triangulation technique to determine the equipment's location by analyzing the signal propagation durations from the tag to the receivers [84]. In [85], the feasibility of commercially available UWB systems for tracking equipment, materials, and workers within a large construction site is investigated.

In [73], UWB and an attitude and heading reference system (AHRS) are utilized to record the positions and boom angles of trucks. In [86], the construction site is divided into dumping, hauling, loading, and excavation zones according to the locations derived from UWB sensors to identify the activities of a truck and an excavator.

RFID employs electromagnetic transmission for detecting and tracking tags attached to objects. The RFID system comprises readers and tags, with tags attached to equipment transferring digital data to readers using radio waves. RFID finds applications in distance estimation, scene analysis, and proximity. The distance from the tag to the readers can be calculated utilizing the triangulation algorithm based on signal propagation time. In equipment monitoring, readers with predetermined power levels define specific detection ranges for RFID tags. Consequently, equipment locations can be calculated by placing tags in various work zones [16]. In [87], RFID readers are deployed at the entry points of loading and dumping zones. The loading and dumping durations are estimated by capturing the entrance and exit times recorded by the RFID system. Then, the work cycle of the truck is estimated according to the sequential relations of activities.

The proposed methods using RTLS sensors, including GPS, RFID, and UWB, have significant challenges that limit their applications in real-world construction sites and extensions to other HDMMs. One constraint associated with these positioning sensors is that the collected data are restricted to location and time information, which makes it challenging to distinguish between productive and idling states of the equipment. Additionally, these records lack sufficient information for estimating the cycle time, the quantities of excavated soil, and operating conditions [16].

2.2.2 Vibration and Orientation Sensors

In contrast to RTLS, accelerometers measure the vibration signals produced by the equipment, and gyroscopes measure the orientations of the equipment. Processing the data obtained from the vibration and orientation sensors allows for the estimation of the pose and state of the equipment. The IMU sensor, comprising an accelerometer, a gyroscope, and a magnetometer, acquires acceleration and orientation data of the equipment. Typically, machine learning algorithms are employed to classify the movement data collected by IMUs, aiming for the recognition of the activity and the work cycle of the equipment [16].

In [88], two accelerometers are installed inside the excavator cabin. Three activities, including working, idling, and engine off, are distinguished by examining the overall patterns of the vibration signals, such as increasing and decreasing trends. In [89], IMU sensors are installed on the bed of a truck and the boom of a loader to identify activities using orientation and acceleration data. For instance, an increase in the boom angle relative to the horizontal line, combined with a stable bed angle near zero, shows that the loader is lifting its boom while the truck awaits loading. In the next step, a discrete event simulation (DES) model is employed to simulate the work cycle of both pieces of equipment based on the detected activities. In [90], two smartphones are utilized to gather accelerometer and gyroscope data from a loader. Firstly, raw data are characterized using 12 features, such

as mean, variance, peak, root mean values, etc. Then, an SVM and a CNN are employed to categorize these features and identify the activities of the loader, including engine off, idling, moving, scooping, and dumping. The results of the activity recognition algorithm are utilized as input, and the durations are estimated by considering the logical relationship between the activities. In [18], the possibility of assessing operational efficiency is explored by utilizing accelerometer data to categorize engine off, idling, and working states of four types of excavators. Four supervised learning methods, including Naive Bayes (NB), instance-based learning (IBL), decision tree (DT), and multi-layer perceptron (MLP) are employed in this research study. In [91], a smartphone is installed in the excavator cabin to record the 3D acceleration. In the next step, eight supervised classifiers are trained to estimate the excavator cycle time based on activity modes (e.g., wheel-base motion, cabin rotation, and arm/bucket movement of the excavator). The accuracy of cycle time estimation is equal to 75.96%. In [92], a smartphone equipped with an IMU sensor is installed onto the excavator's front window. In the proposed method, the dynamic time warping (DTW) technique and four classifiers, such as random forest, Naive Bayes, decision tree, and sequential minimal optimization (SMO), are employed to identify the excavator's activity. In the next step, the cycle time of the excavator is estimated based on the order of the activities. The accuracy of cycle time estimation is equal to 91.83%. In [93], DTW is employed to recognize the task of an excavator, including digging, leveling, and trenching, using joystick signals. In [94], two IMU sensors are installed on the body of a roller to identify six activities using LSTM. In [95], synthetic training data are generated using time-series data augmentation techniques on acceleration and orientation data. A recurrent neural network (RNN) is employed for the activity classification of four different types of excavators and front-end loaders. In [96], three IMU sensors are installed on the bucket, arm, and boom of an excavator to recognize different activities utilizing an SVM, a k-nearest neighbor (KNN), and an artificial neural network (ANN). The results demonstrate that the best place to collect motion information is the bucket. In [97], accelerometer data and a CNN are used to automatically identify the activities of an excavator, including idling, traveling, scooping, dropping, and rotation (left/right), and a roller compactor, including forward (high/low/no vibration) and backward (high/low/no vibration). In [98], a random forest classifier is integrated with the fractional calculus-based feature augmentation technique to identify construction equipment activities. The method is applied to several case studies, such as two different models of excavators, a scaled remotely controlled excavator, and a roller. In [69], a deep learning-based algorithm is presented to determine equipment productivity using kinematic data collected from smartphone sensors installed in an excavator. The excavator activities are classified into active and inactive classes to estimate the utilization ratio.

Vibration and orientation sensors, such as IMUs, can provide a promising solution to the challenges of CV-based and other sensor-based methods in activity recognition, cycle time estimation, and productivity monitoring. Even though IMUs require to be directly attached to the equipment, which is time-consuming in a large fleet, these sensors have many advantages since they are affordable, not restricted, can be easily installed, or have been already installed on different machines. IMUs are robust and resilient in challenging environments, in contrast to CV-based methods [99]. These methods can work easily

without any lines of sight. Moreover, the accuracy of IMUs is satisfactory. The methods can achieve a high level of accuracy, around 80–100%, in activity recognition and cycle time estimation. Also, they do not need high computational power and can be easily implemented in real-time [70]. The costs in small-sized worksites are within the range of [$100–$1,000], and in medium-sized worksites are within the range of [$1,000–$10,000]. Furthermore, in recent years, in order to estimate the bucket position for automated machine guidance (AMG) or automated machine control (AMC) systems, equipment manufacturers [166] and third-party businesses [167], [168] have begun mounting IMUs on the equipment. The sensors can be utilized for activity recognition and productivity monitoring purposes [174], [16], [74]. Although there are some approaches for the activity recognition and cycle time estimation of HDMMs using IMUs, still there are many potentials in using machine learning and IMUs for the activity recognition in different levels of detail and improving cycle time estimation. Also, IMU sensors, alongside other onboard sensors, can be utilized for automatic theoretical productivity and working conditions estimations.

2.2.3 Audio Sensors

Recently, audio-based methods have been introduced which are capable of identifying the activities of HDMMs utilizing the sounds produced by the equipment. Audio signals encompass diverse acoustic patterns associated with the equipment's operational processes. This identification comprises four key steps: (1) collecting sound data from equipment using a microphone; (2) filtering or augmenting the signals; (3) extracting features; and (4) training supervised classifiers [100]. In [72], [101], audio signals are employed to distinguish between major and minor activities of excavators, loaders, and dozers through the utilization of short-time Fourier transform (STFT) features and an SVM classifier. In [102], STFT and continuous wavelet transform (CWT) features are combined with an SVM classifier to identify the activities of an excavator and a dozer. In the next step, a Markov chain filter is employed to assess the cycle time and the number of cycles per hour. Then, the productivity of the backhoe as the volume of excavated soil per hour is determined based on the average fill factor.

Compared to CV-based methods, the obstacles in worksites cannot affect the quality of the recorded data in audio-based methods, and neither high computational power nor large storage space is needed. The audio-based methods have the ability to cover relatively large areas and record sounds from multiple machines. Unlike some sensor-based methods, there is no need to attach several sensors to each machine. The costs of microphones in small-sized worksites are within the range of [$300–$3,000], and in medium-sized worksites are within the range of [$3,000–$30,000]. Nevertheless, the audio-based methods face substantial challenges in crowded and noisy construction sites, which can decrease the accuracy of the methods. Also, some equipment does not generate distinct sound patterns, making it challenging to detect its activities. Moreover, the audio-based methods do not have the ability to accurately distinguish between detailed activities of a machine and then estimate the cycle time. Furthermore, the methods cannot be easily extended to other machines, such as tower cranes, which do not generate sounds [174], [16], [74].

Because of the challenges, the audio-based methods cannot be a solution for cycle time and productivity estimation purposes.

2.2.4 Hybrid Sensors

Hybrid sensors are also employed to obtain more accurate information about equipment and operations. In [103], displacement and pressure sensors are installed on the cylinders of the boom, arm, and bucket of the excavator to record its movements, pose, and actual bucket load. In [104], IMU and microphones are utilized to gather vibration and audio data during excavators' operations. In the next step, two types of data are manually synchronized based on the similarity of signal spikes. Then, an SVM classifier is utilized to distinguish excavator activities, such as stop, shove, move, and turn, achieving an accuracy 20% higher than using only IMU or audio data. In [105], an algorithm is proposed to automatically classify the working stages of an excavator based on the main pump pressure waveform. Three machine learning algorithms, an SVM, a back propagation neural network (BPNN), and logistic regression (LR), are utilized in this research study. In [106], three classifiers, an LSTM network, an RNN, and an SVM, are trained using the control signals of operating handles to recognize the activities of an excavator. In [107], a deep learning-based hybrid kinematic-visual sensing algorithm is designed for equipment activity recognition. Kinematic and visual data are collected using built-in sensors, gyroscopes, accelerometers, and cameras of a smartphone that is installed inside the cabin of an excavator. In [108], a deep neural network (DNN) model is presented to determine the volume of excavated earth per day using telematic data, including equipment weight, bucket volume, volume excavated, fuel rate, total fuel consumed, engine on time, engine on (no dig), engine on (no move), digging, swing time, travel time, and not operating, from 21 days of operation. The main drawback of DNNs is the high computational complexity and requirement for a large dataset. In [109], a method is proposed to identify activities of an excavator, such as excavation, leveling, rock excavation, and drive, using a fusion network that combines sensor and video-based models. This research continues, and in [110], a DNN ensemble called FusionNet is introduced to identify the activities of excavators, including slope digging, ditch digging, rock digging, leveling up-down, leveling front-back, leveling left-right, deep digging, drive, and digging. This algorithm employs the extracted features from sensor data and video frames of on-site excavators.

Additionally, hybrid sensors are applied for monitoring various productivity-related factors. In [111], a decision support system called WEATHER is designed to determine the effect of weather conditions on equipment productivity. In [75], GPS, strain gauges, an accelerometer, and barometric pressure are employed to track equipment location, estimate the load weight of the truck, identify loading and dumping activities of the loader and trucks, and measure weather conditions, respectively. Utilizing the sensor data, an automated data processing algorithm is developed for the near-real-time estimation of earth-moving productivity. In [112], GPS is employed to track the positions of trucks, pavers, and rollers. Also, the temperature of the asphalt mat is monitored utilizing temperature sensors on the pavers. In [113], GPS, IMU, soil water content sensors, and load cells are utilized to assess

the factors affecting earth-moving productivity. These factors included soil conditions, hauling and road conditions, equipment operational conditions, and weather conditions.

2.2.5 Productivity Analysis Methods

Construction equipment commonly operates within diverse and complex construction sites. Equipment productivity can be either predicted using data-oriented methodologies, such as statistical regression models and neural networks if historical data from similar operations are available, or using process-oriented methodologies if no historical data is available [19].

Process-oriented methodologies have been proposed in (a) equipment manufacturers' handbooks [114]–[117], (b) editions from contractors' associations or individual researchers in Germany [118]–[124] and (c) textbook editions [125], [126]. In the process-oriented models, operating conditions, such as swing angle (i.e., the angle between digging and dumping points), digging depth, bucket capacity, skill of human operators, etc., are transformed into several factors to be able to predict productivity. The factors include the rated bucket capacity, the cycle time, the swell factor, the bucket fill factor, the job efficiency factor, the operator skill factor, the equipment availability factor, the swing angle factor, the excavation depth factor, the combined swing angle and digging depth factor, the bucket dump factor, the excavator-truck volumes match factor, the bucket teeth wear factor, and the altitude factor [19].

In data-oriented methodologies, the main productivity influencing factors are supposed known and employed as models' inputs to predict productivity. The models are trained using historical data or using synthetic data generated using process-oriented methodologies. In [127], a linear regression model is designed to determine the productivity of earth-moving equipment. It has been highlighted that the bucket volume, truck travel time, number of trucks, and haul length are key parameters that influence productivity. In [128], a two-layer CNN is utilized to predict the excavator productivity based on the cycle time. The machine weight, digging depth, and swing angle are introduced as three main influencing factors in productivity estimation. Also, in [129], [130], swing angle, machine weight, and digging depth are recognized as the key factors in the productivity of an excavator. In [131], a feed-forward neural network is designed to predict the productivity of excavators using multiple factors, including relative positions between excavators and materials, site obstructions, the skill of the human operator, and the type of soil. In [132], a conjugate gradient algorithm and the feed-forward propagation network are integrated to estimate the earth-moving productivity using the number of excavators and trucks, bucket volume of the excavator, loading capacity of the truck, and type of material. In [133], the loading time of excavators with respect to the relative position with trucks is evaluated. The study highlights that the loading time is influenced by factors such as horizontal and vertical distances and swing angles between the excavator and the truck. In [134], the skill of human operators plays a crucial role in the productivity of an excavator and can influence other factors. The correlation between the skill level of the operator and the productivity of the excavator is investigated using the Caterpillar excavator productivity

model. To enhance the accuracy of productivity estimation, the operator's skill level is incorporated into the model as a factor. In [135], a computer dispatch system is employed to investigate the primary elements impacting the productivity of excavators and trucks in mining projects. The outcomes of the study reveal that the matching between the excavator and truck, such as loading position and truck-shovel combinations, can significantly influence loading efficiency and, consequently, overall productivity. In [76], a linear regression method and various sensors are used to evaluate the impact factors, including humidity, wind speed, temperature, idle time, average speed, etc., on the earth-moving productivity. In [113], a fuzzy model based on expert investigation is designed to detect and assess different factors influencing the productivity of earth-moving operations. The skill of the human operator, snowy road conditions, foggy weather, the water content of the soil, and waiting times are recognized as the most important productivity factors.

Influencing factors, including the excavator's relative position in relation to the truck and soil (i.e., swing angle and digging depth), relative height between the excavator and truck, and site congestion, pose challenges for both sensors and cameras to accurately estimate. These parameters have not yet been estimated through any automated methods and proposed productivity analysis methods only assume that they are known.

Traditionally, surveyors have been responsible for collecting information to monitor progress and conducting surveys at construction sites. The demand for automated monitoring tools has led to the incorporation of 3D sensing technologies, enabling the precise and accurate gathering of on-site data. This data can then be integrated with a planned model based on BIM to evaluate the advancement of the project [136].

Researchers are exploring the usage of BIM and 3D sensing technologies for real-time progress monitoring to address issues related to schedule and cost overruns [137]. This integration was driven by the utilization of BIM across various dimensions. For example, a 4D BIM-based model, also referred to as a schedule model, has been established to sequence activities over time. Another dimension of BIM, the 5D BIM-based model, specifically focuses on tracking activity costs over time [136]. In [138], an object recognition algorithm is designed to evaluate construction progress by matching on-site photographic images with 3D BIM models. This method identifies particular objects in the site images using advanced image processing algorithms to compare them with corresponding 3D objects in the BIM model. In [139], managing and transferring information are introduced as major benefits of BIM that can improve our understanding of planned activities. In [140], modeling and augmented reality are employed to compare the plan with what is actually happening on-site.

Some research studies proposed techniques for processing point cloud data in construction and infrastructure applications [141]. In [142], excavation changes are estimated based on depth differences of the surface using a LiDAR sensor. Obstructions such as piles that block the sensor's vision may reduce the precision and accuracy of volume estimation. In [143], a method is designed using a stereo camera and a LiDAR sensor to establish a 3D visualization of a construction site. In [144], a method is introduced that utilizes point cloud data obtained from a laser mobile mapping system (LMMS) to automatically evaluate the excavation volume required for road widening. In [145], a network-based cloud system is

presented to manage soil volume progress in a construction site. The daily progress volume is determined using the bucket cutting-edge historical data that is gathered from sensors installed on heavy equipment. In [146], a coordinate-based volumetric computational method is proposed to estimate the volume of stockpiles utilizing data from a laser scanner. Also, three mining industry surveying methods, photogrammetry, terrestrial laser scanning (TLS), and aerial laser scanning (ALS), are compared and analyzed. In [147], point clouds, image data, sensors, and computer-aided design (CAD) models are integrated to estimate the excavation volume and monitor the excavation progress at a worksite.

The productivity estimations of quality-centered tasks, including trenching and grading tasks, have been overlooked in the literature review. Recent progress in 3D sensing technologies and BIM can be a promising solution to automatic productivity estimation and progress monitoring in these tasks [175].

3 Scientific Contribution

In this chapter, firstly, the proposed research framework to automatically estimate the productivity of an excavator in different tasks, including loading, trenching, and grading, is elaborated. Afterward, the research gaps and practical challenges identified in the literature review are comprehensively discussed. Then, multiple research questions that are the main targets of the dissertation are introduced.

3.1 Research Framework

In the context of this dissertation, "productivity" means the production rate at the activity level of an operation. Since productivity is defined based on the objective of the task, the definitions of productivity vary for different tasks. Generally, the quantity of material and the operation cycle time are the main factors for the productivity of most cyclical types of machinery. The productivity of an excavator in the loading operation means the quantity of transferred material per unit of time. Although this productivity definition can effectively represent the productivity of an excavator in the loading operation, it cannot correctly show the productivity of an excavator in the trenching and grading operations since quality plays the main role in these operations rather than quantity. In the grading operation, only a small amount of materials are added or removed. Hence, the amount of material cannot reflect the productivity. The productivity of an excavator in a grading operation is defined as the area of the graded surface per unit of time. In the graded area, the error between the model and the actual terrain should be within the specified accuracy requirements. In the trenching operation, it is highly significant that the characteristics and size of the actual trench should be based on the designed model. In this task, contractors typically estimate the productivity in terms of the linear length of the trench per unit of time [115], [148]. Therefore, prior to productivity estimation, an automatic task recognition method is required to identify the duty cycle of the excavator. In the next step, the productivity should be estimated based on the detected duty cycle.

There are different types of productivity definitions that must be taken into account:

- The absolute or actual productivity that shows the real productivity of a machine. The actual productivity is estimated using multiple sensors installed on the machine or the worksite. Another key metric is the actual cycle time, which represents the duration of a work cycle.

- The second productivity definition is the nominal or theoretical productivity that shows the expected productivity level of a machine. The theoretical productivity should be estimated based on the capabilities and characteristics of the machine and ongoing operating conditions. Another important metric is the theoretical cycle time, which represents the duration the machine is capable of performing a particular task under specific working conditions.
- The third productivity definition is the relative productivity or production performance ratio (PPR), which represents the performance level or operational effectiveness of a machine. The relative productivity is obtained by comparing the actual productivity against the theoretical productivity. Another metric is the relative cycle time which is obtained by dividing the theoretical cycle time by the actual cycle time.

As earlier discussed, the actual productivity of an excavator is highly influenced by different parameters and working conditions, such as swing angle, digging depth, size of the excavator, bucket capacity, dumping conditions, type of materials, weather conditions, and skill of human operators. The actual productivity of an excavator cannot lonely represent the performance of a machine since working conditions can significantly impact it. To assess the actual productivity, a benchmark or the theoretical productivity of an excavator is highly required. Then, the relative productivity can effectively illustrate the performance. Hence, automatic methods are needed to estimate the actual and theoretical productivity of an excavator in different tasks, including loading, trenching, and grading operations. In addition, to be able to automatically determine the theoretical productivity, operating conditions, such as swing angle and digging depth, should be automatically estimated.

3.2 Research Gaps

As described in Chapter 2, several methods have been proposed to recognize activities, estimate cycle time, analyze working conditions, and monitor the productivity of an excavator using different types of sensors and data. Still, some challenges should be addressed.

Several approaches have been introduced to detect the activities of excavators, mainly focusing on sub-tasks or low-level information. However, only three research studies [93], [109], [110] have aimed to identify the primary tasks or major activities performed by excavators. In [93], a DTW is suggested for recognizing the main working cycles of an excavator, such as digging, trenching, and leveling, by analyzing joystick measurements. However, the approach encounters significant challenges when applied in real-world scenarios. Joysticks used in different excavator models vary among manufacturers, necessitating substantial time and effort for calibration to interpret joystick output values. Furthermore, the precision of joystick measurements can differ significantly between machines, and the method's accuracy may be heavily influenced by operators' behaviors and skills. Additionally, the proposed technique relies on a complex post-processing algorithm to address errors in the primary algorithm. In [109], [110], a method based on deep learning

is developed to recognize excavators' tasks by integrating sensor data and video frames. Nonetheless, this method faces two main challenges. Firstly, CV-based methods present numerous challenges that have been introduced in Section 2.1.4. Secondly, deep learning models have high computational complexity and demand extensive datasets. Therefore, a method for the excavator's task recognition should be developed to solve the challenges.

Additionally, the majority of presented sensor-based methods focus on recognizing the individual sub-tasks of excavators without providing estimates for cycle time and productivity. The primary challenge lies in accurately estimating the actual cycle time of an excavator during the loading operation. Only two research studies have attempted to estimate excavator cycle time. In [91], the cycle time estimation achieved a low accuracy of 75.96%, which could significantly impact productivity estimation due to errors. In [92], a cycle time estimation accuracy of 91.83% has been achieved. However, in 20% of cycles, the difference between the estimated cycle time and the ground truth obtained from videos exceeded 3 s, leading to substantial errors in productivity estimation. Hence, a method should be designed to improve sub-task recognition and cycle time estimation of an excavator in the loading operation.

Another notable challenge is the lack of a benchmark for assessing estimated cycle time. Because working conditions can impact cycle time, solely relying on actual cycle time cannot accurately indicate whether the machine is operating at optimal performance levels. Hence, there is a necessity for a reference point to evaluate actual cycle time. To establish a theoretical cycle time, it is imperative to automatically estimate working conditions, such as swing angle and digging depth, during the operation.

Based on the literature review, there exists a significant research gap concerning the integration of real-time data with models to offer insights into ongoing activities at construction sites. Moreover, current studies predominantly prioritize the quantity of material, overlooking automated methods for evaluating productivity during grading or trenching operations using BIM. In grading and trenching operations, the paramount focus lies in ensuring quality and accuracy.

3.3 Research Questions

This dissertation aims to develop a series of approaches for the automatic productivity estimation of an excavator in different earth-moving tasks, including loading, trenching, and grading operations, using IMUs and machine learning techniques. In particular, the main focus is on the following research questions:

- How can the task recognition of an excavator be improved using IMUs and machine learning techniques?
- How can the sub-task recognition of an excavator in the loading operation be improved using IMUs and machine learning techniques, and then cycle time be estimated using detected activities?

- How can the operating conditions, including swing angle and digging depth, be automatically estimated using detected activities?

- How can the theoretical productivity of an excavator in the loading operation be automatically estimated based on the operating conditions to determine the relative productivity?

- How can the actual productivity of an excavator be estimated in quality-centered tasks, including trenching and grading operations, using 3D sensing technologies and BIM?

Several methodologies will be proposed to address the research questions outlined. The dissertation's scientific contributions are summarized in Table 3.1. Nevertheless, certain aspects remain unexplored and could be subjects of future investigation. Specifically, the quantification (either in volume or weight) of materials during the loading operation has not been examined within this dissertation because of the extensive existing research on this topic and the satisfactory performance of the proposed methodologies. Additionally, the definition of relative productivity for an excavator during the loading operation has been refined to encompass relative cycle time. This implies that the material quantity in both actual and theoretical productivity is regarded as equivalent. Moreover, the automatic methodologies for estimating the theoretical productivity of an excavator in trenching

Table 3.1: The summary of the scientific contributions for the productivity estimation of an excavator in earth-moving tasks.

	Excavator's tasks recognition		
	Loading operation	Trenching operation	Grading operation
Productivity definition	$\frac{Quantity\ of\ material}{Time}$	$\frac{Length\ of\ trench}{Time}$	$\frac{Area\ of\ graded\ surface}{Time}$
Actual productivity	(1) Excavator's sub-tasks recognition (2) Actual cycle time estimation	(1) Integration of elevation terrain mapping and BIM (2) Actual productivity estimation	(1) Integration of elevation terrain mapping and BIM (2) Actual productivity estimation
Theoretical productivity	(1) Swing angle estimation (2) Digging depth estimation (3) Theoretical cycle time estimation (4) Relative cycle time estimation	–	–

and grading operations have not been explored. This area warrants consideration in subsequent research endeavors.

In Chapter 4, an automatic task recognition method using IMUs is proposed to answer the first research question. In Chapter 5, firstly, a method is proposed to estimate the cycle time of the loading operation using a sub-tasks recognition algorithm. Then, the theoretical productivity of an excavator in the loading operation is estimated using a process-oriented method and automatic working condition estimations. Finally, the relative productivity is estimated. In this chapter, the second, third, and fourth research questions are answered. In Chapter 6, two methods are designed using 3D sensing technologies and BIM to automatically estimate the actual productivity of an excavator in the grading and trenching operations to answer the fifth research question.

4 Excavator Task Recognition

Task recognition is essential for productivity estimation, maximizing efficiency, ensuring safety, maintaining equipment, collecting data, and enhancing training and skill development in construction and excavation operations. In this chapter, a method is designed to automatically recognize the excavator's tasks, including loading, trenching, and grading, using supervised learning algorithms and motion information obtained from IMUs attached to different moving parts of the machine, such as the bucket, arm, boom, and swing body.

4.1 Introduction

Task recognition is a crucial step prior to productivity monitoring since productivity is defined based on the objectives of the tasks. The schematics of the three most important tasks of an excavator, including loading, trenching, and grading, are illustrated in Fig. 1.2 [8]–[10]. The loading task is pivotal in construction and mining industries, which typically consist of four primary activities such as scooping, swinging loaded, dumping, and swinging empty. The productivity of the loading task is defined as the quantity of transferred materials per unit of time [174]. The next important task is the trenching operation. In this task, an excavator is employed to dig trenches according to specified dimensions for the placement of underground utilities. The definition of productivity in this task is equal to the length of the trench per unit of time [115], [148]. The next critical task is the grading (or leveling) operation. In this task, an excavator is used to smooth the ground's surface for building, landscaping, and paving purposes. The productivity of the grading operation is defined as the graded area per unit of time. In the grading and trenching operations, quality is the highest priority instead of quantity [175]. Hence, task or working cycle recognition of an excavator is one of the essential and primary steps before the productivity analysis.

Only three research studies [93], [109], [110] have been proposed to identify the tasks or major activities (loading, trenching, and grading) of an excavator. In [93], a DTW system is proposed to recognize the excavator's working cycles using joystick measurements. The presented approaches face significant challenges in practical implementations. Used joysticks in different machines vary across different manufacturers, and considerable time and effort are required for adjustments to interpret joystick output values. Moreover, the precision of joystick measurements varies among different machines, and the method can be highly susceptible to the behaviors and skills of operators. In addition, the proposed

technique uses an intricate post-processing algorithm to mitigate errors in the primary algorithm. In [109], [110], a deep learning-based method is designed to identify the tasks of an excavator using the integration of sensor data and video frames. However, CV-based methods face several practical limitations in real-world construction sites. They are highly sensitive to lighting and environmental conditions (e.g., dust, snow, rain, fog), and require a clear line of sight, which is difficult to maintain on congested sites. The need for multiple cameras, large storage space, high computational power, and access to diverse training datasets further complicates their use. Privacy concerns and high costs—ranging from $1,000 to $100,000 depending on site size, also limit their applicability [174]. In addition, deep learning models have a high computational complexity and require very large amounts of data.

To address these limitations, our research study proposes an automatic method to recognize the tasks of an excavator, including loading, trenching, and grading, using multiple low-cost IMUs installed on moving parts of the excavator. IMUs offer several advantages, they are affordable, easy to install, already integrated into many machines, and robust against environmental challenges. Their costs range from $100–$1,000 in small-sized worksites to $1,000–$10,000 in medium-sized ones. Major equipment manufacturers and third-party providers have already adopted IMUs for estimating bucket position in AMG or AMC systems. Furthermore, IMUs have low power consumption and are well-suited for use in harsh construction environments, making them a practical and scalable alternative to vision-based systems. The main contribution of this work is the development of a machine learning-based method for automatic task recognition of excavators using IMUs. To the best of our knowledge, this is the first study that applies machine learning techniques to classify excavator's working cycles (loading, trenching, and grading) based on IMU measurements. This sets our approach apart from prior studies that rely on vision data or joystick inputs.

4.2 Methodology

In the proposed method, the excavator's working cycles, including (1) loading, (2) trenching, (3) grading, and (4) idling, are recognized using four IMUs that have been installed on different moving parts of an excavator, including the bucket, arm, boom, and swing body. A dataset lasting 3 h is collected using a medium-rated excavator operated by one experienced and one inexperienced operator. Different operating conditions, such as different swing angles, digging depths, types of material, weather conditions, and the skill levels of operators, have been covered in the dataset to increase the robustness of the data-driven method. In the next step, four machine learning techniques, including a support vector machine (SVM), a k-nearest neighbor (KNN), a decision tree (DT), and Naive Bayes (NB), are trained using the collected dataset. The flowchart of the proposed method is illustrated in Fig 4.1. Then, the effects of different configurations, including time window, overlapping, and feature selection methods, on classification accuracy are

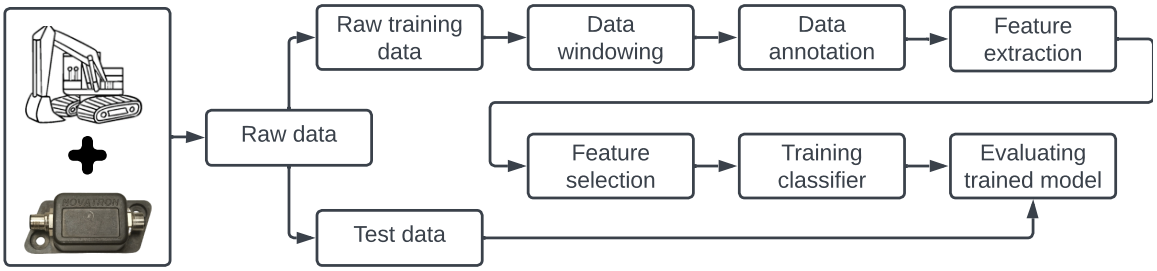

Figure 4.1: Flowchart of the activity recognition algorithm [174].

extensively investigated. Finally, the results show the presented algorithm has the ability to automatically recognize the major tasks or working cycles of an excavator.

4.2.1 Field Data Collection

Firstly, field data was collected using the crawler excavator shown in Fig. 4.2. Although the excavator is old, it has been kept in good condition since it has received regular maintenance and inspections every 500 working hours. The model is a Komatsu® PC138US with a mass of 13.4 tonnes and a typical mono boom structure that is equipped with a Novatron Xsite® machine control system. The bucket was attached to the arm using quick couplers and a tiltrotator. The tiltrotator was not used during the data collection. There was no active construction project in the worksite during the data collection.

There are two standards for heaped bucket capacity, the Society of Automotive Engineers (SAE) standard and the Committee for European Construction Equipment (CECE) standard. The schematics of SAE and CECE standards are illustrated in Fig. 4.3. The angles of repose for material above the strike-off plane in SAE and CECE standards are 1:1 (45°) and 1:2 (~

Figure 4.2: Excavator used in data collection. In the picture, (1) cabin, (2) boom, (3) arm, and (4) bucket are highlighted with red boxes [176].

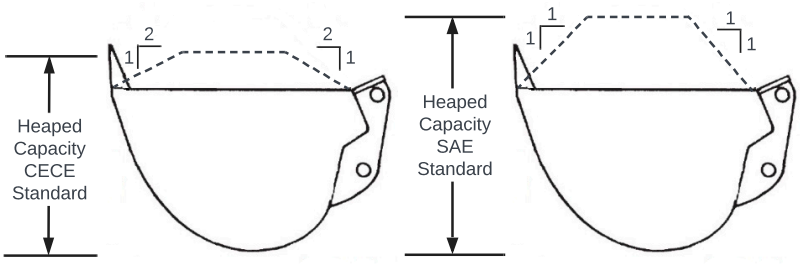

Figure 4.3: Heaping according to the SAE and CECE standards [174].

27°), respectively. It has been observed that $V_{SAE}[m^3] \approx [1.10 - 1.20] \times V_{CECE}[m^3]$ [148]. The heaping bucket capacity of the used excavator in the data collection is equal to 0.37 m^3 according to the SAE standard J-296.

The operations represent realistic construction scenarios, which means no direction is provided to operators on how to do the operations to increase the robustness of the presented method. The collected dataset covers various operating conditions, such as swing angle, digging depth, weather conditions, and types of material. Several types of material, such as sand, gravel, clay, and mixed, were used in the data collection phase. The digging depth increased up to 2 m, and the swing angle varied from 60° to 120°. The operations were performed in different seasons during 18 months by two operators with different levels of competence in a private worksite. The inexperienced operator performed 47% of the experiments, and the rest of the dataset was gathered by the experienced operator.

An IMU is a versatile sensor module widely utilized in different applications, such as orientation tracking, gesture recognition, robotics, and virtual reality, which is equipped with a 3-axis accelerometer and gyroscope. The accelerometer and gyroscope simultaneously measure acceleration along three orthogonal axes and angular velocity, respectively. These two units enable the IMU to capture complex motion dynamics in 3D space to facilitate precise motion analysis and improve the capabilities of various devices ranging from smartphones to unmanned aerial vehicles [97]. The used IMU in the data collection step is shown in Fig. 4.4. This sensor was produced by Novatron® Ltd. and placed in robust casings.

Figure 4.4: The IMU used in the data collection phase [177].

Four IMUs were attached to the moving parts, including the bucket, arm, boom, and swing body, to measure the orientation and angular velocities of the excavator. Attaching the sensor directly to the bucket increases the risk of damage. Therefore, instead of mounting the IMU directly on the bucket, it is positioned on the side link. The configuration of IMUs on the excavator is demonstrated in Fig. 4.5. IMUs were precalibrated utilizing the Xsite® machine control system. The sensor data is transferred with the sampling frequency f_s of 200 Hz using the controller area network (CAN) bus. The CAN bus is connected to the MathWorks® Simulink model using a Kvaser leaf light CAN to USB interface. The length of the dataset is around 3 h, which means that based on the sampling frequency f_s, approximately 2,160,000 data points were collected for each sensor's channel. The amount of data corresponding to each label is presented in Table 4.1.

Table 4.1: The duration of different working cycles in the collected dataset.

	Working Cycle			
	Loading	Trenching	Grading	Idling
Duration [min]	68.43	41.14	35.26	37.27

Each sensor unit measures the quaternion orientation based on the accelerometer and gyroscope's measurements. Afterward, the quaternion measurements are utilized to determine the joint angles between each moving component of the machine connected by the revolute joints. The quaternion to Euler angles conversion is stated in Eq. (4.1c):

$$q(t) = \begin{bmatrix} q_w(t) & q_x(t) & q_y(t) & q_z(t) \end{bmatrix}^T \tag{4.1a}$$

$$|q|^2 = q_w^2 + q_x^2 + q_y^2 + q_z^2 = 1 \tag{4.1b}$$

$$\begin{bmatrix} \phi \\ \theta \\ \psi \end{bmatrix} = \begin{bmatrix} \arctan\left(\frac{2\left(q_w q_x + q_y q_z\right)}{1-2\left(q_x^2+q_y^2\right)}\right) \\ -\pi/2 + 2\arctan\left(\sqrt{\frac{1+2\left(q_w q_y - q_x q_z\right)}{1-2\left(q_w q_y - q_x q_z\right)}}\right) \\ \arctan\left(\frac{2\left(q_w q_z + q_x q_y\right)}{1-2\left(q_y^2+q_z^2\right)}\right) \end{bmatrix} \tag{4.1c}$$

where q indicates the unit quaternion, and ϕ, θ, and ψ represent the roll (rotation around the x-axis), pitch (rotation around the y-axis), and yaw (rotation around the z-axis), respectively [149].

The global angular velocities, which are measured using the gyroscope in the IMU, are utilized to compute the local angular velocity of each moving part. The local angular velocity is the actual angular velocity of the particular body part, which the movements of the other machine parts have been subtracted. The local angular velocity illustrates the movement of the measured body part as a result of the operator's movement of that particular body part. However, the global angular velocity comprises all movements caused by the machine. The local angular velocities and orientation variables are demonstrated in Fig. 4.6. The task recognition algorithm employs the joint angles and angular velocities of

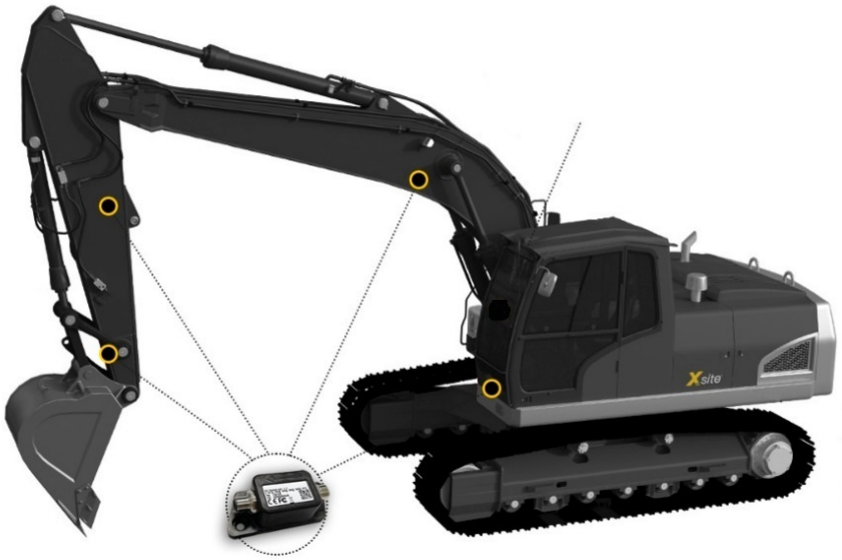

Figure 4.5: The configuration of IMUs on the excavator [177].

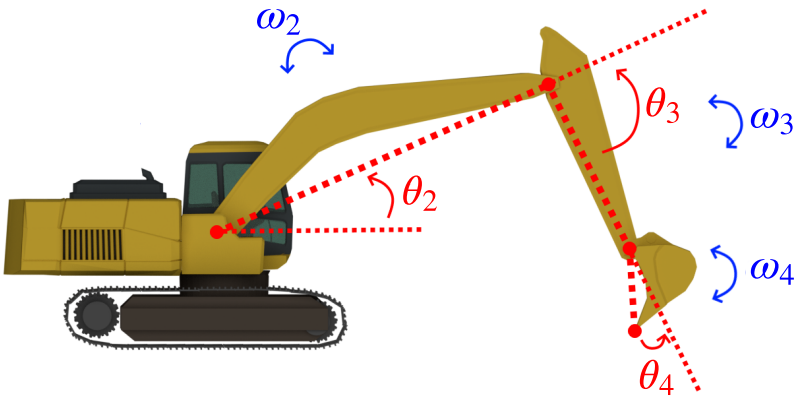

Figure 4.6: The local angular velocities and orientation variables are visualized on an excavator's side profile [177].

the machine parts as input data, and the quaternion data is discarded for further analysis. The input variables comprise the angular velocities of four IMUs (three axes per sensor unit), the local angular velocity of the boom (ω_2), the local angular velocity of the arm (ω_3), the local angular velocity of the bucket (ω_4), the pitch angle of the boom (θ_2), the pitch angle of the arm (θ_3), and the pitch angle of the bucket (θ_4).

4.2.2 Data Windowing

A data windowing scheme is employed in the presented techniques to recognize the tasks of an excavator. The position of a moving part is shown by a single data point at a

single instant of time, while a working cycle is made of sequential motions distributed over a period of time. For example, the loading operation occurs over a period of time, not instantly. In the data windowing scheme, time-series data is divided into numerous smaller and constant-sized pieces using a defined windowing function which is moved along all data. A window is a group of consecutive data points. Because most research studies presented in the literature review mostly concentrate on short-term motions or detailed activities of an excavator, the time window is chosen within a range of [1,5] s. Nonetheless, the tasks, that consist of several sub-tasks and take a much longer time compared to an individual sub-task, are the main targets in our proposed method. The cycle time of an excavator is mostly within the range of [10, 20] s based on the Komatsu® performance handbook [115]. Therefore, a sliding rectangular windowing function with five different window sizes (10, 12, 15, 18, and 20 s) and four overlapping configurations (0%, 25%, 50%, and 75% overlap between two consecutive windows) is employed in the presented technique.

4.2.3 Data Annotation

In the supervised learning algorithms, the data samples must be coupled with so-called ground truth information. To record operations, an external USB webcam with a frame rate of 20 fps was attached inside the cabin of the excavator. The webcam is connected to the MathWorks® Simulink model using the Image Acquisition Toolbox. Then, the dataset is manually labeled using the synced video. During the labeling process, if the activity changes, the user informs the program, and the label is changed. In the next step, the most frequent label in each window is selected as the representative label of that window. The recorded video is used only for the data annotation, and the classifiers employ only the motion information obtained from IMUs.

4.2.4 Feature Extraction

After segmenting the time series data into windows, feature extraction is performed before the model training to extract useful information from each labeled data window. Feature extraction aims to generate variables from raw measurements to maximize the amount of information related to the phenomenon that a classifier will be used to model. Ten time-domain statistical features (also called feature vectors), including (1) mean, (2) maximum, (3) minimum, (4) standard deviation, (5) mean absolute deviation, (6) root mean square, (7) peak-to-peak, (8) interquartile range, (9) skewness, and (10) kurtosis, are extracted from each window in the collected dataset.

4.2.5 Feature Selection

Since some features do not contain value-adding information, they cannot be beneficial for the classification problem and should be discarded for further calculations. In the feature

selection step, a subset of the initially extracted features that contain the most information regarding the classification problem is selected to minimize the feature space and provide a faster and more cost-effective algorithm. In the proposed method, three different subsets of features: (1) selected features using the ReliefF algorithm, (2) selected features using the minimum redundancy maximum relevance (MRMR) algorithm, and (3) selected features using the Chi-squared test, are utilized to train classification models.

4.2.6 Classification Models

Even though activity recognition techniques are presented using both supervised and unsupervised techniques, supervised learning methods demonstrate higher performance in activity recognition problems [17]. The characteristics and size of the dataset specify which classification model should be used. To recognize the tasks based on the given dataset, four classification models, including an SVM, a KNN, a NB, and a DT, are chosen based on the most commonly used supervised classifiers in construction resource activity identification algorithms in the literature review.

4.2.7 Performance Measures

The performance of classification models is evaluated using four standard metrics: *accuracy*, *precision*, *recall*, and $F_1 score$. The *accuracy* metric is calculated using Eq. (4.2):

$$accuracy = \frac{TP + TN}{TP + TN + FP + FN} \times 100\% \tag{4.2}$$

where TP, FP, FN, and TN indicate true positives, false positives, false negatives, and true negatives, respectively. The *accuracy* is a fundamental metric that provides an overall measure of correct predictions by calculating the ratio of correctly predicted instances to the total instances. Even though the *accuracy* metric is informative, it may not be sufficient, particularly in imbalanced datasets, where the class distribution is skewed. The cost of misclassification is analyzed using the *precision* and *recall* metrics. The *recall* metric is the percentage of true instances (i.e., true positive + false negative) that are accurately predicted as positive (i.e., true positive), whereas the *precision* metric is the percentage of predicted positive instances (i.e., true positive + false positive) that are truly positive (i.e., true positive). The *precision* and *recall* metrics are calculated using the following equations:

$$precision = \frac{TP}{TP + FP} \times 100\% \tag{4.3}$$

$$recall = \frac{TP}{TP + FN} \times 100\% \tag{4.4}$$

High *precision* and *recall* values are desirable, but it might be challenging to maximize both metrics for a classification model. The $F_1 score$, which is the harmonic mean of *precision* and *recall* metrics, is computed as follows:

$$F_1 score = 2 \times \frac{precision \times recall}{precision + recall} \tag{4.5}$$

The $F_1 score$ provides a balanced metric that considers both false positives and false negatives [150].

4.3 Results

In this section, the results of the presented method are demonstrated. Firstly, a small part of the dataset is used to show the difference between the skill and behavior of experienced and inexperienced operators. In the next step, the dataset is divided into train and test subsets, and the most informative features are obtained using the introduced feature selection techniques. Then, the supervised learning models are trained using selected features. The impacts of different time windows and overlapping configurations on the performance of the models are assessed. Moreover, k-fold cross-validation is performed to illustrate the robustness of the method.

4.3.1 Data Visualization

The pitch angles of the boom, arm, and bucket in two loading operations that were carried out by experienced and inexperienced operators are illustrated in Fig. 4.7. In order to show the difference between the way of using the excavator by experienced and inexperienced operators, the operating conditions of these operations, including swing angle and type of material are chosen the same. In these two operations, the type of used material is sand, and the swing angle is around 60°. As shown, the experienced operator can effectively control the boom, arm, and bucket of the excavator, and the pitch angles show cyclic behaviors. Nonetheless, the inexperienced operator cannot easily control the manipulator, and different types of movements can be seen.

4.3.2 Classification Model Training and Evaluation

The presented method has been implemented using Statistics and Machine Learning Toolbox in MathWorks® MATLAB R2021a on a laptop with a 1.8 GHz Intel Core i7 CPU and 16 GB of RAM running on a Windows 10 operating system. To assess machine learning techniques, different subsets of the dataset are employed for model training and testing. In this step, the dataset is divided into train and test datasets, with 50% of the data used for the training and 50% used for the test to show the robustness of the proposed method.

Firstly, the feature selection methods introduced in Section 4.2.5 are utilized to select the most important features from the training dataset. Then, after training the models, the performance measures are calculated using the test dataset. The *accuracy*, *precision*, *recall*, and $F_1 score$ of different classification models utilizing different feature selection algorithms with associated time windows and overlapping configurations are shown in Table 4.2. The time window and overlapping configurations indicate the highest *accuracy* for the corresponding classification model and feature selection algorithm. In addition, the best

performance (highest *accuracy*) is highlighted in bold for each classification model. The presented results demonstrate that the proposed data-driven algorithm can automatically recognize the tasks of an excavator with an *accuracy* of more than 99%. Moreover, it can be concluded that the IMU sensors, their placements on moving parts of the machine, and the motion variables are chosen correctly. The confusion matrices of the twelve classification algorithms, which are introduced in Table 4.2, are shown in Table 4.3. Two classification algorithms, including the SVM with MRMR feature selection algorithm, a time window of 20 *s*, and 0% overlapping, and the KNN classifier with MRMR feature selection algorithm, a time window of 20 *s*, and 50% overlapping, have the highest *accuracy* of 99.62%. Each matrix shows the number of correctly and incorrectly classified samples for four excavator activities: loading (L), trenching (T), grading (G), and idling (I). The rows represent the true classes (actual operations), and the columns represent the predicted classes, allowing for detailed analysis of classification performance. Diagonal values indicate correctly classified instances, while off-diagonal entries represent misclassifications. For example, under the ReliefF feature selection method, the SVM classifier correctly identified 217 loading operations, misclassifying 2 as trenching.

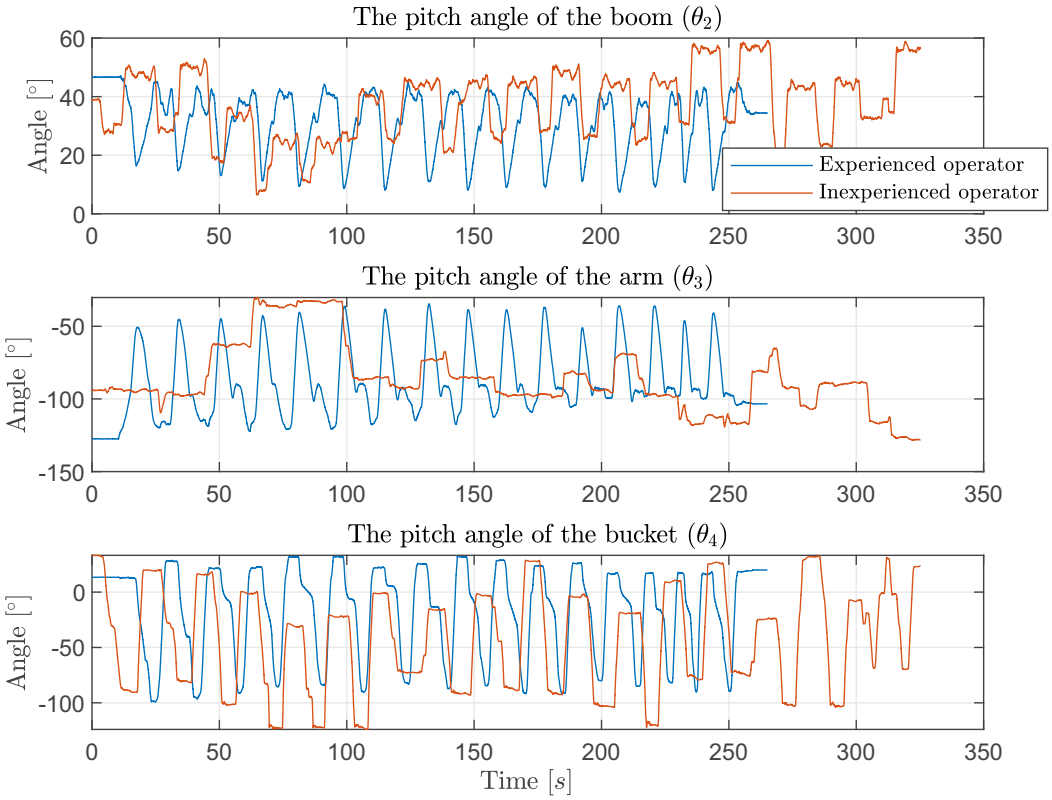

Figure 4.7: The pitch angles of the boom, arm, and bucket in two loading experiments operated by experienced and inexperienced operators [177].

4.3.3 Time Window Analysis

In this step, the effects of the time window on the accuracy of classification algorithms are evaluated. The classification accuracy of the SVM classifier with the MRMR feature selection algorithm using different configurations is presented in Fig. 4.8a. On average, the time windows of 20 *s* and 10 *s* represent the highest and lowest *accuracy* in different overlapping configurations, respectively. In Fig. 4.8b, the classification accuracy of the KNN classifier with the MRMR feature selection algorithm using different configurations is shown. On average, the time windows of 20 *s* and 10 *s* illustrate the highest and lowest *accuracy*, respectively. The classification accuracy of the Naive Bayes classifier with the ReliefF feature selection algorithm and the DT with the MRMR feature selection algorithm are presented in Fig. 4.8c and Fig. 4.8d, respectively. On average, the time windows of 20 *s* and 18 *s* illustrate higher performance compared to the time window of 10 *s*, 12 *s*, and 15 *s*. In Table 4.4, the average classification *accuracy* of different classification algorithms for different time windows is shown.

4.3.4 Overlapping Analysis

In this step, the effects of overlapping configuration on the classification algorithm are analyzed. Figure 4.9a shows the classification *accuracy* of the SVM classifier with the MRMR feature selection algorithm using different overlapping configurations. On average, the overlaps of 75% and 25% demonstrate the highest and lowest classification *accuracy*, respectively. The classification *accuracy* of the KNN classifier with the MRMR feature

Table 4.2: The performance measures for different classifiers with different configurations.

Classification models	Feature selection	Time window	Over-lapping	Metrics			
				accuracy	*precision*	*recall*	F_1*score*
SVM	ReliefF	18 *s*	50%	99.31%	99.33%	99.36%	99.34%
	MRMR	**20 *s***	**0%**	**99.62%**	**99.59%**	**99.50%**	**99.55%**
	Chi-squared	20 *s*	0%	99.24%	99.10%	99.50%	99.30%
KNN	ReliefF	20 *s*	50%	99.23%	99.18%	99.12%	99.15%
	MRMR	**20 *s***	**50%**	**99.62%**	**99.54%**	**99.62%**	**99.58%**
	Chi-squared	18 *s*	50%	99.31%	99.36%	99.28%	99.32%
NB	**ReliefF**	**20 *s***	**75%**	**98.93%**	**98.76%**	**98.91%**	**98.83%**
	MRMR	20 *s*	0%	98.86%	98.94%	98.75%	98.85%
	Chi-squared	20 *s*	50%	98.85%	98.93%	98.65%	98.79%
DT	ReliefF	20 *s*	75%	98.25%	98.01%	98.41%	98.21%
	MRMR	**15 *s***	**75%**	**98.71%**	**98.85%**	**98.59%**	**98.72%**
	Chi-squared	18 *s*	50%	98.11%	98.05%	98.37%	98.21%

selection algorithm is illustrated in Fig. 4.9b. On average, the overlaps of 75% and 0% represent the highest and lowest *accuracy*, respectively. The classification *accuracy* of the Naive Bayes classifier with the RelieF feature selection algorithm and the DT classifier with the MRMR feature selection algorithm are shown in Fig. 4.9c and Fig. 4.9d, respectively. On average, the overlaps of 75% and 50% demonstrate the highest classification *accuracy*. The average classification *accuracy* of different classification algorithms for different overlapping configurations is shown in Table 4.5.

Table 4.3: The confusion matrices of different classification algorithms. The time window and overlapping configurations of the classification algorithms are shown in Table 4.2.

Classification models		Feature selection algorithms											
		ReliefF				MRMR				Chi-squared			
	Pr[b] / Tr[a]	L	T	G	I	L	T	G	I	L	T	G	I
SVM	L[c]	217	2	0	0	100	0	0	0	98	1	1	0
	T[d]	1	131	0	0	0	60	0	0	0	60	0	0
	G[e]	0	1	111	0	0	1	49	0	0	0	50	0
	I[f]	0	0	0	118	0	0	0	54	0	0	0	54
KNN	L	196	0	0	0	196	0	1	0	218	0	0	1
	T	0	118	0	0	0	118	0	0	2	130	0	0
	G	0	3	97	0	0	1	99	0	0	0	111	1
	I	0	0	0	106	0	0	0	106	0	0	0	118
NB	L	385	2	1	0	99	1	0	0	196	1	0	0
	T	1	230	4	0	0	60	0	0	0	118	0	0
	G	0	1	197	0	1	1	48	0	2	1	97	0
	I	0	0	2	208	0	0	0	54	0	2	0	54
DT	L	378	2	8	0	521	3	1	0	213	5	1	0
	T	1	232	1	1	4	311	2	0	3	127	2	0
	G	1	4	193	0	6	2	260	0	0	0	112	0
	I	0	0	0	210	0	0	0	284	0	0	0	118

[a] *Tr* stands for true.
[b] *Pr* stands for prediction.
[c] L stands for loading operation.
[d] T stands for trenching operation.
[e] G stands for grading operation.
[f] I stands for idling.

Table 4.4: The average classification accuracy of different classification algorithms in different time windows (the best performance is highlighted in bold).

Classification models	Feature selection	Over-lapping [%]	Time window [s]				
			10	12	15	18	20
SVM	MRMR	[0, 25, 50, 75]	97.38%	97.90%	97.77%	98.62%	**99.18%**
KNN	MRMR	[0, 25, 50, 75]	96.35%	97.18%	97.82%	98.58%	**98.81%**
NB	ReliefF	[0, 25, 50, 75]	91.81%	93.60%	97.37%	**98.11%**	97.97%
DT	MRMR	[0, 25, 50, 75]	95.93%	95.49%	95.38%	**96.84%**	96.42%

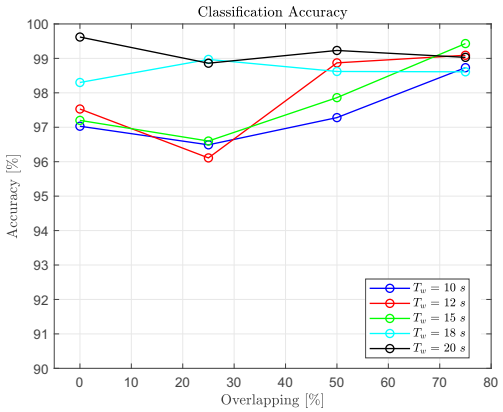

(a) The *accuracy* of the SVM classifier with the MRMR feature selection algorithm.

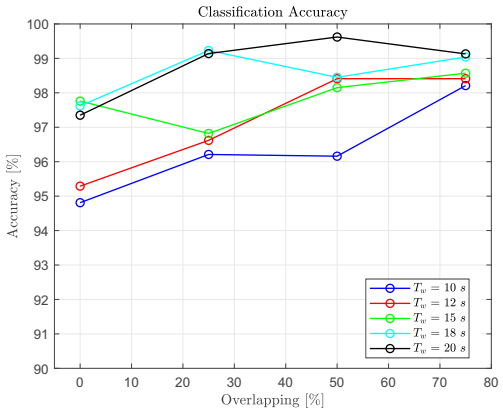

(b) The *accuracy* of the KNN classifier with the MRMR feature selection algorithm.

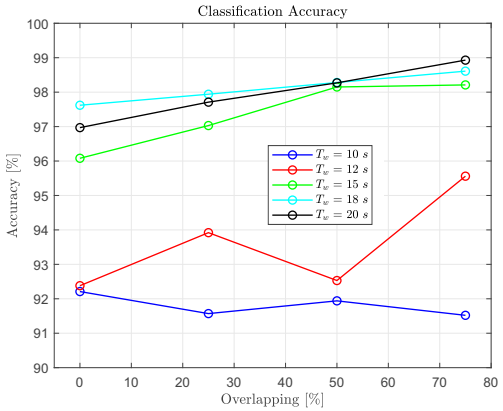

(c) The *accuracy* of the Naive Bayes classifier with the ReliefF feature selection algorithm.

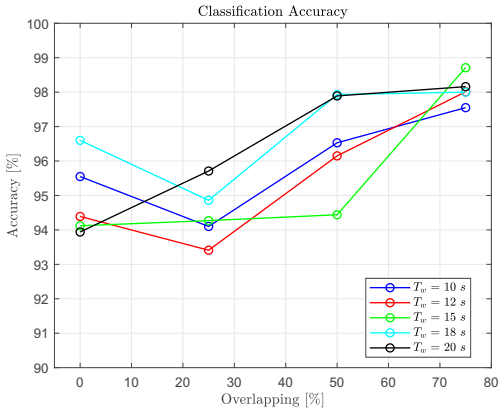

(d) The *accuracy* of the DT with the MRMR feature selection algorithm.

Figure 4.8: The analysis of the impacts of the time window on different classification algorithms and feature selection algorithms. The combinations of classification methods and feature selection techniques are chosen based on the highest *accuracy* in Table 4.2 [177].

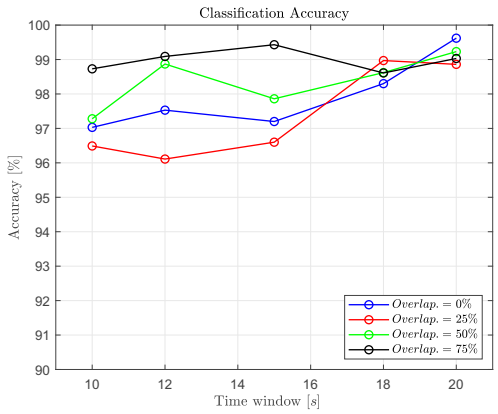

(a) The *accuracy* of the SVM classifier with the MRMR feature selection algorithm.

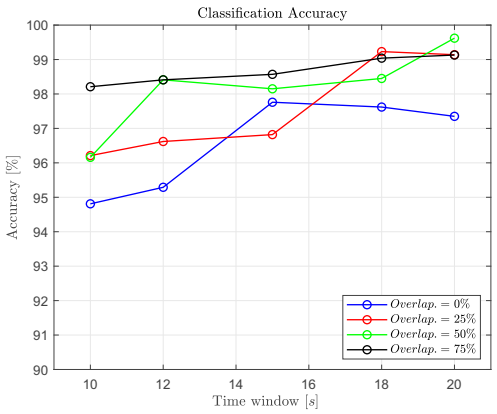

(b) The *accuracy* of the KNN classifier with the MRMR feature selection algorithm.

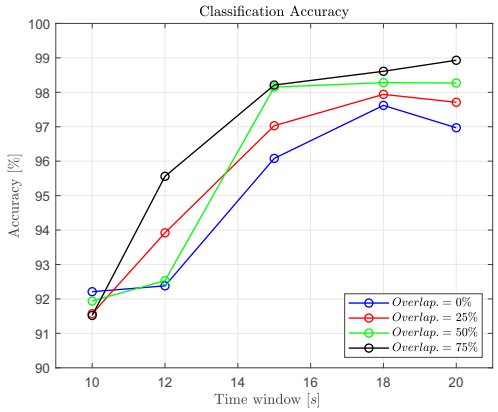

(c) The *accuracy* of the Naive Bayes classifier with the ReliefF feature selection algorithm.

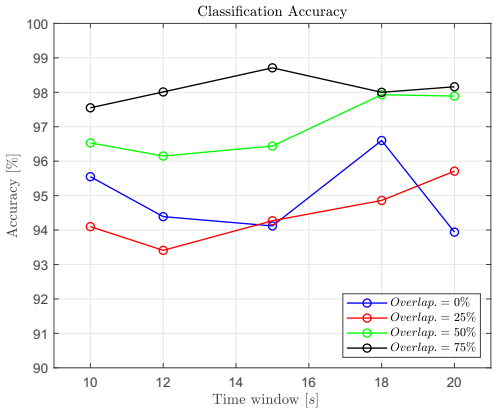

(d) The *accuracy* of the DT with the MRMR feature selection algorithm.

Figure 4.9: The analysis of the impacts of the overlapping configuration on different classification algorithms and feature selection algorithms [177].

Table 4.5: The average classification accuracy of different classification algorithms in different overlapping configurations (the best performance is highlighted in bold).

Classification models	Feature selection	Time window [s]	Overlapping [%]			
			0	25	50	75
SVM	MRMR	[10, 12, 15, 18, 20]	97.94%	97.40%	98.37%	**98.98%**
KNN	MRMR	[10, 12, 15, 18, 20]	96.57%	97.60%	98.16%	**98.67%**
NB	ReliefF	[10, 12, 15, 18, 20]	95.05%	95.63%	95.83%	**96.57%**
DT	MRMR	[10, 12, 15, 18, 20]	94.92%	94.47%	96.99%	**98.09%**

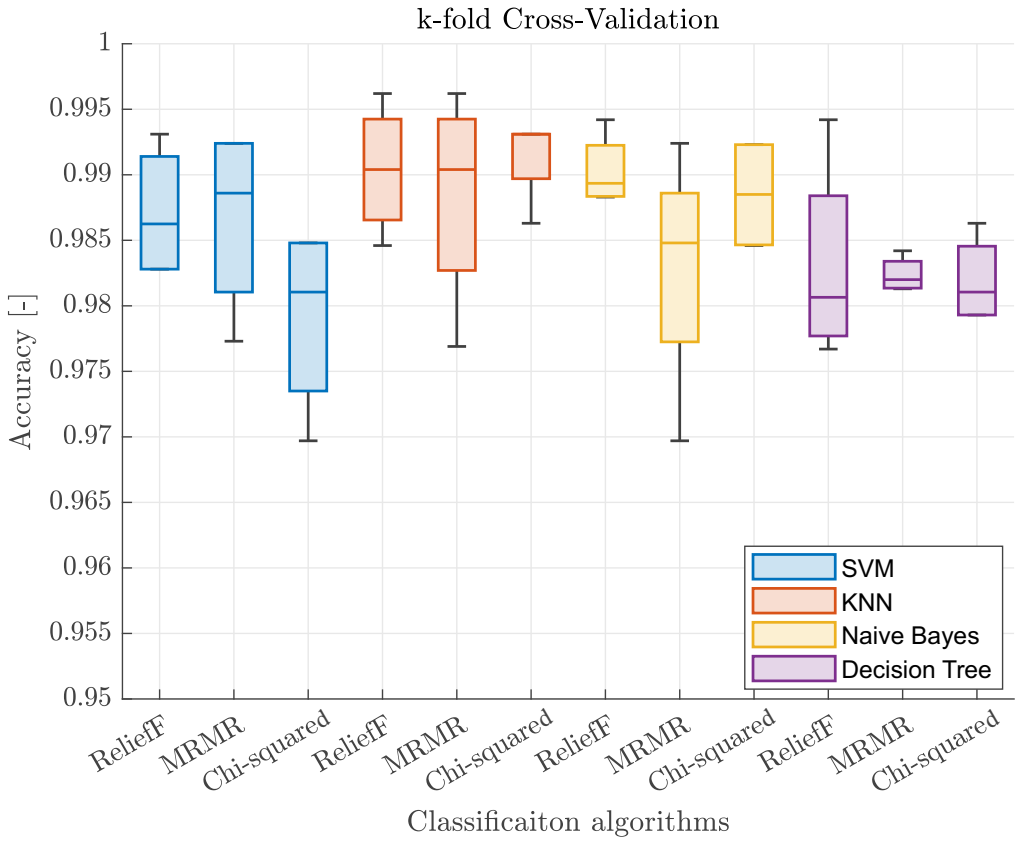

Figure 4.10: Analysis of k-fold cross-validation. Each box chart displays following information: median, lower and upper quartiles, and minimum and maximum values [177].

4.3.5 K-Fold Cross-Validation

The k-fold cross-validation is also conducted to show the robustness of the suggested data-driven method. Cross-validation is a widely used approach in applied machine learning to evaluate how well a model responds to unseen data. A dataset is randomly divided into k folds with the same size. One fold is considered the test dataset, while the other k-1 folds are used to train the model. This scheme is performed k times and the performance is calculated based on the average of the outcomes of the k test datasets. The results of k-fold cross-validation (k equals 4) for the classification algorithms presented in Table 4.2 are shown in Fig. 4.10. The obtained results are approximately equal to the outcomes presented in Table 4.2.

4.4 Conclusions

In this chapter, a data-driven method is designed to recognize the major tasks or duty cycles of an excavator, including loading, grading, trenching, and idling. Initially, a dataset

compromising orientation variables and angular velocities is gathered using a medium-rated excavator equipped with four IMUs mounted on moving parts of the machine, including bucket, arm, boom, and swing body. The tasks were performed by both an experienced and an inexperienced operator in different operating conditions, such as different types of material, swing angles, digging depths, and weather conditions. Four supervised learning methods, including an SVM, a KNN, a DT, and a Naive Bayes classifier, with three feature selection algorithms, including the ReliefF algorithm, MRMR algorithm, and Chi-squared test, are used to automatically recognize tasks. Moreover, the effects of different time windows and overlapping configurations on the classification accuracy are assessed. The comprehensive analyses show the resilience and adaptability of the method in real-world scenarios.

The proposed method can be a robust solution for automating excavator task recognition to improve productivity, operational efficiency, safety, and control. Task recognition and productivity monitoring systems can be integrated to show task-specific metrics, such as task-dependent productivity, completion times for specific tasks, and equipment utilization. Moreover, managers and operators are capable of monitoring progress and identifying areas for improvement. Identification of behavioral patterns that may pose safety risks allows for their incorporation into training programs, ensuring a proactive approach to safety. For example, the system can trigger an alert for a corrective action if an operator engages in unsafe task execution.

Task identification also plays a crucial role in improving collaboration between human workers and automated elements. Task identification data can enhance the accuracy of predictive maintenance for machinery by examining usage patterns, enabling proactive scheduling, and reducing downtime. Analyzing task identification data also helps in recognizing trends and patterns, providing valuable insights for making well-informed decisions regarding resource allocation, equipment upgrades, and process improvements.

In the future, it is proposed to broaden this methodology to encompass other types of HDMMs, including front-end loaders and compactors. The installation of motion sensors, such as IMUs on various moving parts of a machine will enable the tracking of different types of activities. For instance, IMUs can be attached to the bucket, boom, and cabin of front-end loaders to accurately recognize various activities.

The proposed method faces several limitations and challenges. Firstly, the dataset's duration is approximately 3 *h*, and both the test and training datasets are collected from the same machine. To enhance the dataset's effectiveness, it should be expanded by gathering data from a variety of excavators with different sizes. Additionally, it is important to test the resulting model with an operator whose data was not included in the training dataset, as operators utilize machines in different manners. Ensuring the algorithm's robustness requires accounting for various operational conditions during data collection, such as different swing angles, digging depths, material types, and weather conditions. Another drawback of the suggested approach is the labeling of the dataset, which is a crucial and time-consuming step in supervised learning techniques.

5 Excavator Productivity Estimation in Loading Operation

Cycle time and productivity estimation of an excavator in loading operations are highly important since they help in project planning and scheduling, cost management, resource allocation, performance monitoring, optimization opportunities, contractual obligations, and competitive advantage. In this chapter, a method is designed to automatically determine the cycle time and operational effectiveness of an excavator in the loading operation. The proposed method estimates the excavator's actual, theoretical, and relative cycle times in the loading operation. Firstly, a supervised learning method is suggested to identify the excavator's activities in the loading cycle using motion data obtained from four IMUs installed on different moving parts of the machine. Then, the actual cycle time is determined based on the sequence of detected activities. In the next step, the theoretical cycle time is automatically estimated based on the working conditions, such as swing angle and digging depth. Two approaches are proposed to automatically estimate the swing angle and digging depths. Afterward, the relative cycle time is calculated by dividing the theoretical cycle time by the actual cycle time. The relative cycle time can efficiently monitor the performance of an excavator in the loading operation.

5.1 Introduction

The loading operation stands as a pivotal task within the construction and mining industries. It entails utilizing the excavator's manipulator to pick up and move materials from one place to another, encompassing activities such as digging or gathering materials for site preparation or loading them onto trucks for transportation. Precise estimation of an excavator's productivity during loading operations offers guidance to contractors and project managers in effectively planning and budgeting projects. This can result in cost savings by ensuring efficient resource utilization and timely project completion. Additionally, productivity estimation aids in determining the appropriate size and type of excavator required for the project, thereby optimizing equipment usage and minimizing downtime. Also, deviations from expected productivity levels can be identified early, allowing for corrective actions to be taken to keep the project on track. In many cases, construction contracts have specific productivity requirements or performance metrics that contractors must meet. Accurate estimation of productivity helps ensure that contractual obligations are fulfilled, reducing the risk of penalties or disputes. Construction projects are often bid on by multiple contractors, and productivity estimates can be a significant factor in

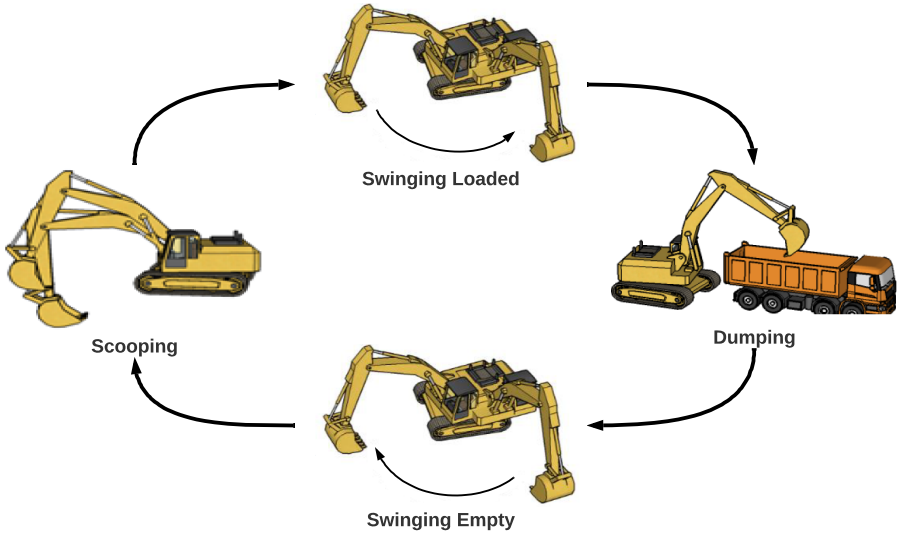

Figure 5.1: Excavator loading cycle [32].

winning bids. Contractors who can provide more accurate estimates and demonstrate higher productivity levels are more likely to secure contracts and gain a competitive edge in the industry [176].

The productivity of most cyclical types of machinery is commonly estimated by assessing both the quantity of material and the cycle time of the operation. For excavators, the loading operation encompasses four main steps: (1) scooping, (2) swinging loaded, (3) dumping, and (4) swinging empty. Figure 5.1 illustrates the schematic of an excavator during the loading task. The cycle time of an excavator in the loading operation depends on the various working conditions [16], including:

1. Excavator
    a) Size of the excavator
    b) Bucket capacity
2. Relative position between the excavator and material
    a) Digging depth
3. Relative position between the excavator and dumping position
    a) Swing angle
    b) Relative height
    c) Dumping condition
4. Site conditions
    a) Type of material
    b) Site congestion

5. Skills of the human operator
6. Weather conditions

In the scooping activity, digging depth and type of material are critical factors. Deeper excavation or harder materials inherently prolong the scooping sub-task [95]. Additionally, the swing angle is a crucial parameter affecting the swinging time, both when loaded and empty, thus impacting the overall cycle time. Furthermore, the size of the machine can significantly affect the swinging time since smaller machines can generally swing faster than larger machines. Moreover, the proficiency of the operator also plays an important role in the excavator's productivity [98].

As discussed in Chapter 2, multiple approaches have been presented to recognize the activities of an excavator in the loading operation. CV and audio-based methods have many challenges that have been completely described. Moreover, most presented sensor-based methods recognize the sub-tasks of an excavator without estimating the cycle time and productivity. The first critical challenge is the estimation of the actual cycle time of an excavator in the loading operation. Only two research studies have been presented that estimate the excavator's cycle time. In [91], the cycle time of an excavator is estimated with a low accuracy of 75.96%. This error can cause a significant error in productivity estimation. In [92], the cycle time is estimated with an accuracy of 91.83%. In 20% of cycles, the difference between the cycle time estimation and ground truth obtained from videos is more than 3 s, which can bring about a huge error in productivity estimation. Another significant challenge is the lack of a benchmark to evaluate the estimated cycle time. Since the working conditions can affect the cycle time, the actual cycle time cannot solely represent whether the machine is working at high or low performance. Therefore, a reference is needed to assess the actual cycle time. To determine the theoretical cycle time, the working conditions, such as swing angle and digging depth, should be estimated automatically during the operation.

Designing an automatic method for the cycle time estimation of an excavator in the loading operation is the primary purpose of this chapter. Initially, a machine learning-based method is proposed to identify the excavator's sub-tasks in the loading operation using IMUs' measurements mounted on different moving parts of the machine. Then, based on the sequence of identified activities, the cycle time is determined. The accuracy of estimated cycle time using the presented method is approximately equal to 97%, which shows higher accuracy compared to the proposed methods in the literature review. In the next step, to estimate the theoretical cycle time based on the operating conditions, the online estimation of the swing angle, digging depth, and information about the excavatability level of the material in the operation are highly required. Finally, the relative cycle time is estimated by dividing the theoretical cycle time by the actual cycle time. The performance of the machine is divided into three classes (satisfactory, average, and poor performance) based on the relative cycle time and simple thresholding.

Construction companies, contractors, and worksite managers can monitor and track the operational effectiveness of each machine during the loading operation using the actual cycle time and relative cycle time index. They have the capability to detect project challenges,

address issues promptly, refine planning and operational parameters, promote efficient resource utilization, enhance equipment usage, and accurately forecast future project budgets. Additionally, the suggested algorithm could serve as a feature for construction machinery manufacturers, facilitating automatic productivity monitoring. Researchers could utilize the relative cycle time index to contrast the effectiveness of autonomous solutions against human operators with varying levels of experience. Demonstrating that autonomous operations yield higher productivity than manual ones is a crucial and challenging task. Furthermore, training institutions can utilize the provided data as feedback to enhance the proficiency of human operators.

5.2 Methodology

Two important variables in defining productivity in the loading operation are the amount of transferred materials and cycle time. Excavator weighing systems have already been developed and are commercially available. Therefore, the development of a new weighing method is not considered necessary, as the area is already mature. Instead, attention is directed toward the estimation of cycle time, which remains relatively underdeveloped. Firstly, the activity recognition method for an excavator in the loading operation is introduced. The presented method is very similar to the task recognition method proposed in Chapter 4. Then, the actual cycle time is estimated based on the sequence of detected activities. In the next step, two methods are proposed to estimate the swing angle and digging depth. The proposed methods employ the recognized activities. The theoretical cycle time is calculated using the BML model [121], information about the excavatability level of the material, and estimated swing angle and digging depth. Finally, the relative cycle time is estimated by dividing the theoretical cycle time by the actual cycle time.

5.2.1 Activity Recognition

The initial step of the proposed method involves employing a supervised learning method to recognize the excavator's activities. The activities during the loading operation comprise (1) scooping, (2) swinging loaded, (3) dumping, (4) swinging empty, and (5) idling. Motion sensors are employed to capture data concerning various movements and actions performed by the excavator. Firstly, a dataset is collected to offline train classifiers. The crawler excavator used in the operations has been shown in Fig. 4.2. The collected dataset covers different working conditions, such as swing angles, digging depth, weather conditions, and types of material. The swing angles vary from 60° to 120°, and the digging depths increase up to 2 m. Two types of material, such as sand and gravel, are used in the operations. Two operators with different levels of competence performed the loading operations in different weather conditions during 18 months. In the experiments, operators were not given instructions on how to perform the tasks, reflecting real construction situations. This was done to make the algorithms more robust and reduce the impact of human behavior on the classification process.

Four IMUs have been mounted on the bucket, arm, boom, and swing body of the excavator to measure the orientation and angular velocities of the moving parts of the machine. The configuration of IMUs on the machine has been illustrated in Fig. 4.5. The duration of the dataset is around 75 *min*, which means that based on the sampling frequency f_s of 200 *Hz*, approximately 900,000 data points have been collected for each channel of the sensor. An inexperienced operator performed roughly 35% of the operations, and the rest of the dataset was collected by an experienced operator.

In Chapter 4, motion variables obtained from IMUs have been completely described. The joint angles and angular velocities of the machine parts are used as input data in the activity recognition algorithm. The local angular velocities and orientation variables have been demonstrated in Fig. 4.6. The input variables comprise the angular velocities of four IMUs (3 axes per sensor unit), the local angular velocity of the boom (ω_2), the local angular velocity of the arm (ω_3), the local angular velocity of the bucket (ω_4), the pitch angle of the boom (θ_2), the pitch angle of the arm (θ_3), and the pitch angle of the bucket (θ_4).

In the next step, data windowing approaches are implemented to recognize sub-tasks or short-term motions of an excavator. The overlapping configuration is chosen the same as the task recognition. Nonetheless, the length of time window should be chosen smaller compared to the task recognition method since a sub-task takes shorter than a task or a duty cycle. In the method, a sliding rectangular windowing function with four different window sizes (0.5, 1, 2, 3 *s*) and with four overlapping configurations (0%, 25%, 50%, and 75% overlap between two consecutive windows) are used. In the next step, the data annotation step is performed using the recorded videos to divide the dataset into five groups: (1) scooping, (2) swinging loaded, (3) dumping, (4) swinging empty, and (5) idling. The extracted features are completely the same as the task recognition algorithm introduced in Section 4.2.4. Next, four different subsets of features, including (1) all features, (2) selected features using the ReliefF algorithm, (3) selected features using the MRMR algorithm, and (4) selected features using the Chi-squared test, are used to train the classification models. Four supervised learning models, including a support vector machine (SVM), a k-nearest neighbor (KNN), a decision tree (DT), and a Naive Bayes (NB), are trained using the collected dataset. All performance metrics have been introduced in Section 4.2.7.

5.2.2 Actual Cycle Time Estimation

In the previous step, the processes of data collection and training of the classification models have been outlined. The trained models can subsequently be deployed online to identify the activities of excavators. In this step, the actual cycle time of an excavator is determined by analyzing the sequence of activities within a work cycle. Initially, the work cycle and cycle time should be defined. In [151], a definition for a work cycle of construction equipment is presented: “A work cycle is an activity performed in a finite time-frame by the equipment where all the states of the equipment are in the same range at the start and the end of the work cycle”. The loading task comprises four sub-tasks, including scooping, swinging loaded, dumping, and swinging empty. In [92], the cycle time is defined based on the time between two consecutive anti-clockwise rotations if

there is one clockwise rotation between them. In our proposed method, to mitigate the effects of classification errors and increase the robustness, the cycle time is defined based on the time between two consecutive scooping activities if there are at least one swinging loaded activity, one dumping activity, and one swinging empty activity between them. The accuracy definition, introduced in [92], is used to compare the results of the proposed method with the literature review. The real cycle time or ground truth information is obtained based on the recorded video by manually measuring the cycle times. The accuracy of the estimated cycle time is computed by the ratio of deviation between the estimated cycle time and real cycle time to the total real cycle time. The accuracy of cycle time estimation is formalized by Eq. (5.1):

$$accuracy_{CT} = 1 - \frac{\Sigma_{i=1}^{n} |\hat{t}_i - t_i|}{\Sigma_{i=1}^{n} t_i} \tag{5.1}$$

where $accuracy_{CT}$ denotes the accuracy of cycle time estimation $[-]$, $\hat{t}_i$ is the estimated cycle time $[s]$, t_i denotes the real cycle time $[s]$, and n is the total number of cycles.

5.2.3 Theoretical Cycle Time Estimation

As mentioned earlier, relying solely on the actual cycle time may not effectively depict the machine's performance, given the various factors that can impact the excavator's productivity. To assess or analyze the estimated actual cycle time, it is necessary to establish a theoretical cycle time. This theoretical cycle time serves as a standard or comparison point for evaluating the actual cycle time of an excavator. In this section, the theoretical cycle time of an excavator in the loading operation is computed, taking into account factors such as swing angle, digging depth, and the excavability level of the material. Construction equipment manufacturers, Komatsu® [115] and Caterpillar® [117] have developed two models aimed at calculating the theoretical cycle time and productivity of excavators. However, the proposed model by Caterpillar®, cannot be used in an automatic manner since it is a descriptive model requiring human input. Additionally, an industry guideline introduced an alternative model [121]. The BML guideline was developed collaboratively by the Central Association of German Construction Companies (Zentralverband des Deutschen Baugewerbes) and the Federation of the German Construction Industry (Hauptverband der Deutschen Bauindustrie). In this study, the BML approach is adopted because it is more conservative and offers a theoretical cycle time that aligns more closely with reality, unlike the Komatsu model, which tends to be more optimistic [178].

The BML model formalizes the cycle time of an excavator in the loading operation through Eq. (5.2):

$$t_{theoretical} = t_{initial} \times \frac{1}{f_{swing}} \times \frac{1}{f_{depth}} \tag{5.2}$$

where $t_{theoretical}$ denotes the theoretical cycle time $[s]$, $t_{initial}$ shows the initial guess of theoretical cycle time $[s]$, f_{swing} is the swing angle factor $[-]$, and f_{depth} is the digging depth factor $[-]$.

Within the BML model, the initial guess of the theoretical cycle time $t_{initial}$ is determined by considering the heaped bucket capacity alongside the soil excavability categories outlined in Table 5.1. The initial estimate of the theoretical cycle time for materials characterized by high excavability, such as sand and gravel is formalized by Eq. (5.3):

$$\frac{t_{initial}}{s} = -0.50 \times \frac{V_{CECE}^2}{m^{3^2}} + 4.19 \times \frac{V_{CECE}}{m^3} + 13.13 \tag{5.3}$$

and the calculation for materials with medium and low excavability, such as hard compacted clay, is determined by Eq. (5.4):

$$\frac{t_{initial}}{s} = -0.07 \times \frac{V_{CECE}^2}{m^{3^2}} + 3.30 \times \frac{V_{CECE}}{m^3} + 15.52 \tag{5.4}$$

where V_{CECE} is heaped bucket capacity according to the standard of CECE. The BML model does not provide an estimation for the theoretical cycle time of materials categorized as having very low excavability [178], [152].

Next, the initial estimation of the theoretical cycle time is adjusted based on two factors related to the swing angle and digging depth of the operation. In the loading process, the swing angle refers to the horizontal angle between scooping and dumping positions. The BML method approximates the swing angle factor f_{swing} using Eq. (5.5):

$$f_{swing} \approx 1.754 \times \theta_{sw}^{-0.1258}; \quad \theta_{sw} \in [45°, 180°] \tag{5.5}$$

Table 5.1: Material categories in the BML model.

Excavability	Material
High	Loose or even compressed sand, gravel sand mix, gravel with <15% (of mass) binding components and <30% stones of 63–100 *mm* diameter, clay with organic components, soft, cuttable such as sea chalk, rotting mud; piles with <30% stones of <200 *mm* diameter such as rough gravel
Medium	Ground with solid components of mixed size (15–40% binding components), soft, such as meadow loam or loam with <30% stones of 63–100 *mm* diameter; clay with >40% binding components, soft (various examples of clay or loam types)
Low	Ground with solid components of mixed size (>30% stones of 63–100 *mm* diameter), stiff; piles with 30–60% stones of <200 *mm* diameter or 30% stones of 0.01–0.1 m^3, such as gravel at the bottom of cliffs; clay with >30% stones of 63–100 *mm* diameter, stiff and glutinous
Very low	Loosely packed stones that are brittle; rock that was blasted or ripped apart (edge lengths <300 *mm*); clay with very high dry toughness and a lot of stone inclusions

where θ_{sw} indicates the swing angle [°] of the operation. Variations of swing angle within the range of [45°,180°] affect ±10% variations in the cycle time.

In the BML method, the digging depth factor f_{depth} for soil types categorized as low and very low excavability is roughly determined using Eq. (5.6):

$$f_{depth} \approx h_d^{-0.1039}; \quad h_d \geq 1\ m, \tag{5.6}$$

and for materials classified as high and medium excavability, the digging depth factor f_{depth} is approximately evaluated using Eq. (5.7):

$$f_{depth} \approx h_d^{-0.1164}; \quad h_d \geq 1\ m \tag{5.7}$$

where h_d shows the digging depth $[m]$ of the operation. When the digging depth h_d is less than 1 m, the digging depth factor f_{depth} is assumed to be one. As the digging depth increases, it only negatively affects the cycle time, leading to an increase of up to 20% in extreme cases (i.e., for h_d greater than 8 m).

To automatically estimate the theoretical cycle time of an excavator during the loading operation, it's essential to have real-time automatic estimations of the swing angle and digging depth at the end of each cycle. The following sections describe how the swing angle and digging depth are estimated based on the identified excavator activities.

5.2.3.1 Swing Angle Estimation

Swing angle is a vital operational parameter that significantly affects the cycle time and productivity of an excavator in the loading operation. In [176], a method is presented

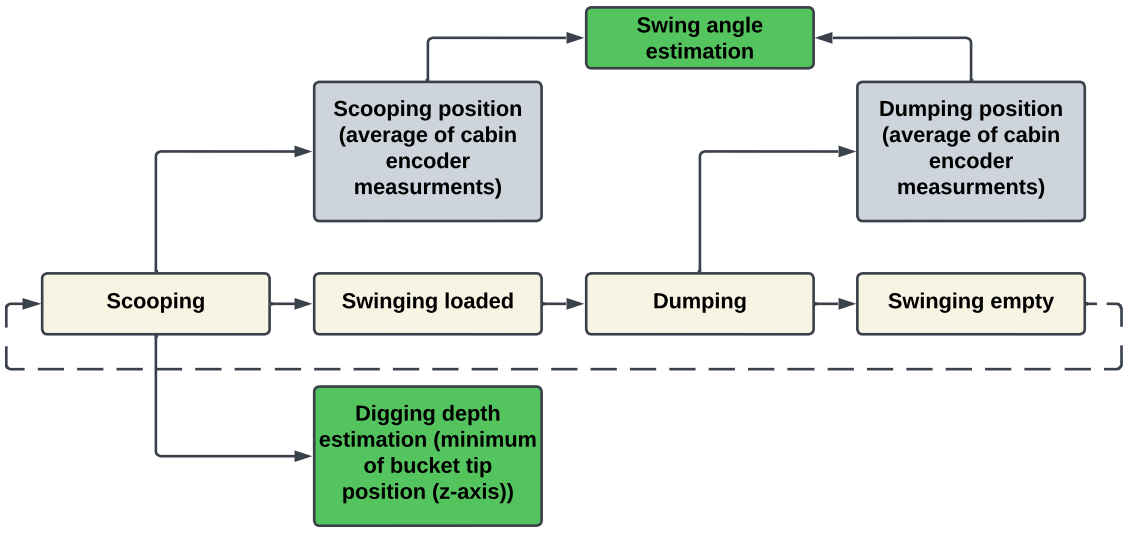

Figure 5.2: Flowchart of methods for swing angle and digging depth estimations based on activity recognition algorithm [174].

that employs Otsu's technique, known for achieving optimal thresholding by maximizing variance between classes. In the section, an algorithm is introduced to estimate the swing angle by utilizing cabin encoder measurements and the excavator activity recognition algorithm. All excavators are equipped with cabin encoders, which provide measurements specifying the horizontal angle of the excavator cabin during operation. The swing angle is defined as the absolute deviation of horizontal angles between the scooping and dumping positions. To determine the horizontal angles of the scooping and dumping positions in the loading operation, the scooping and dumping activities need to be detected. The start and end of each cycle are identified using the method proposed in Section 5.2.2. In each cycle, four sets of activities occur (scooping, swinging loaded, dumping, and swinging empty). The average of the horizontal angles (cabin encoder measurements) during the identified scooping and dumping activities are considered as the scooping and dumping positions, respectively. Figure 5.2 illustrates the flowchart of the method for swing angle estimation.

5.2.3.2 Digging Depth Estimation

The digging depth is another crucial factor to consider in estimating the theoretical cycle time. As the digging position becomes deeper, it requires more time to complete the scooping task. In this study, digging depth is estimated based on both bucket position estimation and the excavator activity recognition algorithm. As previously mentioned, each cycle comprises four activities. The digging depth is determined as the minimum of the vertical axes of the bucket position estimation during the identified scooping activities. The scooping activity is recognized using the trained classification model, and the bucket position is estimated using IMUs and the forward kinematics of the machine. The flowchart of the method for estimating digging depth is depicted in Fig. 5.2.

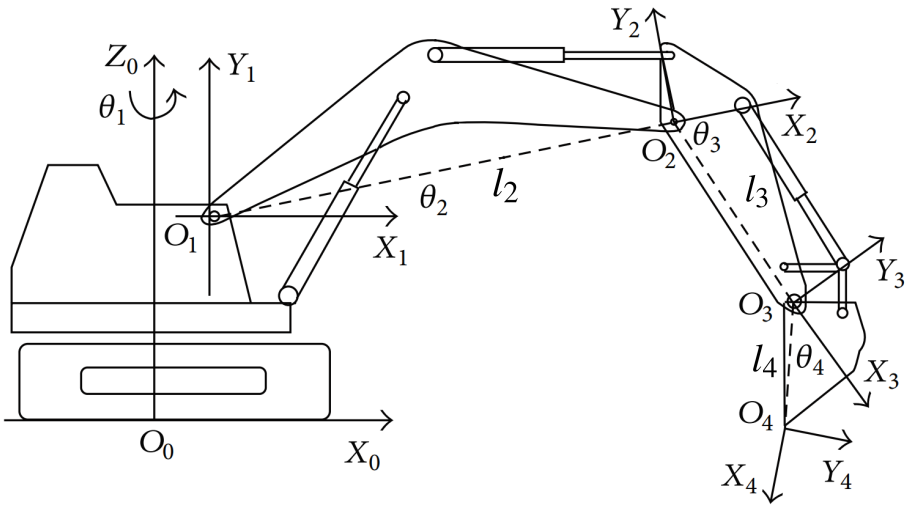

Figure 5.3: Excavator coordinate systems in Denavit-Hartenberg convention [153].

The movement of the excavator's manipulator is described using kinematic equations, excluding the consideration of driving forces and torques. An excavator can be modeled as an open-loop articulated chain comprising a boom, arm, and bucket. In an excavator, a sequence of rigid bodies, referred to as links, are interconnected by revolute joints [154]. Figure 5.3 displays the forward kinematics of an excavator.

Each link has its own Cartesian coordinate system, which moves with the link itself. The local coordinate system for each link is constructed based on the Denavit-Hartenberg (D-H) convention (refer to Table 5.2), wherein the z-axis aligns with the direction of rotation of the revolute joint, and the x-axis aligns with the adjacent joint within the same link. Hence, the direction of the y-axis is determined using the right-hand rule [153]. The

Table 5.2: Denavit-Hartenberg parameters [153].

Link_i	d_i	a_i	α_i	θ_i
1	0	l_1	90°	θ_1
2	0	l_2	0°	θ_2
3	0	l_3	0°	θ_3
4	0	l_4	0°	θ_4

angle $\theta_i,\ i \in \{1, 2, 3, 4\}$ are calculated using quaternion measurements, and the conversion formula (Eq. (4.1)). In addition, the length $l_i,\ i \in \{1, 2, 3, 4\}$ are obtained from machine specifications. Forward kinematic equations are employed to determine the positions of the manipulator links based on the joint angles and lengths of the links. A transformation matrix between two consecutive coordinate systems (from $(i+1)_{th}$ to i_{th}) on a link can be expressed using the Denavit-Hartenberg convention:

$$
{}^{i}T_{i+1} = \begin{bmatrix} \cos\theta_{i+1} & -\cos\alpha_{i+1}\sin\theta_{i+1} & \sin\alpha_{i+1}\sin\theta_{i+1} & a_{i+1}\cos\theta_{i+1} \\ \sin\theta_{i+1} & \cos\alpha_{i+1}\cos\theta_{i+1} & -\sin\alpha_{i+1}\sin\theta_{i+1} & a_{i+1}\sin\theta_{i+1} \\ 0 & \sin\alpha_{i+1} & \cos\alpha_{i+1} & d_{i+1} \\ 0 & 0 & 0 & 1 \end{bmatrix} \tag{5.8}
$$

where ${}^{i}T_{i+1}$ denotes the transformation matrix from $(i+1)_{th}$ coordinate system to i_{th} coordinate system, θ_{i+1} is the rotation angle about z_i-axis, α_{i+1} is the rotation angle of z_i-axis about x_{i+1}-axis, d_{i+1} is the offset along the z_i-axis, and a_{i+1} is the length of the link [153]. Any point in any local coordinate system can be represented in the origin coordinate system using the coordinate transformation matrix as follows:

$$
{}^{0}P = {}^{0}T_n\,{}^{n}P = {}^{0}T_1\,{}^{1}T_2\,{}^{2}T_3 \ldots {}^{n-1}T_n\,{}^{n}P, \tag{5.9}
$$

where ${}^{0}P$ represents the position vector in the origin coordinate system, ${}^{0}T_n$ denotes the transformation matrix from the n_{th} coordinate system to the origin coordinate system, and ${}^{n}P$ indicates the position vector in the n_{th} coordinate system [153].

5.2.4 Relative Cycle Time Estimation

Finally, the relative cycle time is derived by comparing the actual cycle time to the theoretical cycle time:

$$t_{relative} = \frac{t_{theoretical}}{t_{actual}} \tag{5.10}$$

where $t_{relative}$ represents the relative cycle time $[-]$, $t_{theoretical}$ denotes the theoretical cycle time $[s]$, which is computed according to the model introduced in Section 5.2.3, and t_{actual} shows the actual cycle time $[s]$, estimated using the method outlined in Section 5.2.2. A higher relative cycle time indicates better performance. This metric can be utilized by worksite managers to assess both excavator and operation performance, enhancing project planning and scheduling. Additionally, the relative cycle time can serve as feedback to evaluate the proficiency and skill level of human operators.

5.3 Implementation and Case Studies

In this section, the presented method is evaluated using the dataset. Initially, classification models are trained offline, and then, the method is applied and tested through two case studies presented in Section 5.3.2. These case studies investigate the accuracy of cycle time estimation, wherein swing angle, digging depth, theoretical, and relative cycle time are all assessed. Finally, using the obtained relative cycle time index, the performance of experienced and inexperienced operators is compared. The designed method has been implemented using Statistics and Machine Learning Toolbox in MathWorks® MATLAB R2021a on a laptop with a 1.8 GHz Intel Core i7 CPU and 16 GB of RAM running on a Windows 10 operating system.

5.3.1 Classification Model Training and Evaluation

Initially, the accuracy of classifiers with different feature selection algorithms is examined. Additionally, it assesses the effects of different window sizes and overlapping configurations

Table 5.3: Accuracy of different classifiers and feature selection algorithms: The numbers represent "the best accuracy (time window, overlapping configuration)".

Feature selection algorithms	Classification models			
	SVM	KNN	Naive Bayes	Decision Tree
All features	0.9203(3, 75%)	0.9173(2, 75%)	0.8915(2, 25%)	0.9054(1, 75%)
ReliefF	0.9438(2, 75%)	0.9433(2, 50%)	0.9129(2, 75%)	0.9443(1, 75%)
MRMR	**0.9523(2, 75%)**	0.9356(2, 75%)	0.9274(2, 25%)	0.9371(2, 75%)
Chi-squared	0.9041(3, 0%)	0.9273(3, 0%)	0.7727(3, 0%)	0.9068(3, 0%)

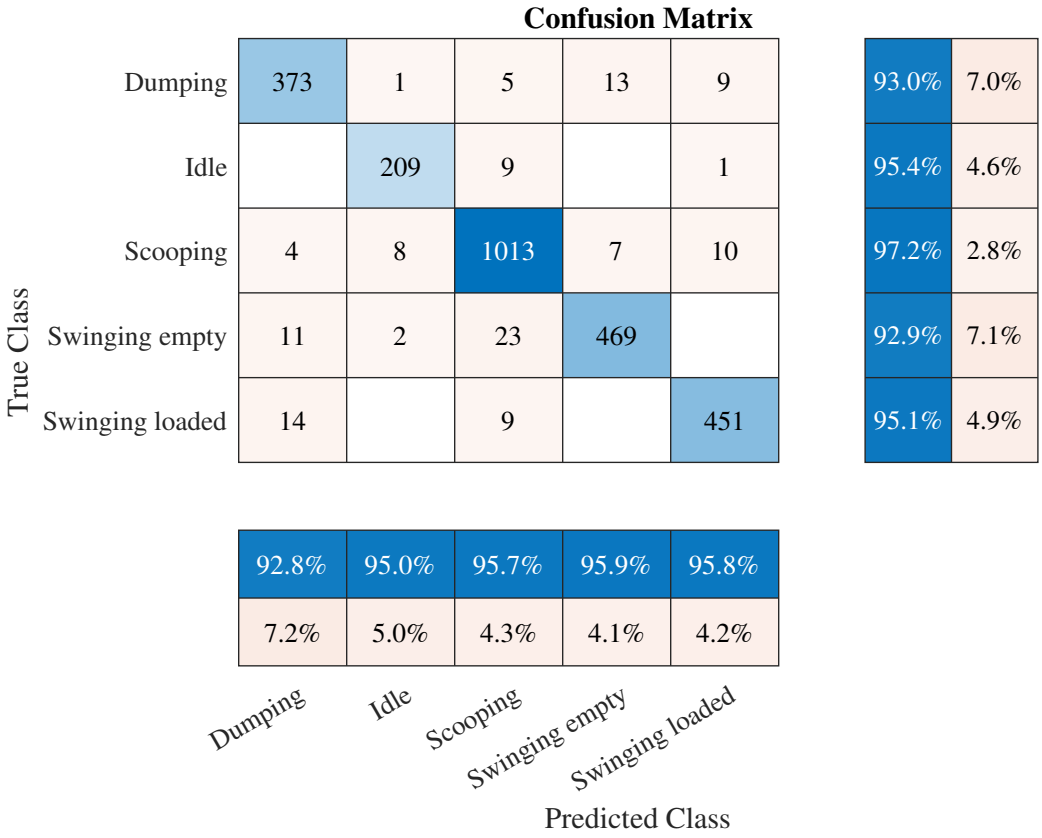

Figure 5.4: Confusion matrix of SVM classifier and MRMR feature selection algorithm with 2 *s* time window and 75% overlapping [174].

Table 5.4: Accuracy of the SVM classifier and MRMR feature selection algorithm with different time windows and overlapping configurations.

Overlapping	Time window [*s*]			
	0.5	1	2	3
0%	0.9322	0.9397	0.9366	0.9136
25%	0.9327	0.9485	0.9433	0.9334
50%	0.9418	0.9404	0.9516	0.9385
75%	0.9189	0.9422	**0.9523**	0.9501

on classification accuracy. When comparing multiple data-driven modeling techniques, different subsets of the dataset must be utilized for model training and testing. To achieve this, the entire dataset was divided into training and testing subsets, with 70% of the data allocated for training and the remaining 30% for testing purposes. The accuracy of different classifiers and feature selection algorithms with the associated time window and overlapping configurations is presented in Table 5.3. The SVM classifier with the MRMR feature selection algorithm shows the highest accuracy. The MRMR feature selection algorithm not only demonstrates superior accuracy compared to the ReliefF algorithm but

also proves to be more cost-effective and entails lower computational complexity than ReliefF. Table 5.4 displays the accuracy of the SVM classifier and MRMR feature selection algorithm across various time windows and overlapping configurations. The highest accuracy is attained when the time window is set to 2 *s*, with an overlapping rate of 75%. Figure 5.4 depicts the confusion matrix of the proposed supervised learning algorithm using the optimal configurations. The central matrix displays the number of correctly and incorrectly classified samples for each excavator activity. The diagonal elements represent correct classifications, while the off-diagonal elements show misclassifications between activity classes. To enhance readability, a color gradient has been applied: darker blue cells indicate a higher number of correctly classified instances, while lighter shades represent fewer correct classifications. The right-hand column shows per-class recall (true positive rate) and false negative rate, where darker blue indicates higher recall. The bottom row shows per-class precision and false positive rate, using the same blue gradient to highlight high precision.

Additionally, k-fold cross-validation (k equals 4) is conducted to demonstrate the robustness of the proposed classification algorithm. The outcomes of k-fold cross-validation for

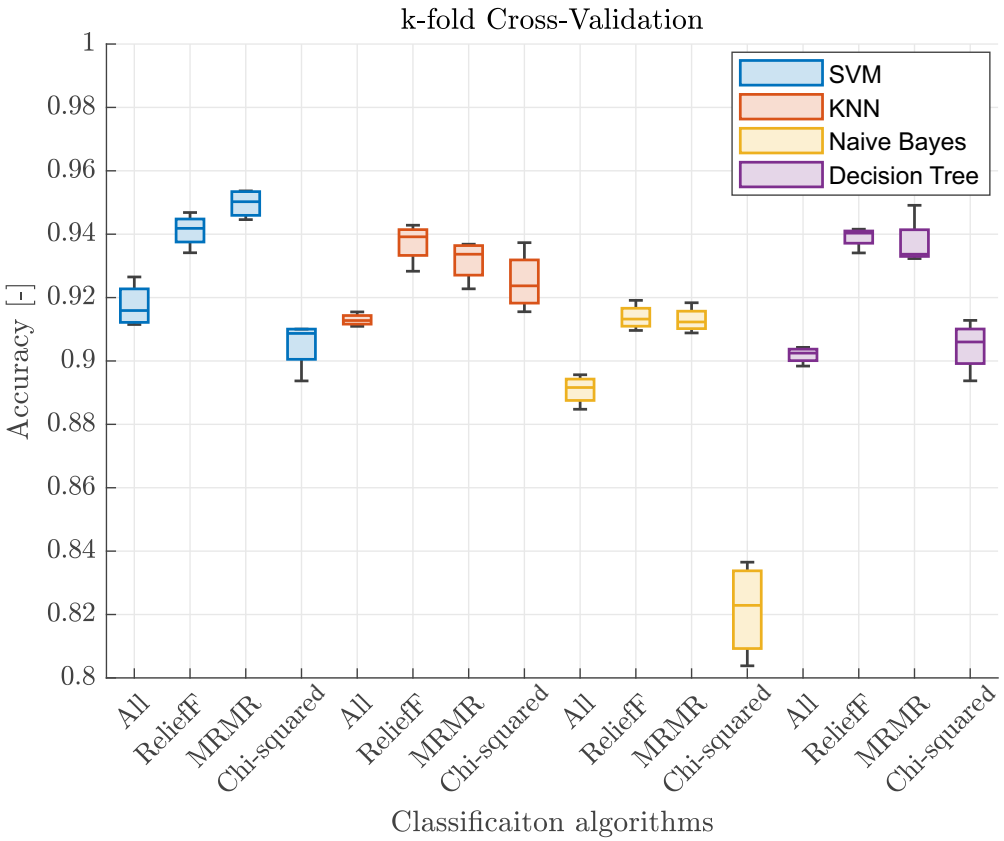

Figure 5.5: Analysis of k-fold cross-validation. Each box chart displays the following information: median, lower and upper quartiles, and minimum and maximum values [174].

different classification models and feature selection algorithms are illustrated in Fig. 5.5. The accuracy of the classification algorithms aligns closely with the results presented in Table 5.3.

In the next sections, the trained classification model is employed to online recognize machine activities. Then, the actual cycle time, swing angle, and digging depth are computed based on the detected activities.

5.3.2 Case Studies

The performance of the presented method is demonstrated through implementation in two case studies. Each case study comprises two experiments conducted by experienced and inexperienced operators, with the digging depth being nearly zero due to the material being on the ground surface. In the first case study, the swing angle is approximately 120°, with sand as the material type, while in the second case study, the swing angle is around 60°, with gravel as the material type. Each experiment lasts approximately 5 *min*, resulting in the collection of roughly 60,000 data points per sensor channel at the data sampling frequency f_s of 200 *Hz*. Further details are provided in Table 5.5. Additionally, the operation is recorded using a camera to obtain ground truth for the cycle time.

Table 5.5: Specifications of case studies.

Case Study	Operator	Digging Depth	Swing Angle [°]	Material	Duration [*min*]
Inexp. 1[a]	Inexperienced	Ground surface	120°	Sand	5.3
Exp. 1[b]	Experienced	Ground surface	120°	Sand	5.2
Inexp. 2	Inexperienced	Ground surface	60°	Gravel	5.4
Exp. 2	Experienced	Ground surface	60°	Gravel	4.4

[a] Inexp. stands for an inexperienced operator.
[b] Exp. stands for an experienced operator.

5.3.3 Actual Cycle Time Estimation

Figure 5.6, displays the cycle time estimations for the first case study. As illustrated, the cycle time in case study Exp. 1 which is conducted by the experienced operator is lower than in case study Inexp. 1. It can have a notable influence on the overall productivity of the operation. The cycle time estimations in the second case study are depicted in Fig. 5.7. As anticipated, the cycle time of case study Inexp. 2 is higher than the estimated cycle time in case study Exp. 2. The presented method demonstrates its effectiveness in accurately estimating the cycle time, achieving an error of less than 1.5 *s* in both case studies. The accuracy of cycle time estimations, as defined by Eq. (5.1), is shown in Table 5.6. In the case studies, only 5 out of 66 cycles (approximately 7.5%) exhibit absolute error exceeding 1 *s*.

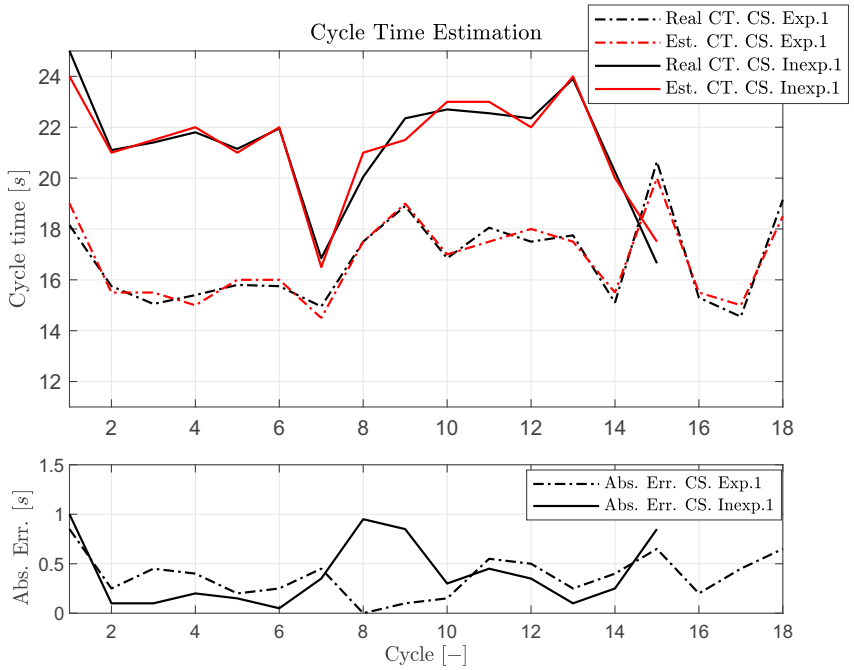

Figure 5.6: Cycle time estimations in the first case study ($\theta_{sw} \approx 120°$) [174].

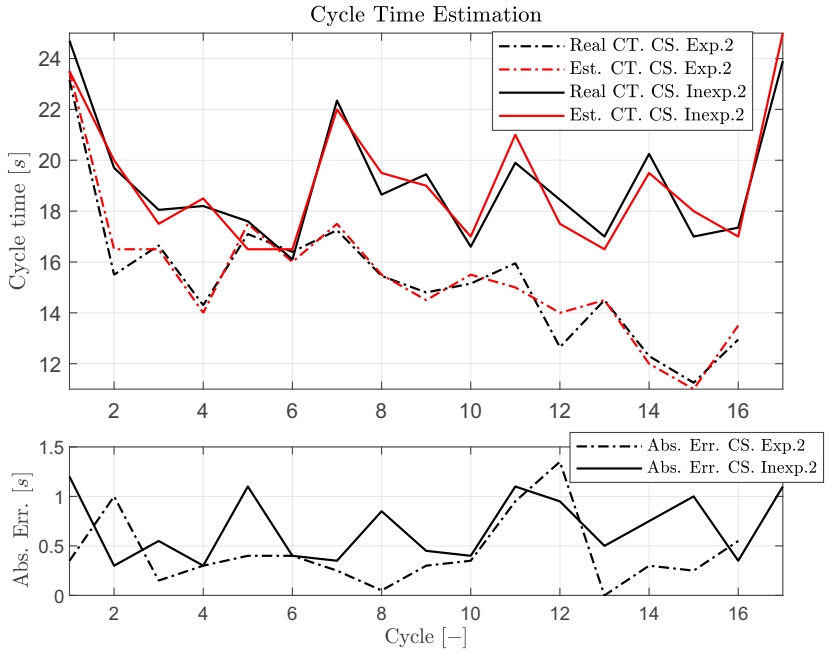

Figure 5.7: Cycle time estimations in the second case study ($\theta_{sw} \approx 60°$) [174].

Table 5.6: Accuracy of cycle time estimations based on Eq. (5.1) for each case study.

	Case study			
	Inexp. 1	Exp. 1	Inexp. 2	Exp. 2
$accuracy_{CT}$	0.9811	0.9777	0.9642	0.9717

5.3.4 Swing Angle Estimation

To compute the theoretical cycle time, estimations of the swing angle and digging depth are needed. In this section, the swing angle is estimated utilizing the method described in Section 5.2.3.1. Figure 5.8 presents the estimations of the swing angle for the first case study. In this particular study, operators aimed to maintain the horizontal angle between the scooping and dumping positions at approximately 120°. Notably, the experienced

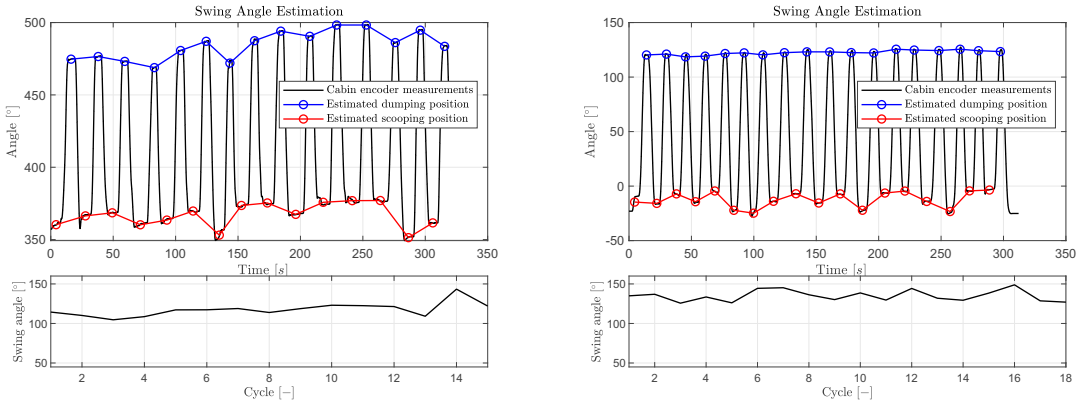

(a) Case study Inexp.1

(b) Case study Exp.1

Figure 5.8: Swing angle estimations in the first case study ($\theta_{sw} \approx 120°$) [174].

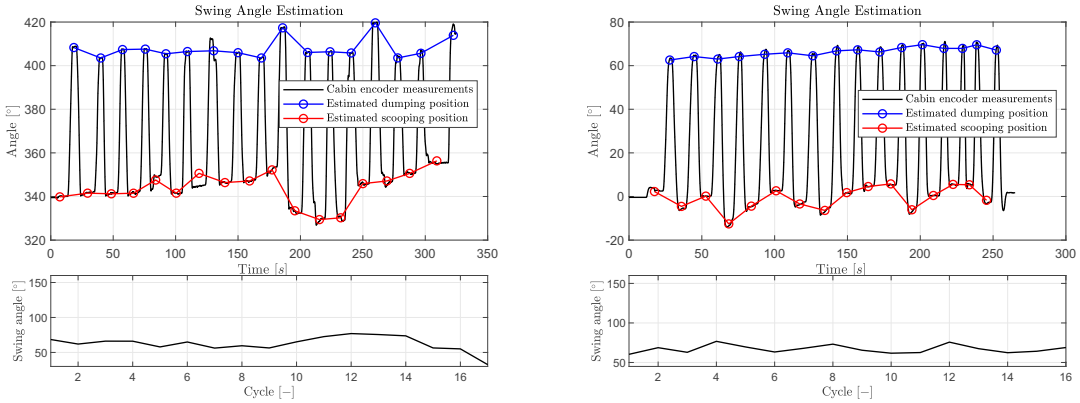

(a) Case study Inexp.2

(b) Case study Exp.2

Figure 5.9: Swing angle estimations in the second case study ($\theta_{sw} \approx 60°$) [174].

operator demonstrates adept control over the swing motion of the cabin, resulting in minimal variations. Figure 5.9 displays the estimations of the swing angle for the second case study. In this scenario, operators aim to maintain the swing angle around 60°. The proposed method accurately identifies the scooping and dumping activities in both scenarios, effectively estimating the swing angle.

5.3.5 Digging Depth Estimation

In this section, the digging depth of the operation is estimated utilizing the technique outlined in Section 5.2.3.2. Figure 5.10 shows the digging depth estimations for the first case study. The estimations are approximately zero, consistent with the fact that the pile of material is situated on the ground surface. The digging depth estimation for the second case study is depicted in Fig. 5.11. The method accurately estimates the digging depth

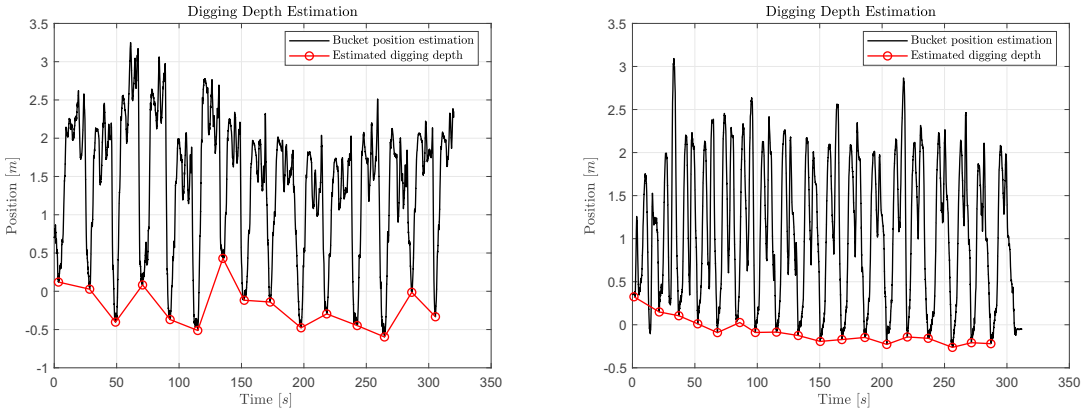

(a) Case study Inexp.1 (b) Case study Exp.1

Figure 5.10: Digging depth estimations in the first case study ($\theta_{sw} \approx 120°$) [174].

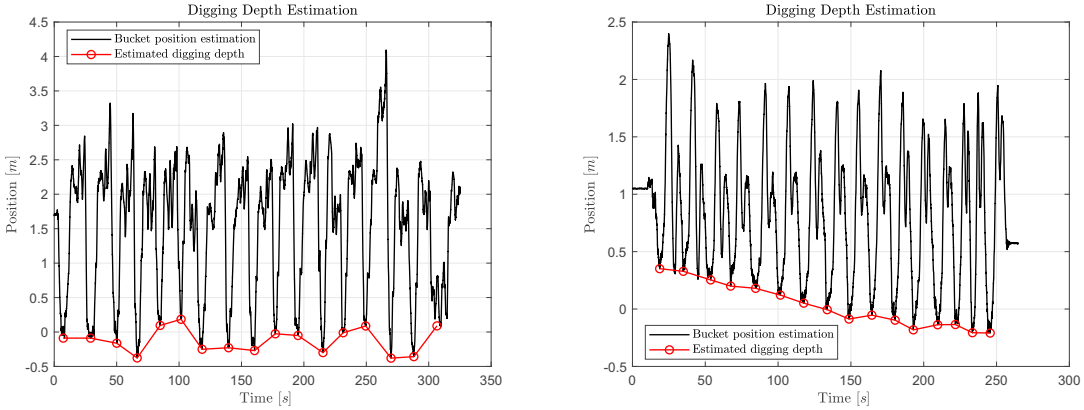

(a) Case study Inexp.2 (b) Case study Exp.2

Figure 5.11: Digging depth estimations in the second case study ($\theta_{sw} \approx 60°$) [174].

during the operations. As anticipated, the experienced operator demonstrates greater control over the bucket position, resulting in fewer variations in bucket movements. Conversely, there are numerous fluctuations in bucket movements when the inexperienced operator performs the task. Despite the significant difference in human operators' skills, the proposed supervised learning method effectively manages this challenge.

5.3.6 Relative Cycle Time Estimation

In this section, the theoretical cycle time is initially computed using the estimated swing angle, digging depth, and the type of material. Subsequently, the relative cycle time is determined based on the estimated and theoretical cycle times.

The theoretical, estimated, and relative cycle times for the first case study are illustrated in Fig. 5.12. In the first case study, the theoretical cycle times for both experiments are nearly identical due to similar operating conditions. In this figure, areas above 0.8 are colored green, indicating satisfactory performance, while areas between 0.6 and 0.8 are colored yellow, representing average performance. Conversely, regions below 0.6 are colored red, indicating poor performance. The colors have been inspired by traffic lights to be easily understandable for everybody. In the case study Inexp. 1, operated by the inexperienced operator, most of the cycles exhibit relative cycle times in the yellow area, indicating average performance. Conversely, in Exp. 1, operated by the experienced operator, nearly all cycles show relative cycle times exceeding 0.8, representing satisfactory performance. Figure 5.13 illustrates the relative, estimated, and theoretical cycle times for the second

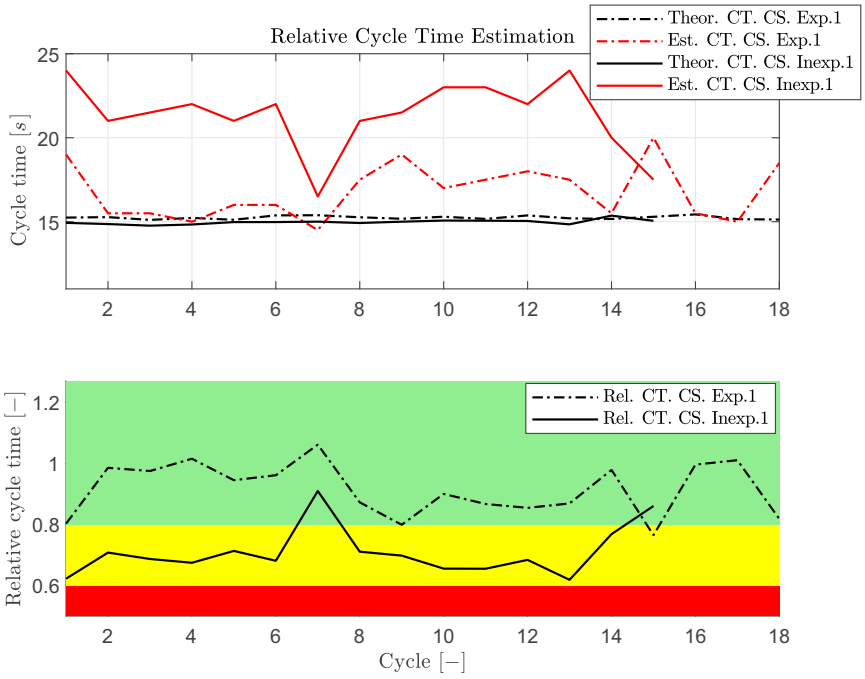

Figure 5.12: Relative cycle time estimations in the first case study ($\theta_{sw} \approx 120°$) [174].

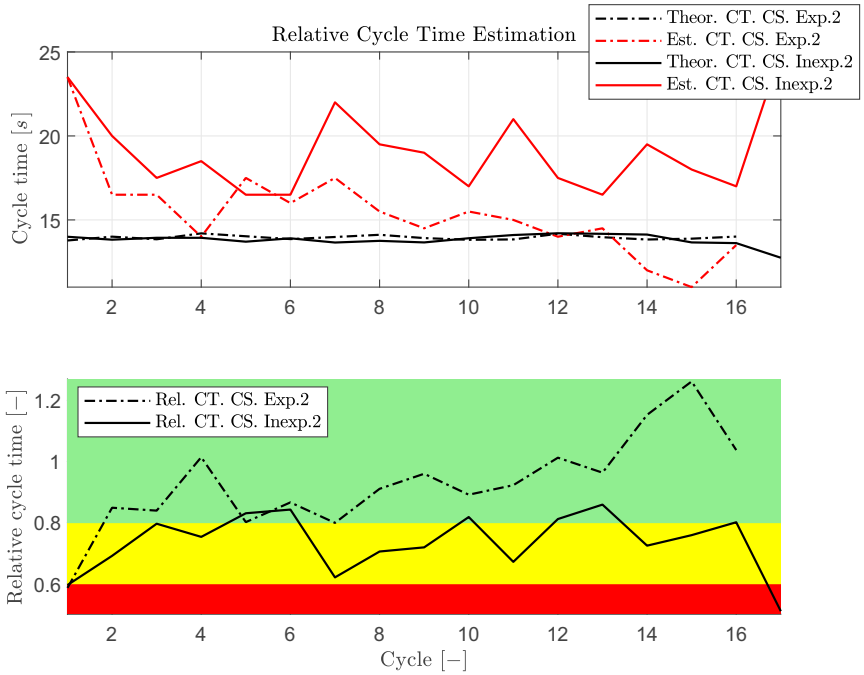

Figure 5.13: Relative cycle time estimations in the second case study ($\theta_{sw} \approx 60°$) [174].

case study. In Inexp. 2, operated by the inexperienced operator, the relative cycle time falls within the yellow area, indicating average performance. However, in Exp. 2, the relative cycle time demonstrates satisfactory performance.

5.4 Conclusions

This chapter proposes a method to estimate the actual, theoretical, and relative cycle times of an excavator during the loading operation. Initially, a supervised learning algorithm is introduced to recognize excavator activities, utilizing orientation variables and angular velocities collected from four IMUs installed on different moving parts of the machine. Multiple classification algorithms and feature selection methods are tested on the collected dataset. In addition, the impacts of various time windows and overlapping configurations on the activity recognition method are evaluated. The model can recognize the activities with an accuracy of approximately 95%. Subsequently, the cycle time is estimated based on the sequence of identified activities. Then, the theoretical cycle time is calculated using the BML model and ongoing operating conditions to assess the actual cycle time. The calculation of the theoretical cycle time needs automatic estimations of swing angle and digging depth. Two approaches are presented for these estimations based on recognized activities. Relative cycle time is then derived from the actual and theoretical cycle times, serving as an index of operational effectiveness, with higher values indicating superior performance. The method is evaluated through implementation in two case studies performed by experienced and inexperienced operators. The working

conditions, such as swing angle and type of material, are varied in the two case studies. Results demonstrate that the method can estimate the actual cycle time, with an average accuracy of approximately 97%. Furthermore, relative cycle time comparisons highlight differences between experienced and inexperienced operators, facilitating classification into three performance levels (satisfactory, average, and poor) via simple thresholding.

The suggested approach can be employed across various excavators for automated monitoring of cycle time, productivity, and operational efficiency. By incorporating data on the quantity of material, the concept of actual, theoretical, and relative cycle times can be extended to actual, theoretical, and relative productivity. These approaches have the potential to significantly reduce cost in the overall process by optimizing machine usage. They provide worksite managers with valuable insights into the productivity of each machine and its operators, enabling them to enhance operator training and streamline processes. Future plans include expanding the presented method to other applications, such as trenching and grading operations for excavators, as well as short and long loading cycles for front-end loaders.

Currently, there is a substantial demand for automated monitoring of productivity and performance in HDMMs. Based on existing data, there seems to be a lack of automated methods for evaluating the relative cycle time and operational efficiency of an excavator during loading operations under current operational circumstances. The proposed method offers automated monitoring of an excavator's cycle time and performance during loading operations. This data enables worksite managers and contractors to promptly identify issues, leading to significant reductions in operation time, improved scheduling, and enhanced productivity. Additionally, the method accounts for how operating conditions, such as swing angle and digging depth, can impact cycle time and productivity, marking another innovative aspect of the proposed method.

This study gathers a dataset by operating one excavator with both an experienced and inexperienced operator at a private worksite to train the classification models. The same machine is used to collect the test dataset. A significant limitation of the proposed method, as well as data-driven algorithms in general, is the limited amount of data available. Expanding the dataset is crucial, using data gathering from excavators of different sizes operated by individuals in varying competency levels. To enhance accuracy and consider differing operating conditions, data collection should encompass diverse swing angles, digging depths, material types, and weather conditions since the variables significantly impact the accuracy of the algorithm and the machine's productivity. Additionally, a notable limitation is the labeling of the dataset, a fundamental time-intensive process for supervised classification algorithms.

Material type plays a significant role in influencing both the cycle time and productivity of an excavator during loading operations. However, a limitation of the proposed method is the assumption of knowing the excavability level of the material. Project managers or operators should provide this information to the system. An artificial intelligence (AI)-driven approach for automatically identifying materials on construction sites could offer a promising solution, addressing certain challenges in productivity estimation algorithms. Another crucial variable to estimate during loading operations is the quantity of material

handled in each cycle. This can be accomplished by estimating the weight of material in the bucket through dynamic bucket payload estimation methods or by estimating the volume of material using advanced sensors, such as LiDAR. Typically, bucket volume estimation algorithms are more expensive and intricate, and they tend to offer lower accuracy compared to dynamic bucket payload estimation methods.

6 Excavator Productivity Estimation in Trenching and Grading Operations

In this chapter, two automatic methods are proposed to automatically estimate the productivity of an excavator in the trenching and grading operations. Firstly, a grid-based height map from working areas is obtained using a Livox Horizon® LiDAR sensor and localization data from the Global navigation satellite system (GNSS), and IMUs. In addition, BIM is employed to obtain information regarding the designed model and required accuracy. The productivity is determined based on the map comparison between the working areas and the target model. The obtained information can help worksite managers and contractors to analyze the productivity of each individual machine and enhance planning and time-scheduling.

6.1 Introduction

As described in the previous chapter, conventional manual productivity monitoring methods are time-consuming, costly, labor-intensive, and prone to errors. Additionally, in grading and trenching tasks, the quantity of material moved does not matter; but, precision within specified tolerances is crucial [165]. Hence, there is a need for an automated method to estimate the productivity of HDMMs in grading and trenching operations, which depends on predefined target models [16], [147].

In a grading operation, an excavator is employed to level and refine the ground surface, often for building or landscaping objectives. This preparation can involve leveling a site for construction or creating an even surface for paving. The excavator utilizes its bucket to shift and distribute material, ensuring a smooth and level terrain. Unlike other tasks, grading demands heightened precision, typically within ± 0.05 or ± 0.1 m, and in certain instances, accuracy as fine as ± 0.02 m is necessary [165]. Figure 6.1 depicts an excavator engaged in a grading task. The excavator's productivity in this operation is significantly influenced by various factors such as the type and condition of the material, the desired surface's size and complexity, the required level of accuracy, the excavator's size and capabilities, the specifications of the bucket, and the proficiency of the operator.

Productivity assessment should align with the goals of the duty cycle. Typically, the quantity of material and the cycle time are two crucial elements in the productivity definition of the most cyclical types of machinery. While quantifying an excavator's productivity by material moved per time unit is common, it cannot be used for grading

Figure 6.1: The grading operation using an excavator [169].

tasks. The quality and time of the grading operation are given utmost priority by worksite management since only a small amount of materials are added or removed. Therefore, material volume alone fails to adequately capture the operation's productivity. In this study, excavator productivity in grading tasks is quantified by the area of the graded surface per time unit:

$$Q_{grading} = \frac{a}{t} \tag{6.1}$$

where $Q_{grading}$ indicates the excavator's productivity in the grading operation $[m^2/s]$, a is the area of the graded surface $[m^2]$, and t is the time $[s]$.

Trenching operations entail the use of an excavator to dig trenches in the earth for laying underground utilities, such as water and sewer pipes. The operator utilizes the excavator to dig into the ground, shaping a trench to meet specific size and depth requirements. Various factors play a crucial role in determining the productivity of an excavator during trenching operations. These include the excavator's size and capabilities, the type and condition of the ground, the operator's proficiency and experience, the trench's depth and width requirements, and the type and size of the bucket. In trenching operations, contractors commonly estimate productivity based on the linear length of the trench per time unit [117], [155], [156]. Figure 6.2 depicts the trenching operation conducted with an excavator. In this study, productivity in the trenching operation is defined as the length of the trench per unit of time:

$$Q_{trenching} = \frac{l}{t} \tag{6.2}$$

where $Q_{trenching}$ indicates the excavator's productivity in the trenching operation $[m/s]$, l shows the length of the trench $[m]$, and t is the time $[s]$. Productivity depends on

Figure 6.2: The trenching operation using an excavator [170].

several factors, including the type of material, swing angle, bucket size and type, cross-sectional area of the trench, the skill of the human operator, and weather conditions. This productivity definition enables contractors and managers to monitor operation productivity effectively. It aids in estimating the time required to finish trenching work and determining the number of excavators needed to adhere to project deadlines. Furthermore, worksite managers can utilize the estimated productivity to plan future projects.

Traditionally, progress tracking and construction site surveys have relied on manual methods performed by surveyors. However, the demand for automated monitoring tools has led to the integration of 3D sensing technologies for the precise and accurate collection of on-site data. By combining this data with a BIM-based planned model, project progress can be effectively assessed [136].

According to the literature review presented in Chapter 2, there is a noticeable gap in research focusing on integrating real-time data with models to provide insights into ongoing activities on construction sites. Additionally, existing studies predominantly emphasize the quantity of material as a primary concern. Several key challenges identified in existing studies include the absence of input from the construction industry regarding their specific requirements and practical use cases, inadequate integration with BIM systems, and the failure to develop efficient visualization tools for assessing the performance of construction equipment. Furthermore, there is a notable lack of automated approaches for assessing productivity during grading or trenching operations utilizing BIM. Quality and accuracy have the highest priority in the grading and trenching operations and must be taken into account.

This study introduces two innovative algorithms for estimating the actual productivity of an excavator in grading and trenching operations, leveraging target models derived from BIM. The productivity metrics for grading and trenching operations are defined as the area of graded surface per unit of time and the length of the trench per unit of time, respectively. A LiDAR sensor installed on top of the excavator is employed to map the surrounding areas using an elevation terrain mapping technique. The positions of the bucket, arm, and boom are estimated utilizing the excavator's forward kinematics and IMUs mounted on different moving parts of the excavator. This allows for the removal of redundant points resulting from the movements of the excavator's manipulator. Furthermore, BIM provides the designed surface and trench models. The algorithm compares the acquired actual maps with the desired model to compute productivity, ensuring that the margin of error remains within the specified accuracy threshold. Finally, the methods are tested by implementation on a real dataset. The dataset is gathered using a medium-rated excavator in a private worksite, and the operations are conducted by a skillful operator. The outcomes indicate that the proposed methods can efficiently estimate the actual productivity of an excavator and monitor the operation progress.

This study makes a notable contribution to the construction domain by introducing an automated approach for estimating excavator productivity in grading and trenching tasks. The research demonstrates the efficiency of this method in accurately estimating and monitoring productivity, providing valuable assistance to project managers in tracking project progress. It streamlines project management processes, facilitates cost estimation and budgeting, and overcomes the challenges associated with manual data collection. Furthermore, the study highlights the underexplored potential of leveraging BIM in productivity estimation algorithms for HDMMs, emphasizing the significance of precision and quality in grading and trenching tasks, rather than merely the material quantity. Overall, this research offers a promising solution to improve cost-effectiveness, minimize environmental footprint, and elevate management strategies in earth-moving operations.

6.2 Methodology

This section provides a comprehensive description of the proposed techniques. Initially, it details the process of elevation terrain mapping, leveraging LiDAR sensor data, GNSS, and IMUs to cover the working area of the excavator. Additionally, the algorithm uses a forgetfulness scheme [157] to adapt to dynamic conditions efficiently. Next, the algorithm estimates the positions of the excavator's revolute joints to eliminate the manipulator from the 3D point clouds. Subsequently, the concept of BIM and its benefits are elaborated. Lastly, productivity estimation involves comparing the heights between the desired model and the actual map from the surrounding areas. Given the different productivity definitions for grading and trenching, two methodologies are presented for calculating productivity.

6.2.1 Elevation Terrain Mapping

In this method, acquiring a height map of operational zones is crucial for assessing the excavator's productivity in grading and trenching tasks. Typically, this map is generated by integrating sensor data from LiDAR, stereo cameras, and radio detection and ranging (RADAR), along with localization information from the GNSS, IMUs, or wheel odometry. A common data representation for characterizing a robot's environment is the elevation map. Each cell within a grid-based height map represents the terrain's height within that cell relative to a designated reference level, such as elevation above sea level. The accuracy and precision of localization data and sensor calibrations greatly influence the map's accuracy in the global frame [158].

A LiDAR sensor is a typical mapping tool. It captures measurements in its Spherical coordinate system and transforms them into a global Cartesian coordinate system to create a 3D point cloud of spatial data. However, errors can occur in this transformation process if the LiDAR sensor's actual position and orientation differ from the measured values. The final elevation map is typically constructed through a series of transformations, from the sensor's coordinate frame to the machine's body frame and eventually into the global frame. However, the cumulative effect of minor transformation errors can lead to substantial inaccuracies in the resulting map.

6.2.1.1 Transformation

To utilize LiDAR measurements for mapping purposes, the data initially provided in the sensor's Spherical coordinate system must be transformed into point clouds in a global Cartesian coordinate system. This transformation is achieved through a series of coordinate transformations. Three frames $A_i \in \{g, m, s\}$ indicate the main frames in coordinate transformations where g, m, and s represent the global, machine, and sensor frames, respectively. An affine coordinate transformation is formalized by Eq. (6.3):

$$ {}^{j}T_i = \begin{bmatrix} {}^{j}R_i & {}^{j}P_i \\ 0_{1\times3} & 1 \end{bmatrix} \tag{6.3a} $$

$$ {}^{j}R_i\left({}^{j}\varphi_i,\ {}^{j}\theta_i,\ {}^{j}\psi_i\right) = R_{roll}\left({}^{j}\varphi_i\right) R_{pitch}\left({}^{j}\theta_i\right) R_{yaw}\left({}^{j}\psi_i\right) \tag{6.3b} $$

$$ {}^{j}P_i = \left[{}^{j}x_i,\ {}^{j}y_i,\ {}^{j}z_i\right]^T \tag{6.3c} $$

where ${}^{j}T_i$ shows the 4 by 4 transformation matrix from i_{th} frame to j_{th} frame, ${}^{j}R_i$ indicates the 3 by 3 rotation matrix from i_{th} frame to j_{th} frame, ${}^{j}P_i$ represents the 3 elements translation vector from i_{th} frame to j_{th} frame, $R_{roll}\left({}^{j}\varphi_i\right)$ is the rotational matrix around the x-axis, $R_{pitch}\left({}^{j}\theta_i\right)$ indicates the rotational matrix around the y-axis, $R_{yaw}\left({}^{j}\psi_i\right)$ shows the rotational matrix around the z-axis, ${}^{j}\varphi_i$, ${}^{j}\theta_i$, and ${}^{j}\psi_i$ represent roll, pitch and yaw angles, respectively [159].

A single LiDAR measurement is represented by either Spherical coordinates (r, θ, ϕ) or Cartesian coordinates (x, y, z). The relationship between Spherical and Cartesian coordinates is illustrated in Fig. 6.3. The point ${}^{g}P$ in the global frame is calculated utilizing

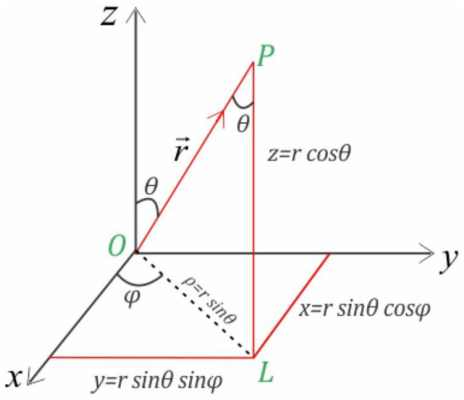

Figure 6.3: Relationship between Spherical coordinates and Cartesian coordinates [171].

the point ${}^{s}P$ in the sensor frame and a chain of transformations:

$$ {}^{g}P = {}^{g}T_{m}\,{}^{m}T_{s}\,{}^{s}P, \tag{6.4} $$

where ${}^{m}T_{s}$ shows the transformation matrix from the sensor frame to the machine frame and ${}^{g}T_{m}$ indicates the transformation matrix from the machine frame to the global frame. The transformation matrix from the sensor to the machine is acquired through a target-based calibration method. During calibration, the frames of the sensor and the machine are precisely aligned using spherical targets with known dimensions and positions relative to the machine frame. These targets serve as reference points, and corresponding points in both the sensor and machine coordinate frames are required to compute the transformation matrix [160]. The transformation matrix from the machine frame to the global frame is obtained using IMU and GNSS measurements. This method integrates the machine's acceleration and angular velocity data from the IMU, along with position data from GNSS (latitude, longitude, and altitude), using an extended Kalman filter (EKF). By fusing information from multiple sensors, this approach ensures a high-accuracy and drift-free estimation of the machine's position in the global frame.

Initially, the EKF employs a mathematical model, known as the "priori" estimate, to predict the current state of the machine. Subsequently, it updates this estimate by comparing it with the current sensor measurements, generating a "posteriori" estimate through a process known as the measurement update. This update involves applying the Kalman gain to weigh the relative contributions of the a priori estimate and the sensor measurements. This prediction and update cycle is iteratively performed at regular intervals using the latest sensor data [161].

In a 2D grid, known as a height map, the average and variance of heights are recorded within individual cells. To construct this height map, each point within the 3D point cloud is allocated to a specific cell based on its x and y coordinates. Subsequently, the z coordinate values of all 3D points assigned to a particular cell are treated as new measurements for that cell.

Employing a Bayesian updating approach, the existing estimation within a cell is adjusted based on the new measurements. The proposed algorithm incorporates a forgetfulness

scheme [157] to handle dynamic conditions effectively. The height observations z_t are modeled using a Gaussian distribution $N(z_t, \sigma_{z_t}^2)$. Using the observation z_t recorded at time t and the Kalman filter, the height estimate $\hat{h}$ is updated as follows:

$$\hat{h}(t) = \frac{1}{\sigma_{z_t}^2 + \sigma_{\hat{h}(t-1)}^2} \left(\sigma_{z_t}^2 \hat{h}(t-1) + \sigma_{\hat{h}(t-1)}^2 z_t \right), \tag{6.5}$$

$$\sigma_{\hat{h}(t)}^2 = \frac{1}{\frac{1}{\sigma_{\hat{h}(t-1)}^2} + \frac{1}{\sigma_{z_t}^2}}. \tag{6.6}$$

The primary impact originates from the latest measurements. The update procedure escalates the variance of the current estimate proportionally to the time elapsed between the prior and current measurements. Points with variance exceeding a predefined threshold are excluded from processing, effectively filtering out uncertain information [159]. In the subsequent stage, the height map undergoes cropping using a rectangular filter. The dimensions of this filter are determined based on the excavator's maximum digging reach and width, ensuring coverage of the entire working area.

6.2.1.2 Revolute Joints' Positions

As the LiDAR sensor is mounted on top of the excavator to map the working area, the presence of the boom, arm, and bucket adds extra points that do not accurately reflect the ground's height. Furthermore, the dynamic movement of these components means their locations are not fixed. Therefore, it is necessary to eliminate these extra points from the acquired point clouds. In the proposed method, the positions of the excavator's revolute joints are initially estimated, followed by the removal of points in proximity to the estimated positions. To determine the positions of the revolute joints, the forward kinematics of an excavator introduced in Section 5.2.3.2 are employed.

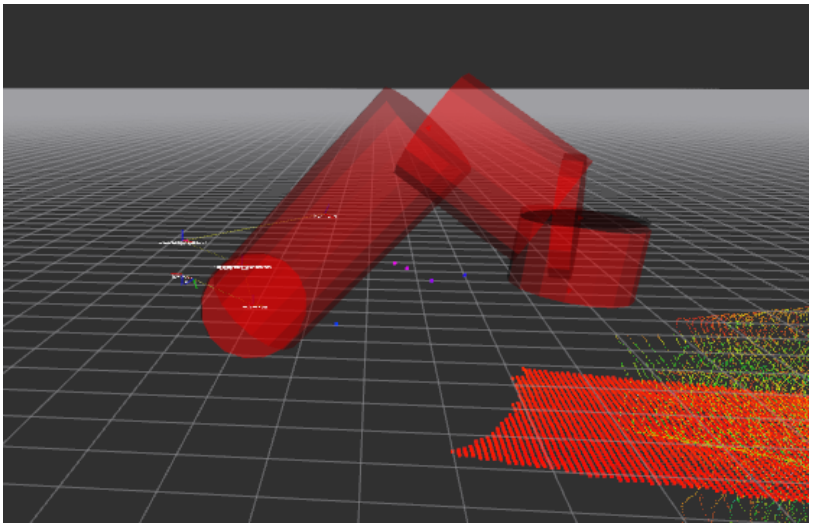

Figure 6.4: Schematics of the modeled boom, arm, and bucket using cylinders [175].

Next, each link is modeled as a simple cylinder, where the axis of the cylinder corresponds to the line connecting two adjacent coordinate systems. All cylinders have a constant radius value. The schematics of the modeled boom, arm, and bucket are illustrated in Fig. 6.4. Points that intersect with both the cylinders and the point clouds are discarded, leaving behind the remaining points for use in the elevation terrain mapping process. Occasionally, when the bucket is in close proximity to the ground, some ground points may be removed. However, this is not an issue since as the bucket moves away from the surface, the previously obscured area becomes visible and can be incorporated into the height map.

6.2.2 Building Information Modeling (BIM)

BIM is a methodology used to generate and manage digital representations of both the physical and functional aspects of construction projects throughout their entire lifespan. These models encompass detailed information about the project's geometry, construction elements, systems, and various components. Although BIM has been in development since the 1970s, its widespread adoption only occurred in the early 2000s. BIM is supported by a wide range of technologies and software tools to facilitate its implementation and usage. The initial stage of the BIM process involves creating a 3D model of the construction project, which is continuously revised to incorporate alterations and updates throughout the design and construction phases. BIM enables visualization of the construction project and facilitates simulation of its performance. Furthermore, it allows the estimation of costs and time requirements for the project, along with identifying and resolving any potential issues or conflicts [108], [136].

Furthermore, Infrastructure BIM, often referred to as InfraBIM, encompasses the application of BIM principles and methodologies in the planning, design, construction, and maintenance of infrastructure projects. InfraBIM finds applications across various infrastructure projects such as roads, bridges, tunnels, airports, rail systems, as well as water and wastewater treatment facilities. InfraBIM facilitates real-time monitoring of progress by comparing as-built data with the initial design. Additionally, it aids in monitoring resource allocation and utilization, thereby ensuring efficient use of resources throughout the project lifecycle. Moreover, it can enable the integration of various disciplines and the coordination of intricate systems, fostering collaboration and communication among stakeholders, boosting efficiency and overall project quality, and streamlining decision-making processes while minimizing errors and rework [172], [162].

Currently, the integration of BIM and machine control systems, such as Xsite® PRO 3D, can greatly facilitate construction projects. The Xsite® PRO 3D system is depicted in Fig. 6.5. Using machine control systems, operators can efficiently and precisely execute tasks by comparing the position of the bucket tip with the target model. These target models are designed by construction professionals utilizing 3D design software programs.

Figure 6.5: Xsite® PRO 3D system that is installed in the excavator cabin [173].

6.2.3 Productivity Estimation

In this section, two approaches are introduced for estimating the actual productivity of excavators in grading and trenching operations. These algorithms begin by designing a target model using BIM, and then the operator executes the task according to this model. The Xsite® PRO 3D system, located within the cabin, assists the human operator in aligning the bucket tip position with the target model. Concurrently, the elevation terrain mapping algorithm continuously updates the height map of the working areas at regular intervals during operations. These methodologies calculate productivity by comparing the desired model with the actual maps obtained from the surrounding areas.

6.2.3.1 Grading Operation

During the grading operation, it is crucial that the height difference between the initial and target surfaces is less than the bucket's height. If the height difference is more than the bucket's height, preliminary digging operations become necessary. In the proposed approach, initially, a region of interest (ROI) around the i_{th} point of the desired model is

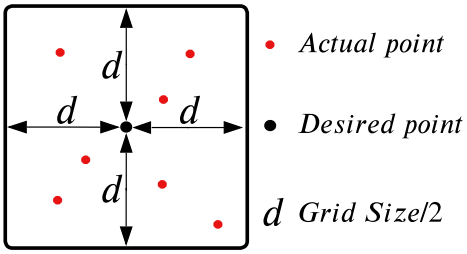

Figure 6.6: The desired and actual points within the ROI in the grading operation [175].

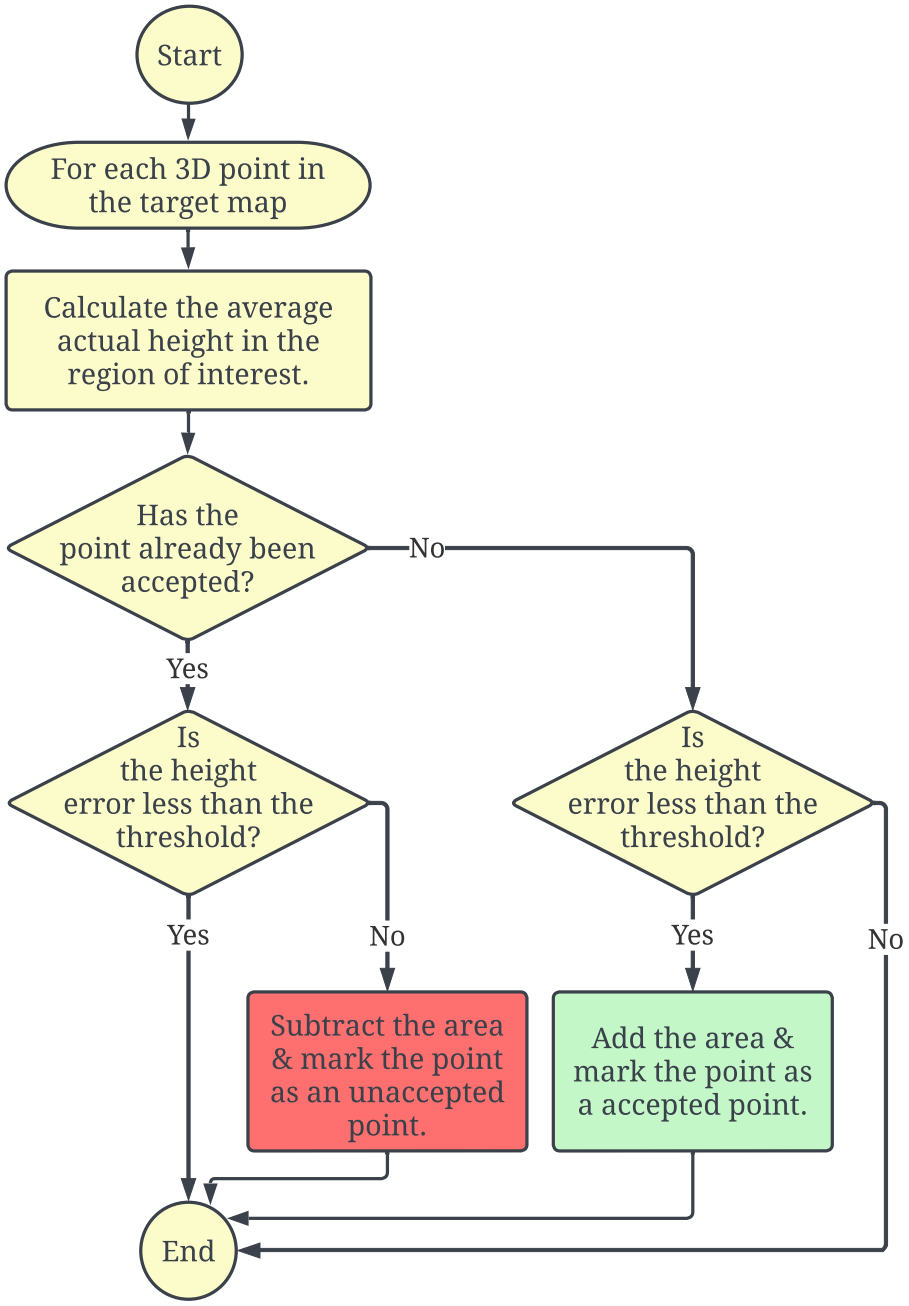

Figure 6.7: Flowchart of the productivity estimation in the grading operation [175].

selected. The point is located in the center of the square-shaped ROI. The size of the ROI is equal to the grid size of the target model. Subsequently, the actual points inside the defined ROI are identified. A simplified schematic of desired and actual points inside an ROI is illustrated in Fig. 6.6.

The desired height, denoted as $Z_{desired}$, corresponds to the z coordinate value of the i_{th} point in the model. Equation (6.7) formalizes the average height of actual points within the ROI:

$$Z_{actual} = \frac{\Sigma_{j=1}^{N} z_j}{N}; \quad j \in \{1, 2, 3, \ldots, N\}, \tag{6.7}$$

where Z_{actual} shows the average actual height, z_j denotes the z coordinates of the j_{th} point within the ROI, and N indicates the total number of points within the ROI. The flowchart of the presented method is illustrated in Fig. 6.7. In this method, the ROI area is added to the productivity calculation when the point has not been labeled as a valid point yet, and the deviation between the actual and desired height values falls below the specified accuracy threshold. Moreover, it is necessary to verify the current height of a point previously validated, as it could have altered. If the error exceeds the designated accuracy level, the point is marked as unaccepted, and the ROI area is subtracted from the productivity calculation. This scenario could lead to negative productivity, indicating that the error exceeds the threshold.

6.2.3.2 Trenching Operation

As previously outlined, the actual productivity of the trenching operation is defined as the length of the trench per unit of time. In this method, the ROI represents a narrow strip of the trench. Figure 6.8 provides a basic illustration of the desired and actual points within an ROI in the trenching operation. The desired height $Z_{desired}$ for a strip corresponds to

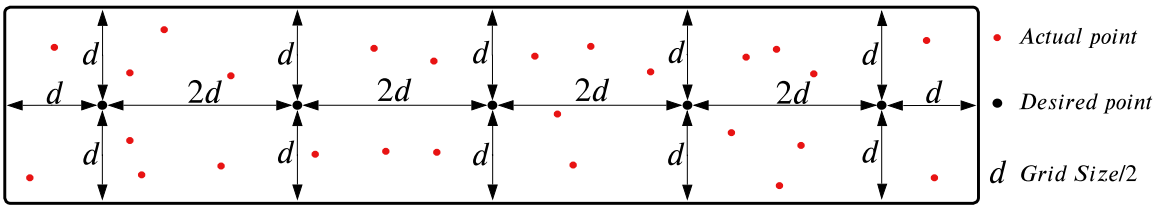

Figure 6.8: The desired and actual points within the ROI in the trenching operation [175].

the average of the z coordinates of desired points within the ROI. It is computed using Eq. (6.8):

$$Z_{desired} = \frac{\Sigma_{i=1}^{M} z_i}{M}; \quad i \in \{1, 2, 3, \ldots, M\}, \tag{6.8}$$

where z_i shows the z coordinates of i_{th} desired point within the ROI, and M indicates the total number of the desired points inside the strip. The average height of actual points inside a strip is calculated using Eq. (6.9):

$$Z_{actual} = \frac{\Sigma_{j=1}^{N} z_j}{N}; \quad j \in \{1, 2, 3, \ldots, N\}, \tag{6.9}$$

where Z_{actual} indicates the average actual height, z_j denotes the z coordinates of j_{th} actual point inside the ROI, and N shows the total number of the actual points within the ROI.

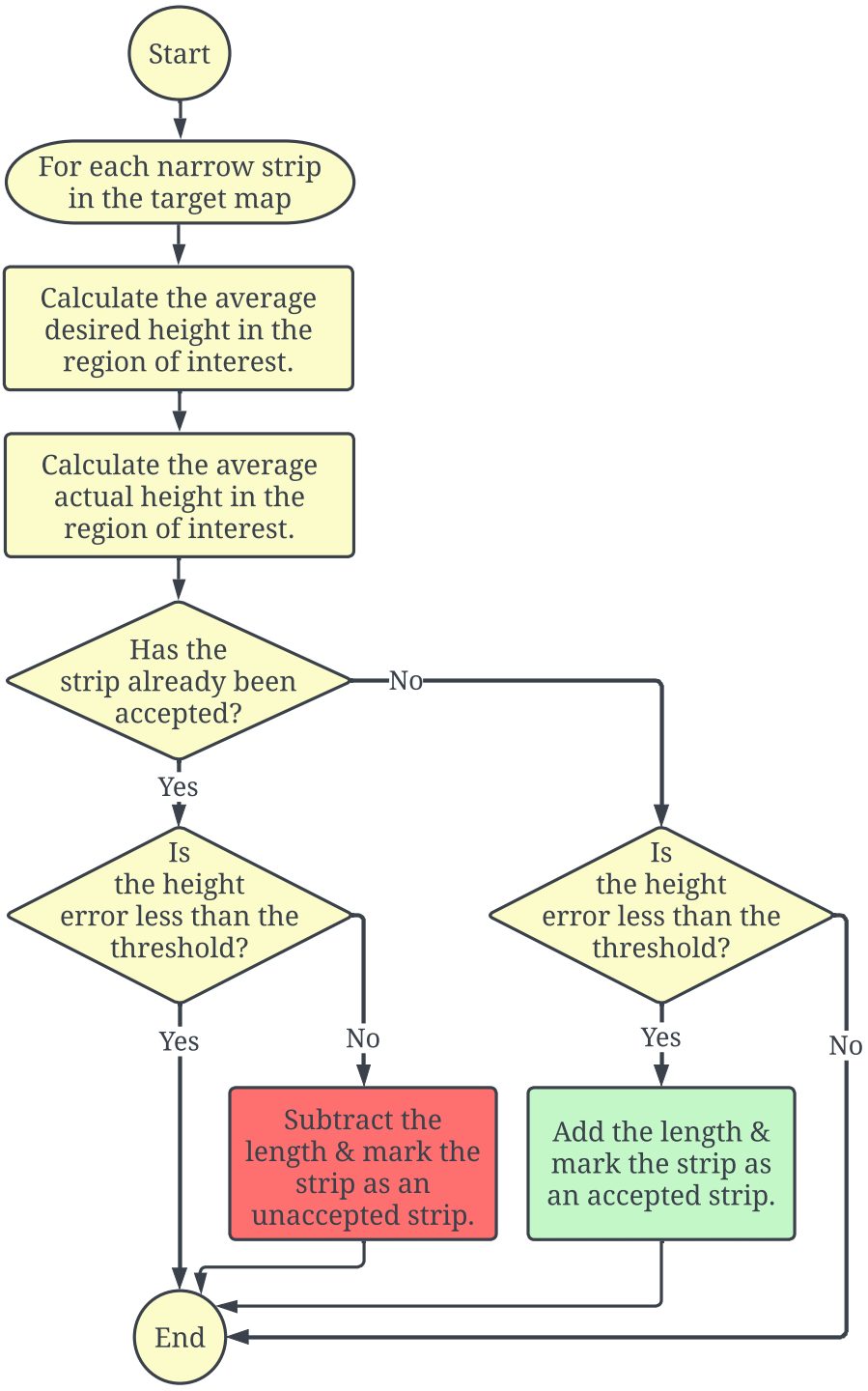

Figure 6.9: Flowchart of the productivity estimation in the trenching operation [175].

Figure 6.9 illustrates the flowchart of the proposed method for estimating the actual productivity of an excavator in trenching operations.

In the algorithm outlined, the length of a strip contributes to the productivity estimation if the strip has not been previously accepted as a valid strip and if the deviation between the average actual and desired heights falls below the specified accuracy threshold. Additionally, the actual heights of previously validated strips must be verified for potential changes. If the error exceeds the specified accuracy threshold, the strip's length is deducted from the productivity estimation, and the strip is labeled as an unaccepted strip. This scenario, where the error exceeds the required accuracy, results in negative productivity.

6.3 Results

In this section, the effectiveness of the proposed methods is illustrated through their applications in grading and trenching operations. Initially, the sensor setups and data acquisition procedure are elaborated. Subsequently, the actual and aggregate productivity of the excavator in both grading and trenching tasks are estimated. The suggested methods have been implemented using MathWorks® MATLAB R2021a on a laptop with a 1.8 GHz Intel Core i7 CPU and 16 GB of RAM running on a Windows 10 operating system.

6.3.1 Data Collection Procedure

During the tests, data was collected using a Komatsu® PC138US excavator. The crawler excavator utilized in the experiments is depicted in Fig. 4.2. A Livox Horizon® LiDAR was mounted on top of the excavator cabin, providing a field-of-view (FOV) of 25.1° vertically and 81.7° horizontally. The LiDAR's coverage area was aligned with the area that the

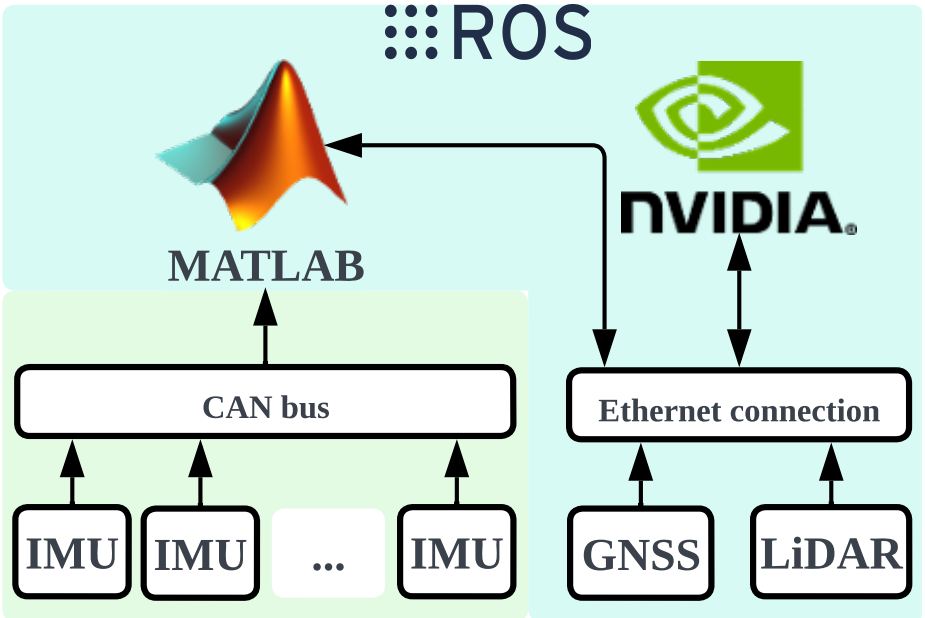

Figure 6.10: Schematic of various connections in the excavator [175].

bucket could reach. Data collection took place at a private worksite without any active construction activity. The experiments were conducted by a skilled operator, and two types of materials, clay and a mix of sand and gravel were used for the grading and trenching operations, respectively.

The data from the excavator is collected using the robot operating system (ROS) and the MathWorks® Simulink model. ROS serves as a communication interface that ensures seamless compatibility between programs written in various languages and operating on diverse platforms [163]. This communication framework facilitates the access of various components to different measurements and variables, including the height map and the positions of the revolute joints. Figure 6.10 illustrates the schematic of the connections between different sensors and processors. In this setup, the NVIDIA® Jetson AGX Xavier functions as the ROS master, while Simulink® generates and links its own ROS node to it. IMU measurements are transmitted via the CAN bus at a sampling frequency f_s of 200 Hz. To connect Simulink® to the CAN bus, a Kvaser leaf light CAN to USB interface is used. Ethernet connections are utilized to link the LiDAR, GNSS, NVIDIA® Jetson AGX Xavier, and Simulink® to the ROS framework. Figure 6.11 depicts the configuration of the IMUs, GNSS, Xsite® PRO 3D, and LiDAR sensor on the excavator.

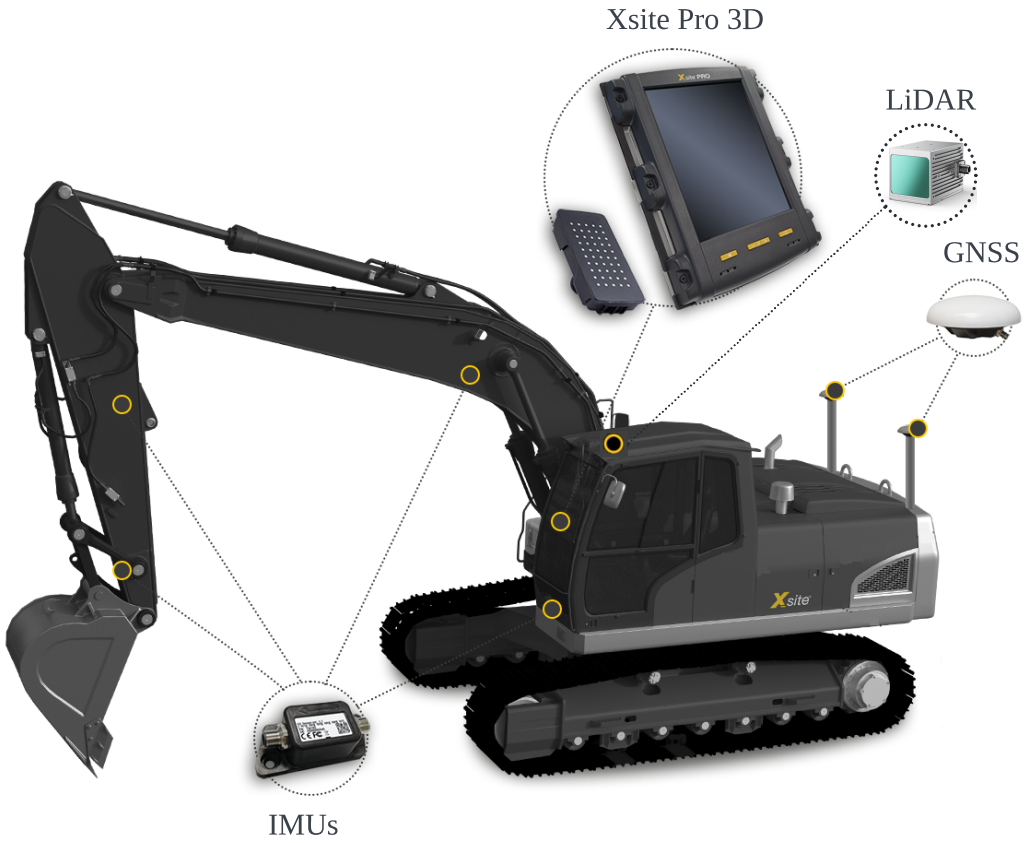

Figure 6.11: The configuration of IMUs, GNSS, Xsite® PRO 3D, and LiDAR sensor on the excavator [175].

6.3.2 Grading Operation

Initially, the operator inside the excavator's cabin utilizes the Xsite® PRO 3D to design a surface as the target model for the grading operation. Subsequently, the 3D-Win® software program is utilized to generate a 3D point cloud. Figure 6.12 displays the 3D point cloud of the desired model in the grading operation, representing a roughly 3 $m \times 4$ m rectangular surface. The desired surface is set to be 0.5 m deeper than the ground surface, and the

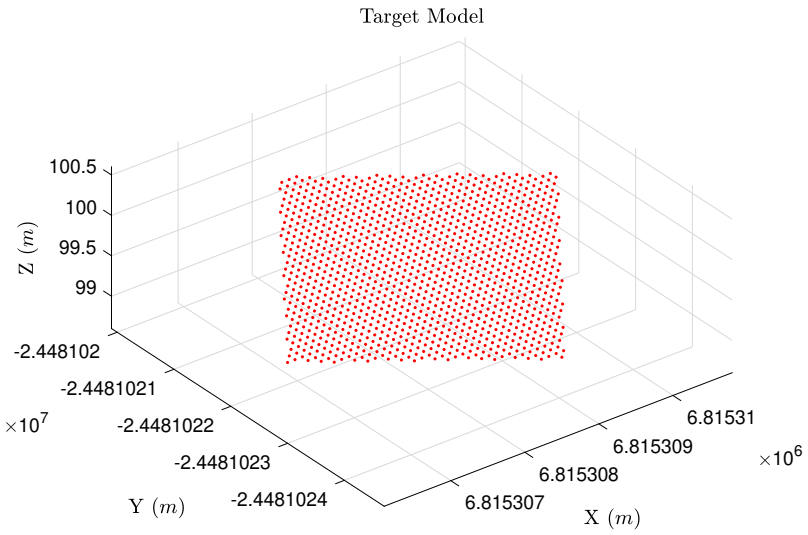

Figure 6.12: The target model designed in BIM in the grading operation [175].

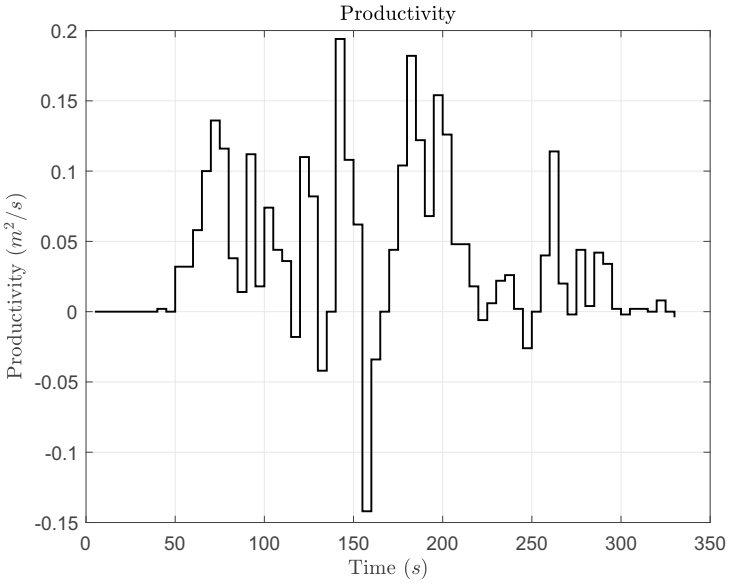

Figure 6.13: The productivity of the excavator in the grading operation [175].

slopes of the desired surface and the initial terrain are both equal to zero. In the operation, the BIM model's required accuracy and the point cloud's grid size are both set to 0.1 m.

The elevation map from the surrounding areas is updated at intervals of 5 s. Figure 6.13 depicts the actual productivity of the excavator in the grading operation. As shown, the productivity occasionally falls below zero. Negative productivity arises when the deviation between the desired and actual heights exceeds the specified accuracy threshold. For instance, this occurs when a large volume of material spills from the bucket onto a section that has already been graded or when the bucket digs too deeply, leading to an error that exceeds the threshold.

Figure 6.14 illustrates the aggregate productivity of the excavator during the grading operation. The total area of the target model is approximately 12 m^2. In this operation, the average actual productivity is approximately 0.037 m^2/s. In certain parts, the aggregate productivity experiences a decline, primarily due to instances of negative productivity in the operation. Towards the end of the operation, the aggregate productivity aligns closely with the entire area of the target model. It means that almost in the whole area, the deviation between the target model and the actual map is within the specified accuracy threshold. Figure 6.15 depicts the progress of the operation at four different time points. Areas where the error exceeds the specified accuracy threshold are highlighted in red, while those with errors within the accuracy threshold are depicted in green. Using the described algorithm, both managers and contractors gain a convenient means to monitor productivity and track operational progress. This productivity data proves beneficial for project managers in scheduling tasks and conducting cost analyses. Additionally, the comparison of the machine's productivity to industry benchmarks or other machines offers insights into potential productivity enhancements and efficiency optimizations.

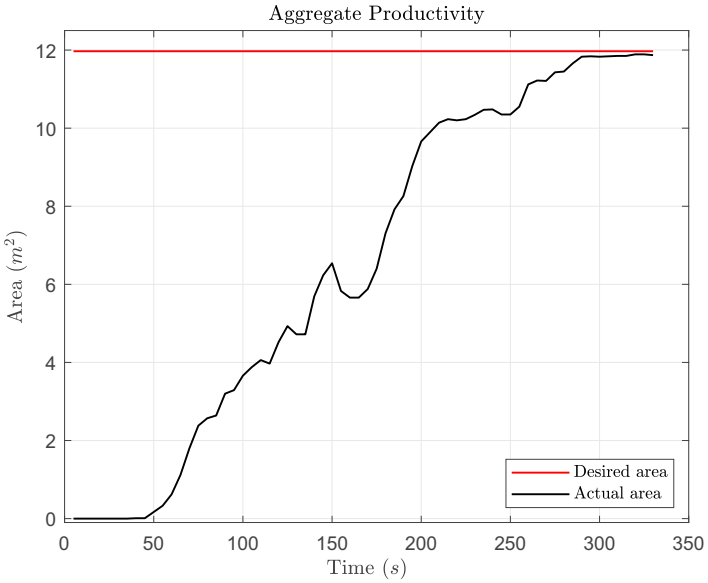

Figure 6.14: The aggregate productivity of the excavator in the grading operation [175].

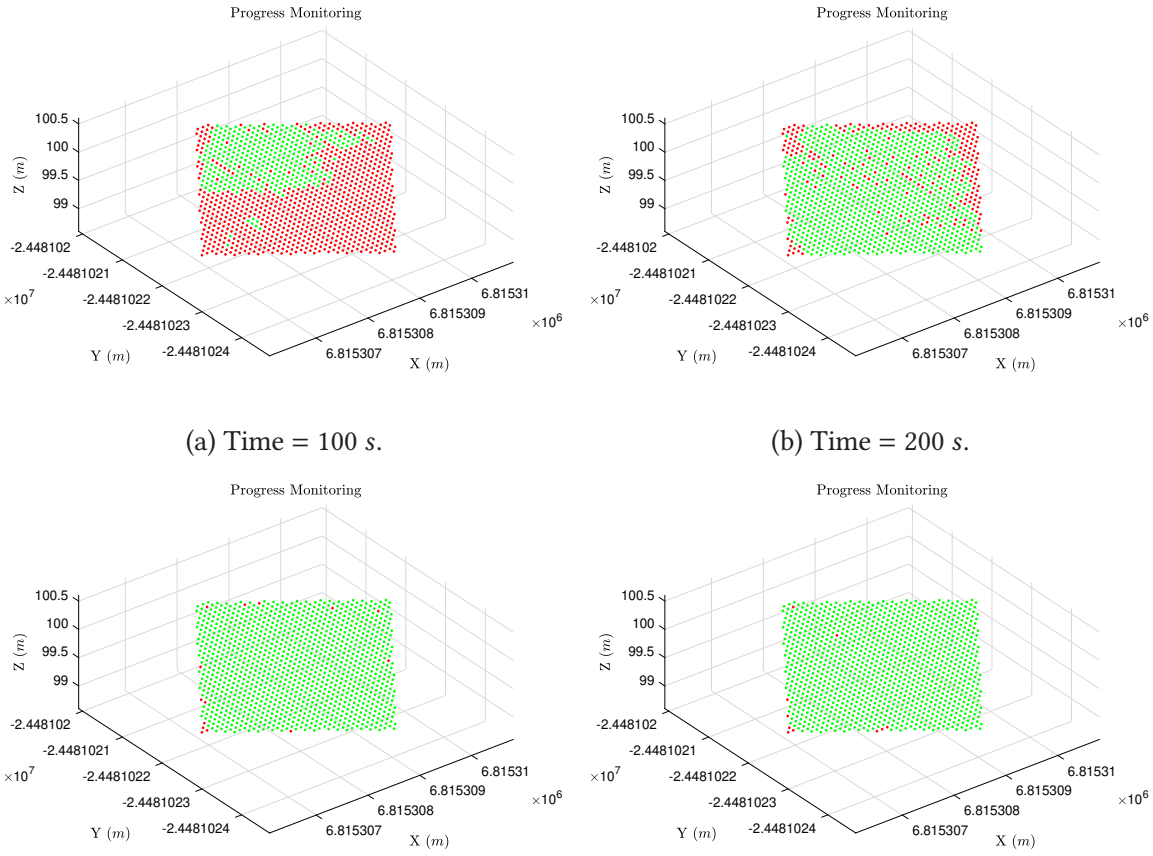

(a) Time = 100 *s*.

(b) Time = 200 *s*.

(c) Time = 300 *s*.

(d) Time = 330 *s*.

Figure 6.15: Progress monitoring during the grading operation: (•) green points indicate the area where the error is less than the required accuracy, and (•) red points represent the area where the error is higher than the required accuracy [175].

Furthermore, human operators can leverage the provided feedback to improve their skills and execute operations with high accuracy in a short time.

6.3.3 Trenching Operation

In the second use case, the performance of the suggested method is demonstrated through its application in the trenching operation. Initially, a target model is designed to align with the project's specifications and requirements, utilizing the Xsite® PRO 3D system installed inside the excavator's cabin. Subsequently, the 3D point cloud representing the desired trench is generated using the 3D-Win® software, as depicted in Fig. 6.16. The trench's dimensions include a depth of 1 *m* and a width of 0.825 *m*. The total length of the trench is approximately 23.8 *m*. In the trenching operation, the BIM model's required accuracy and the elevation map's grid size are equal to 0.1 *m*.

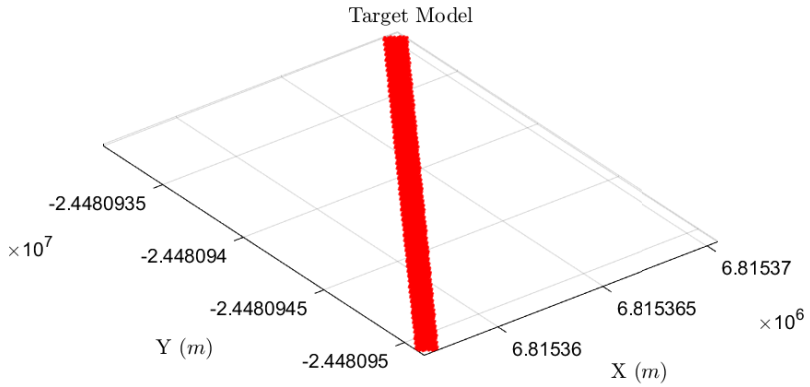

Figure 6.16: The target model designed in BIM in the trenching operation [175].

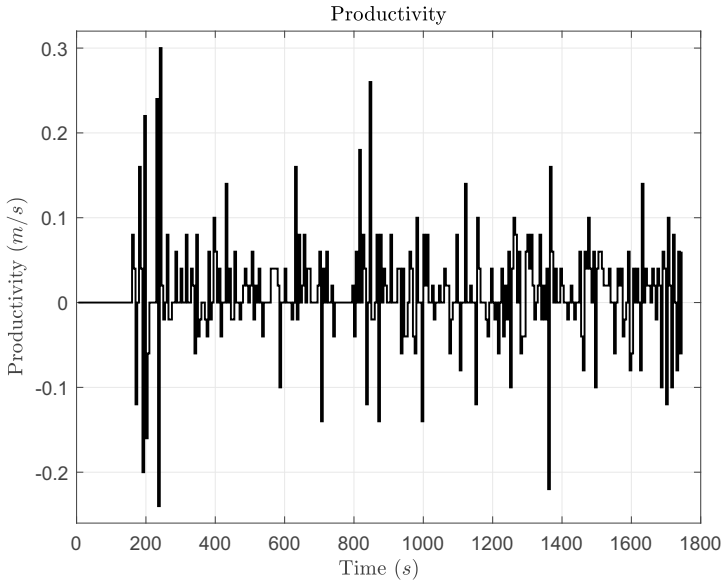

Figure 6.17: The productivity of the excavator in the trenching operation [175].

As previously described, the actual productivity in the trenching operation is defined as the length of the trench excavated per unit of time. The excavator's actual productivity in the trenching operation is depicted in Fig. 6.17. Similar to the grading operation, instances of negative productivity are observed, typically occurring when materials spill from the bucket or trench sides or when the operator digs too deeply.

Figure 6.18 illustrates the aggregate productivity of the excavator in the trenching operation. On average, the excavator achieves a productivity rate of approximately 0.01 m/s. The

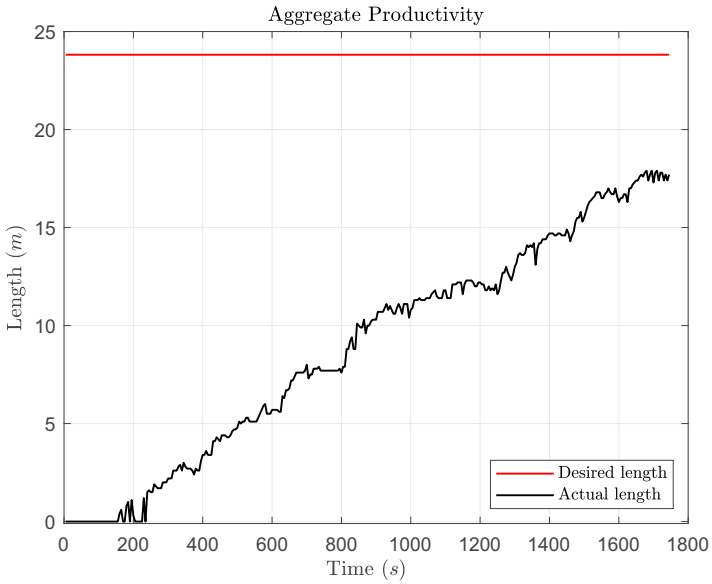

Figure 6.18: The aggregate productivity of the excavator in the trenching operation [175].

aggregate productivity at the end of the operation does not match the entire length of the trench. This discrepancy arises because, in certain sections of the trench, the error between the model and the actual map exceeds the defined threshold. Figure 6.19 depicts the progress of the trenching operation at four different time intervals. It is evident that the quality of the operation is inadequate at both the beginning and end of the trench. At the beginning of the trench, the error between the model and the actual map is higher than the defined threshold. At the end of the trench, the operation suddenly stopped due to safety concerns, resulting in the operator being unable to complete the task.

6.4 Conclusions

Trenching and grading operations stand as pivotal tasks across diverse worksites. These tasks prioritize attaining high-quality outcomes, placing a focus on precision and accuracy rather than mere quantity. Existing methodologies in the literature predominantly focus on material quantity rather than the operational quality of these tasks. The productivity metrics for grading and trenching operations entail the area of graded surface per unit of time and the length of trench per unit of time, respectively. This paper introduces two innovative approaches aimed at autonomously estimating the productivity of an excavator in these operations. The suggested algorithms encompass three primary stages: (1) elevation terrain mapping, (2) BIM, and (3) productivity calculation. Initially, the elevation profile of working areas is determined and updated every few seconds using a LiDAR sensor installed on top of the machine and the elevation terrain mapping algorithm. In the subsequent stage, the removal of additional points resulting from manipulator

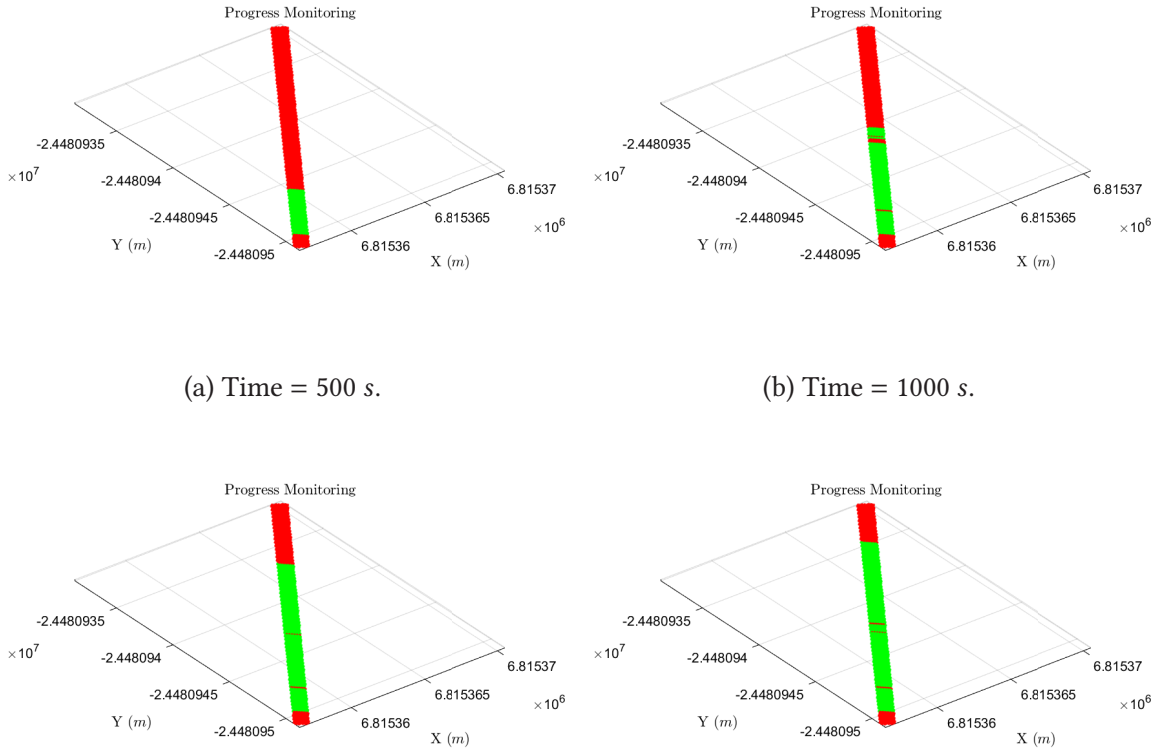

(a) Time = 500 *s*.

(b) Time = 1000 *s*.

(c) Time = 1500 *s*.

(d) Time = 1745 *s*.

Figure 6.19: Progress monitoring during the trenching operation: (•) green points show the area where the error is less than the required accuracy, and (•) red points indicate the area where the error is higher than the required accuracy [175].

movements, such as the bucket, arm, and boom, is addressed by computing the positions of revolute joints. The excavator's forward kinematics alongside IMUs mounted on various moving components of the machine are used to estimate the revolute joints. Next, the shape of the desired surface or trench is retrieved from BIM. Estimation of actual productivity involves comparing maps derived from the target model with elevation maps. For trenching productivity calculation, the ROI is a narrow strip, whereas for grading productivity calculation, it is a small square. The presented algorithms are applied to a dataset obtained from a real excavator performing grading and trenching tasks. The outcomes show that the proposed methods efficiently estimate actual productivity and monitor operation progress. Monitoring progress and estimating productivity provide valuable insights for contractors and worksite managers to analyze operations and identify issues. Additionally, they can compare individual machine productivity to industry standards or the productivity of other machines. Furthermore, human operators can utilize productivity estimation as feedback to enhance their skills based on performance evaluation.

Effectively managing ongoing projects and ensuring precise costing and budgeting for future projects are crucial aspects in diverse worksites. The suggested automated methods for productivity estimation and progress monitoring represent a significant move towards achieving autonomous functionality in excavators. Autonomous machines rely on performance data to optimize their operations. Nonetheless, a limitation of the presented algorithms is their specificity to grading and trenching tasks, making them unsuitable for other operations. In the future, the methods should be expanded to encompass a broader range of tasks and machinery, including bulldozers and compactors, based on their unique operational needs.

The proposed algorithms aim to assess the excavator's actual productivity in the grading and trenching tasks. In the future, it would be beneficial to compute the theoretical or highest feasible productivity given specific task requirements, objectives, and working conditions, such as material type, swing angle, trench's cross-sectional area, bucket and machine size, etc. This theoretical productivity can serve as a benchmark to normalize the actual productivity. By establishing the relative productivity or the production performance ratio, it becomes possible to determine the machine's operational effectiveness based on the current operating conditions.

Another challenge is that the required accuracy in certain tasks and applications is $\pm\, 0.02\, m$. Attaining such high precision in elevation terrain mapping algorithms poses challenges due to the need for exceptionally accurate and costly sensors, as well as time-consuming calibration procedures.

7 Conclusions and Future Directions

The construction industry is not just an essential sector of the economy; it is the backbone that supports economic growth globally. Moreover, it serves as a crucial link between various industries. However, despite its importance, the construction sector faces several challenges, including low productivity and outdated practices. One of the key issues plaguing the construction industry is its relatively low productivity growth. This slow pace of improvement stands in stark contrast to other industries, highlighting the urgent need for innovation and efficiency enhancement within the construction sector.

HDMMs are integral to various construction projects, with equipment costs often accounting for a significant portion of total project expenses. Among these machines, excavators play a central role, undertaking diverse earth-moving tasks. However, assessing the performance of these machines has traditionally been a labor-intensive and error-prone process, relying on manual data collection and on-site observations. To address these challenges, there is a growing recognition of the importance of accurately measuring the productivity of HDMMs. This research study focuses specifically on excavators and aims to develop innovative approaches for assessing their productivity. By leveraging advanced technologies, the study seeks to streamline productivity estimation and progress monitoring for excavators across different tasks and working conditions. By better understanding and managing excavator productivity, the construction industry can anticipate challenges more effectively, refine planning and operating parameters, reduce costs, and ultimately deliver projects more successfully.

Chapter 2 of the dissertation explores the current state of research in monitoring the productivity of HDMMs. Traditional methods for monitoring productivity rely heavily on manual observations, proving time-consuming and prone to errors. To address these limitations, researchers have turned to integrating information technology for automated data collection. The chapter delves into the latest developments in this field, focusing on two main categories: CV-based techniques and sensor-based techniques. CV-based approaches involve gathering operational data from cameras, while sensor-based methods deploy various sensors or tags to capture position and pose information. The chapter discusses the challenges and potential of both approaches, highlighting their applicability and limitations in real-world construction scenarios. CV-based methods encounter considerable practical challenges in real applications. It is suggested that vibration and orientation sensors, such as IMUs, present a promising alternative for overcoming the challenges associated with CV-based and other sensor-based methods in activity recognition, cycle time estimation, and productivity monitoring.

It also explores the use of process-oriented and data-oriented methodologies for predicting equipment productivity. Additionally, the integration of BIM and 3D sensing technologies for real-time progress monitoring and productivity estimation is discussed, emphasizing the potential for improving understanding and management of construction tasks. Lastly, the chapter notes a gap in the literature, specifically the lack of focus on productivity estimation for quality-centered tasks, such as trenching and grading.

Chapter 3 of the dissertation outlines the scientific contributions of the research. It begins by detailing the proposed research framework for automatically estimating the productivity of an excavator across various tasks, such as loading, trenching, and grading. The framework aims to address the identified research gaps and practical challenges discussed in the literature review. The chapter introduces multiple research questions that serve as the primary targets of the dissertation. These questions revolve around improving task and sub-task recognition of an excavator, estimating cycle time, automatically assessing operating conditions, such as swing angle and digging depth, and determining theoretical and actual productivity using IMUs and machine learning techniques. Furthermore, the dissertation aims to bridge the gap in integrating real-time data with planned models to provide insights into construction site activities, particularly focusing on quality-centered tasks, such as trenching and grading. In addition, certain unexplored aspects that could be subjects of future investigations, including the automatic estimation of theoretical productivity in trenching and grading operations and adding the quantity of materials to the actual, theoretical, and relative cycle time concepts, have been discussed. These areas represent potential subjects for further research, contributing to the ongoing advancement of productivity monitoring techniques in construction contexts.

Chapter 4 of the dissertation presents a method for automatically recognizing tasks performed by an excavator using supervised learning algorithms and motion data obtained from IMU sensors attached to different parts of the machine. It highlights the essential tasks of an excavator, such as loading, trenching, and grading, with different productivity definitions, and emphasizes the significance of task recognition for productivity estimation. The proposed data-driven method is positioned as a robust solution for automating excavator task recognition. The method collects orientation and angular velocity data from the excavator's moving parts, and then four supervised learning algorithms are employed, along with feature selection techniques, to automatically recognize tasks. The method's resilience and adaptability in real-world scenarios are demonstrated through comprehensive analyses.

Moreover, it discusses the integration of task recognition and productivity monitoring systems, enabling task-specific metrics and progress monitoring. The potential for enhancing collaboration between human workers and automated elements, predictive maintenance, and decision-making through trend analysis is also highlighted. Future directions for research include broadening the methodology to encompass other types of HDMMs, such as front-end loaders and compactors, by installing motion sensors on moving parts. Also, the integration of task recognition and DES can be utilized for management purposes in construction sites. The chapter acknowledges limitations, such as the duration and scope of the dataset, emphasizing the need for expansion and robustness testing under various

operational conditions. Additionally, the time-consuming labeling process in supervised learning techniques is noted as a challenge. Addressing these challenges is essential for ensuring the effectiveness and applicability of the proposed method in real-world scenarios.

Chapter 5 of the dissertation introduces a method for estimating the actual cycle time and operational effectiveness of an excavator in the loading operation. It emphasizes the importance of accurate productivity estimation for project planning, cost management, resource allocation, and competitive advantage in the construction and mining industries. Existing challenges in estimating cycle time and productivity are outlined, including limitations of current methods and the lack of a theoretical value for evaluating actual cycle time. The proposed method aims to address these challenges by automatically determining the actual, theoretical, and relative cycle times of an excavator during loading operations.

The proposed approach involves utilizing supervised learning algorithms to identify excavator activities based on motion data from IMUs mounted on different machine parts, estimating actual cycle time based on the sequence of identified activities, and automatically estimating theoretical cycle time using swing angle and digging depth information. Afterward, the relative cycle time is calculated by comparing actual and theoretical cycle times to indicate the machine's operational effectiveness.

The chapter also discusses potential applications and benefits of the proposed method, including automated cycle time and productivity monitoring, performance evaluation, and optimization of machine usage. Future research directions are suggested, such as extending the method to other excavator operations and addressing limitations related to dataset size, material type identification, and material quantity estimation. Overall, the proposed method offers a promising solution for enhancing productivity estimation and operational efficiency in excavator loading operations.

Chapter 6 introduces cutting-edge methods designed to automate the estimation of excavator actual productivity in trenching and grading operations, where precision and accuracy are paramount. Traditionally, manual productivity monitoring in earth-moving operations is time-consuming, labor-intensive, and prone to errors, necessitating automated solutions to accurately estimate productivity. Also, existing methods often prioritize material quantity over operational quality. Two automated methods are proposed based on an elevation terrain mapping algorithm and BIM to compare actual maps with target models. These methods allow for the estimation of actual productivity in quality-centered tasks based on predefined target models.

By emphasizing precision and quality over material quantity, these methods address the specific requirements of quality-centered tasks. They offer valuable insights for contractors and worksite managers, enabling them to analyze operations, identify issues, and compare machine productivity to industry standards. Challenges include algorithm specificity to grading and trenching tasks and the need for high precision in elevation mapping, which requires costly sensors and calibration. Future research directions include expanding the

methods to other tasks and machinery, such as bulldozers and compactors, thereby broadening their applicability and impact in the construction domain. Also, productivity can be used as a reward function in reinforcement learning algorithms. Future improvements could also involve computing theoretical productivity benchmarks for normalization and operational effectiveness evaluation.

List of Figures

List of Tables

Bibliography

[1] S. Dixit, S. N. Mandal, J. V. Thanikal, and K. Saurabh, "Evolution of studies in construction productivity: A systematic literature review (2006–2017)", *Ain Shams Engineering Journal*, vol. 10, no. 3, pp. 555–564, 2019. DOI: 10.1016/j.asej.2018.10.010.

[2] V. K. Reja, M. S. Pradeep, and K. Varghese, "A systematic classification and evaluation of automated progress monitoring technologies in construction", in *Proceedings of the 39th International Symposium on Automation and Robotics in Construction (ISARC)*, Bogotá, Colombia: International Association for Automation and Robotics in Construction (IAARC), Jul. 2022, pp. 120–127. DOI: 10.22260/ISARC2022/0019.

[3] M. Geimer, *Mobile Working Machines*. Warrendale, Pennsylvania: SAE International, 2020. DOI: 10.4271/9780768094329.

[4] D. A. Deshmukh and P. S. Mahatme, "Factors affecting performance of excavating equipment: An overview", *International Journal of Science and Research*, pp. 1250–1253, 2016. DOI: 10.21275/v5i1.nov153044.

[5] H. Lingard, R. Wakefield, and N. Blismas, "If you cannot measure it, you cannot improve it: Measuring health and safety performance in the construction industry", in *19th Triennial CIB World Building Congress, Queensland University of Technology, Brisbane, Queensland, Australia*, 2013, pp. 1–12. [Online]. Available: https://researchrepository.rmit.edu.au/esploro/outputs/9921859226601341.

[6] Y. Nakanishi, T. Kaneta, and S. Nishino, "A review of monitoring construction equipment in support of construction project management", *Frontiers in Built Environment*, vol. 7, p. 632 593, 2022. DOI: 10.3389/fbuil.2021.632593.

[7] D. Kempecova and M. Kozlovska, "Sensing technologies for construction productivity monitoring", *MATEC Web Conf.*, vol. 385, p. 01 032, 2023. DOI: 10.1051/matecconf/202338501032.

[8] M. Helmus and M. Fecke, *Standardisierung definierter lastzyklen und messmethoden zur energieverbrauchsermittlung von baumaschinen*, Wuppertal, Germany, 2015. DOI: 10.2314/GBV:86993631X.

[9] C. Holländer, "Untersuchungen zur beurteilung und optimierung von baggerhydrauliksystemen", PhD thesis, TU Braunschweig, Braunschweig, Germany, 1998.

[10] M. Vukovic, R. Leifeld, and H. Murrenhoff, "Reducing fuel consumption in hydraulic excavators—a comprehensive analysis", *Energies*, vol. 10, no. 5, p. 687, 2017. DOI: 10.3390/en10050687.

[11] *Earth-Moving Machinery-Fuel Consumption on Hydraulic Excavator-Test Procedure*. Tokyo, Japan: JCMAS H020:2007;Japan Construction Machinery and Construction Association for Hydraulic Excavators, 2007.

[12] E. R. Azar, S. Dickinson, and B. McCabe, "Server-customer interaction tracker: Computer vision–based system to estimate dirt-loading cycles", *Journal of Construction Engineering and Management*, vol. 139, no. 7, pp. 785–794, 2013. DOI: 10.1061/(ASCE)CO.1943-7862.0000652.

[13] J. Kim and S. Chi, "Adaptive detector and tracker on construction sites using functional integration and online learning", *Journal of Computing in Civil Engineering*, vol. 31, no. 5, p. 04 017 026, 2017. DOI: 10.1061/(ASCE)CP.1943-5487.0000677.

[14] A. Montaser, I. Bakry, A. Alshibani, and O. Moselhi, "Estimating productivity of earthmoving operations using spatial technologies1this paper is one of a selection of papers in this special issue on construction engineering and management", *Canadian Journal of Civil Engineering*, vol. 39, no. 9, pp. 1072–1082, 2012. DOI: 10.1139/l2012-059.

[15] J. Louis and P. S. Dunston, "Integrating IoT into operational workflows for real-time and automated decision-making in repetitive construction operations", *Automation in Construction*, vol. 94, pp. 317–327, 2018. DOI: 10.1016/j.autcon.2018.07.005.

[16] C. Chen, Z. Zhu, and A. Hammad, "Critical review and road map of automated methods for earthmoving equipment productivity monitoring", *Journal of Computing in Civil Engineering*, vol. 36, no. 3, p. 03 122 001, 2022. DOI: 10.1061/(ASCE)CP.1943-5487.0001017.

[17] M. Golparvar-Fard, A. Heydarian, and J. C. Niebles, "Vision-based action recognition of earthmoving equipment using spatio-temporal features and support vector machine classifiers", *Advanced Engineering Informatics*, vol. 27, no. 4, pp. 652–663, 2013. DOI: 10.1016/j.aei.2013.09.001.

[18] C. R. Ahn, S. Lee, and F. Peña-Mora, "Application of low-cost accelerometers for measuring the operational efficiency of a construction equipment fleet", *Journal of Computing in Civil Engineering*, vol. 29, no. 2, p. 04 014 042, 2015. DOI: 10.1061/(ASCE)CP.1943-5487.0000337.

[19] A. Panas, J. P. Pantouvakis, and M. Kalogiannaki, "Comparative assessment of deterministic methodologies for estimating excavation productivity", *Organization, Technology and Management in Construction: an International Journal*, vol. 15, no. 1, pp. 63–78, 2023. DOI: 10.2478/otmcj-2023-0007.

[20] E. R. Azar and B. McCabe, "Automated visual recognition of dump trucks in construction videos", *Journal of Computing in Civil Engineering*, vol. 26, no. 6, pp. 769–781, 2012. DOI: 10.1061/(ASCE)CP.1943-5487.0000179.

[21] M. Memarzadeh, M. Golparvar-Fard, and J. C. Niebles, "Automated 2D detection of construction equipment and workers from site video streams using histograms of oriented gradients and colors", *Automation in Construction*, vol. 32, pp. 24–37, 2013. DOI: 10.1016/j.autcon.2012.12.002.

[22] H. Tajeen and Z. Zhu, "Image dataset development for measuring construction equipment recognition performance", *Automation in Construction*, vol. 48, pp. 1–10, 2014. DOI: 10.1016/j.autcon.2014.07.006.

[23] E. Rezazadeh Azar and B. McCabe, "Part based model and spatial–temporal reasoning to recognize hydraulic excavators in construction images and videos", *Automation in Construction*, vol. 24, pp. 194–202, 2012. DOI: 10.1016/j.autcon.2012.03.003.

[24] J. Zou and H. Kim, "Using hue, saturation, and value color space for hydraulic excavator idle time analysis", *Journal of computing in civil engineering*, vol. 21, no. 4, pp. 238–246, 2007. DOI: 10.1061/(ASCE)0887-3801(2007)21:4(238).

[25] S. Chi and C. H. Caldas, "Automated object identification using optical video cameras on construction sites", *Computer-Aided Civil and Infrastructure Engineering*, vol. 26, no. 5, pp. 368–380, 2011. DOI: 10.1111/j.1467-8667.2010.00690.x.

[26] H. Kim, K. Kim, and H. Kim, "Vision-based object-centric safety assessment using fuzzy inference: Monitoring struck-by accidents with moving objects", *Journal of Computing in Civil Engineering*, vol. 30, no. 4, p. 04 015 075, 2016. DOI: 10.1061/(ASCE)CP.1943-5487.0000562.

[27] M. Bügler, A. Borrmann, G. Ogunmakin, P. A. Vela, and J. Teizer, "Fusion of photogrammetry and video analysis for productivity assessment of earthwork processes", *Computer-Aided Civil and Infrastructure Engineering*, vol. 32, no. 2, pp. 107–123, 2017. DOI: 10.1111/mice.12235.

[28] M. Bügler, G. Ongunmakin, J. Teizer, P. A. Vela, and A. Borrmann, "A comprehensive methodology for vision-based progress and activity estimation of excavation processes for productivity assessment", in *Proceedings of the EG-ICE Workshop on Intelligent Computing in Engineering*, Cardiff, Wales, Jul. 2014, pp. 1–10. DOI: 10.13140/RG.2.1.4630.2561.

[29] E. R. Azar, "Construction equipment identification using marker-based recognition and an active zoom camera", *Journal of Computing in Civil Engineering*, vol. 30, no. 3, p. 04 015 033, 2016. DOI: 10.1061/(ASCE)CP.1943-5487.0000507.

[30] H. Kim, H. Kim, Y. W. Hong, and H. Byun, "Detecting construction equipment using a region-based fully convolutional network and transfer learning", *Journal of Computing in Civil Engineering*, vol. 32, no. 2, p. 04 017 082, 2018. DOI: 10.1061/(ASCE)CP.1943-5487.0000731.

[31] D. Roberts and M. Golparvar-Fard, "End-to-end vision-based detection, tracking and activity analysis of earthmoving equipment filmed at ground level", *Automation in Construction*, vol. 105, p. 102 811, 2019. DOI: 10.1016/j.autcon.2019.04.006.

[32] C. Chen, Z. Zhu, and A. Hammad, "Automated excavators activity recognition and productivity analysis from construction site surveillance videos", *Automation in construction*, vol. 110, p. 103 045, 2020. DOI: 10.1016/j.autcon.2019.103045.

[33] W. Fang, L. Ding, B. Zhong, P. E. Love, and H. Luo, "Automated detection of workers and heavy equipment on construction sites: A convolutional neural network approach", *Advanced Engineering Informatics*, vol. 37, pp. 139–149, 2018. DOI: 10.1016/j.aei.2018.05.003.

[34] J. Kim, J. Hwang, S. Chi, and J. Seo, "Towards database-free vision-based monitoring on construction sites: A deep active learning approach", *Automation in Construction*, vol. 120, p. 103 376, 2020. DOI: 10.1016/j.autcon.2020.103376.

[35] W. Liu, D. Anguelov, D. Erhan, *et al.*, "SSD: Single Shot MultiBox Detector", in *Computer Vision – ECCV 2016*, Cham: Springer International Publishing, 2016, pp. 21–37.

[36] J. Redmon, S. Divvala, R. Girshick, and A. Farhadi, "You Only Look Once: Unified, Real-Time Object Detection", in *Proceedings of the IEEE Conference on Computer Vision and Pattern Recognition (CVPR)*, Jun. 2016.

[37] J. Kim, S. Chi, and J. Seo, "Interaction analysis for vision-based activity identification of earthmoving excavators and dump trucks", *Automation in Construction*, vol. 87, pp. 297–308, 2018. DOI: 10.1016/j.autcon.2017.12.016.

[38] Z. Kalal, K. Mikolajczyk, and J. Matas, "Tracking-learning-detection", *IEEE Transactions on Pattern Analysis and Machine Intelligence*, vol. 34, no. 7, pp. 1409–1422, 2012. DOI: 10.1109/TPAMI.2011.239.

[39] J. Gong and C. H. Caldas, "An object recognition, tracking, and contextual reasoning-based video interpretation method for rapid productivity analysis of construction operations", *Automation in Construction*, vol. 20, no. 8, pp. 1211–1226, 2011. DOI: 10.1016/j.autcon.2011.05.005.

[40] M.-W. Park, A. Makhmalbaf, and I. Brilakis, "Comparative study of vision tracking methods for tracking of construction site resources", *Automation in Construction*, vol. 20, no. 7, pp. 905–915, 2011. DOI: 10.1016/j.autcon.2011.03.007.

[41] J. Teizer, "Status quo and open challenges in vision-based sensing and tracking of temporary resources on infrastructure construction sites", *Advanced Engineering Informatics*, vol. 29, no. 2, pp. 225–238, 2015. DOI: 10.1016/j.aei.2015.03.006.

[42] K. Kim, H. Kim, and H. Kim, "Image-based construction hazard avoidance system using augmented reality in wearable device", *Automation in Construction*, vol. 83, pp. 390–403, 2017. DOI: 10.1016/j.autcon.2017.06.014.

[43] B. Xiao and Z. Zhu, "Two-dimensional visual tracking in construction scenarios: A comparative study", *Journal of Computing in Civil Engineering*, vol. 32, no. 3, p. 04 018 006, 2018. DOI: 10.1061/(ASCE)CP.1943-5487.0000738.

[44] J. F. Henriques, R. Caseiro, P. Martins, and J. Batista, "High-speed tracking with kernelized correlation filters", *IEEE Transactions on Pattern Analysis and Machine Intelligence*, vol. 37, no. 3, pp. 583–596, 2015. DOI: 10.1109/TPAMI.2014.2345390.

[45] J. F. Henriques, R. Caseiro, P. Martins, and J. Batista, "Exploiting the circulant structure of tracking-by-detection with kernels", in *Computer Vision – ECCV 2012*, Berlin, Heidelberg: Springer, 2012, pp. 702–715. DOI: 10.1007/978-3-642-33765-9_50.

[46] Z. Zhu, X. Ren, and Z. Chen, "Visual tracking of construction jobsite workforce and equipment with particle filtering", *Journal of Computing in Civil Engineering*, vol. 30, no. 6, p. 04 016 023, 2016. DOI: 10.1061/(ASCE)CP.1943-5487.0000573.

[47] C. Yuan, S. Li, and H. Cai, "Vision-based excavator detection and tracking using hybrid kinematic shapes and key nodes", *Journal of Computing in Civil Engineering*, vol. 31, no. 1, p. 04 016 038, 2017. DOI: 10.1061/(ASCE)CP.1943-5487.0000602.

[48] B. D. Lucas and T. Kanade, "An iterative image registration technique with an application to stereo vision", in *IJCAI'81: 7th international joint conference on Artificial intelligence*, vol. 2, Vancouver, Canada, Aug. 1981, pp. 674–679. [Online]. Available: https://hal.science/hal-03697340.

[49] Z. Kalal, K. Mikolajczyk, and J. Matas, "Forward-backward error: Automatic detection of tracking failures", in *20th International Conference on Pattern Recognition*, 2010, pp. 2756–2759. DOI: 10.1109/ICPR.2010.675.

[50] J. Y. Bouguet, "Pyramidal implementation of the lucas kanade feature tracker", 1999. [Online]. Available: https://api.semanticscholar.org/CorpusID:9350588.

[51] N. Wojke, A. Bewley, and D. Paulus, "Simple online and realtime tracking with a deep association metric", in *IEEE international conference on image processing (ICIP)*, 2017, pp. 3645–3649. DOI: 10.1109/ICIP.2017.8296962.

[52] J. Gong, C. H. Caldas, and C. Gordon, "Learning and classifying actions of construction workers and equipment using bag-of-video-feature-words and bayesian network models", *Advanced Engineering Informatics*, vol. 25, no. 4, pp. 771–782, 2011. DOI: 10.1016/j.aei.2011.06.002.

[53] L. Li, W. Huang, I. Y. H. Gu, and Q. Tian, "Foreground object detection from videos containing complex background", in *Proceedings of the Eleventh ACM International Conference on Multimedia (MULTIMEDIA '03)*, New York, NY, USA: Association for Computing Machinery, 2003, pp. 2–10. DOI: 10.1145/957013.957017.

[54] R. Bao, M. A. Sadeghi, and M. Golparvar-Fard, "Characterizing construction equipment activities in long video sequences of earthmoving operations via kinematic features", in *Construction Research Congress*, 2016, pp. 849–858. DOI: 10.1061/9780784479827.086.

[55] E. R. Azar, "Semantic annotation of videos from equipment-intensive construction operations by shot recognition and probabilistic reasoning", *Journal of Computing in Civil Engineering*, vol. 31, no. 5, p. 04 017 042, 2017. DOI: 10.1061/(ASCE)CP.1943-5487.0000693.

[56] H. Kim, S. Bang, H. Jeong, Y. Ham, and H. Kim, "Analyzing context and productivity of tunnel earthmoving processes using imaging and simulation", *Automation in Construction*, vol. 92, pp. 188–198, 2018. DOI: 10.1016/j.autcon.2018.04.002.

[57] J. Kim, S. Chi, and B.-G. Hwang, "Vision-based activity analysis framework considering interactive operation of construction equipment", *Computing in Civil Engineering*, pp. 162–170, 2017. DOI: 10.1061/9780784480830.021.

[58] J. Kim and S. Chi, "Action recognition of earthmoving excavators based on sequential pattern analysis of visual features and operation cycles", *Automation in Construction*, vol. 104, pp. 255–264, 2019. DOI: 10.1016/j.autcon.2019.03.025.

[59] P. G. D. Scherer, "Methodik zur Bewertung der Energieeffizienz von mobilen Arbeitsmaschinen", German, Ph.D. dissertation, Karlsruher Institut für Technologie (KIT), 2017. DOI: 10.5445/IR/1000066047.

[60] C. Chen, Z. Zhu, A. Hammad, and W. Ahmed, "Vision-based excavator activity recognition and productivity analysis in construction", in *Computing in Civil Engineering*, American Society of Civil Engineers, 2019, pp. 241–248. DOI: 10.1061/9780784482438.031.

[61] J. Zhang, L. Zi, Y. Hou, M. Wang, W. Jiang, and D. Deng, "A deep learning-based approach to enable action recognition for construction equipment", *Advances in Civil Engineering*, vol. 2020, p. 8 812 928, 2020. DOI: 10.1155/2020/8812928.

[62] S. Zhang and L. Zhang, "Vision-based excavator activity analysis and safety monitoring system", in *Proceedings of the 38th International Symposium on Automation and Robotics in Construction (ISARC)*, Dubai, UAE: International Association for Automation and Robotics in Construction (IAARC), Nov. 2021, pp. 49–56. DOI: 10.22260/ISARC2021/0009.

[63] I.-S. Kim, K. Latif, J. Kim, A. Sharafat, D.-E. Lee, and J. Seo, "Vision-based activity classification of excavators by Bidirectional LSTM", *Applied Sciences*, vol. 13, no. 1, p. 272, 2023. DOI: 10.3390/app13010272.

[64] C. Chen, B. Xiao, Y. Zhang, and Z. Zhu, "Automatic vision-based calculation of excavator earthmoving productivity using zero-shot learning activity recognition", *Automation in Construction*, vol. 146, p. 104 702, 2023. DOI: 10.1016/j.autcon.2022.104702.

[65] H. Kim, Y. Ham, W. Kim, S. Park, and H. Kim, "Vision-based nonintrusive context documentation for earthmoving productivity simulation", *Automation in Construction*, vol. 102, pp. 135–147, 2019. DOI: 10.1016/j.autcon.2019.02.006.

[66] J. Dai, Y. Li, K. He, and J. Sun, "R-FCN: Object Detection via Region-based Fully Convolutional Networks", in *Advances in Neural Information Processing Systems*, vol. 29, Curran Associates, Inc., 2016. [Online]. Available: https://proceedings.neurips.cc/paper_files/paper/2016/file/577ef1154f3240ad5b9b413aa7346a1e-Paper.pdf.

[67] J. Kim and S. Chi, "Multi-camera vision-based productivity monitoring of earthmoving operations", *Automation in Construction*, vol. 112, p. 103 121, 2020. DOI: 10.1016/j.autcon.2020.103121.

[68] C.-F. Cheng, A. Rashidi, M. Davenport, and D. Anderson, "Audio signal processing for activity recognition of construction heavy equipment", in *Proceedings of the 33rd International Symposium on Automation and Robotics in Construction (ISARC)*, Auburn, USA: International Association for Automation and Robotics in Construction (IAARC), Jul. 2016, pp. 642–650. DOI: 10.22260/ISARC2016/0078.

[69] E. Mahamedi, K. Rogage, O. Doukari, and M. Kassem, "Automating excavator productivity measurement using deep learning", *Proceedings of the Institution of Civil Engineers - Smart Infrastructure and Construction*, vol. 40, no. 14, pp. 121–133, 2021. DOI: 10.1680/jsmic.21.00031.

[70] A. S. Hanna, *Quantifying the Cumulative Impact of Change Orders for Electrical and Mechanical Contractors*, Austin, Texas, USA, 2001. [Online]. Available: https://search.worldcat.org/title/50690019.

[71] R. Akhavian and A. H. Behzadan, "Simulation-based evaluation of fuel consumption in heavy construction projects by monitoring equipment idle times", in *Winter Simulations Conference (WSC)*, Washington, DC, USA, 2013, pp. 3098–3108. DOI: 10.1109/WSC.2013.6721677.

[72] C.-F. Cheng, A. Rashidi, M. A. Davenport, and D. V. Anderson, "Activity analysis of construction equipment using audio signals and support vector machines", *Automation in Construction*, vol. 81, pp. 240–253, 2017. DOI: 10.1016/j.autcon.2017.06.005.

[73] R. Akhavian and A. H. Behzadan, "Knowledge-based simulation modeling of construction fleet operations using multimodal-process data mining", *Journal of Construction Engineering and Management*, vol. 139, no. 11, p. 04 013 021, 2013. DOI: 10.1061/(ASCE)CO.1943-7862.0000775.

[74] B. Sherafat, C. R. Ahn, R. Akhavian, *et al.*, "Automated methods for activity recognition of construction workers and equipment: State-of-the-Art Review", *Journal of Construction Engineering and Management*, vol. 146, no. 6, p. 03 120 002, 2020. DOI: 10.1061/(ASCE)CO.1943-7862.0001843.

[75] I. Magdy and M. Osama, "Automated productivity assessment of earthmoving operations", *Journal of Information Technology in Construction (ITcon)*, vol. 19, pp. 169–184, 2014. [Online]. Available: https://www.itcon.org/2014/9.

[76] S. Song, E. Marks, and N. Pradhananga, "Impact variables of dump truck cycle time for heavy excavation construction projects", *Journal of Construction Engineering and Project Management*, vol. 7, no. 2, pp. 11–18, 2017. DOI: 10.6106/JCEPM.2017.7.2.011.

[77] S. Ashraf, S. Ahmad, and M. Osama, "Fuzzy-based configuration of automated data acquisition systems for earthmoving operations", *Journal of Information Technology in Construction (ITcon)*, vol. 23, pp. 122–137, 2018. [Online]. Available: http://www.itcon.org/2018/6.

[78] M. Ali and M. Osama, "Truck+ for earthmoving operations", *Journal of Information Technology in Construction (ITcon)*, vol. 19, pp. 412–433, 2014. [Online]. Available: http://www.itcon.org/2014/25.

[79] A. Adel and M. Osama, "Productivity based method for forecasting cost & time of earthmoving operations using sampling GPS data", *Journal of Information Technology in Construction (ITcon)*, vol. 21, pp. 39–56, 2016. [Online]. Available: http://www.itcon.org/2016/3.

[80] S. Ahn, S. Han, and M. Al-Hussein, "Improvement of transportation cost estimation for prefabricated construction using geo-fence-based large-scale GPS data feature extraction and support vector regression", *Advanced Engineering Informatics*, vol. 43, p. 101 012, 2020. DOI: 10.1016/j.aei.2019.101012.

[81] S. Han, T. Hong, and S. Lee, "Production prediction of conventional and global positioning system–based earthmoving systems using simulation and multiple regression analysis", *Canadian Journal of Civil Engineering*, vol. 35, no. 6, pp. 574–587, 2008. DOI: 10.1139/L08-005.

[82] L. Song and N. N. Eldin, "Adaptive real-time tracking and simulation of heavy construction operations for look-ahead scheduling", *Automation in Construction*, vol. 27, pp. 32–39, 2012. DOI: 10.1016/j.autcon.2012.05.007.

[83] N. Pradhananga and J. Teizer, "Automatic spatio-temporal analysis of construction site equipment operations using GPS data", *Automation in Construction*, vol. 29, pp. 107–122, 2013. DOI: 10.1016/j.autcon.2012.09.004.

[84] X. Li, W. Yi, H.-L. Chi, X. Wang, and A. P. Chan, "A critical review of virtual and augmented reality (VR/AR) applications in construction safety", *Automation in Construction*, vol. 86, pp. 150–162, 2018. DOI: 10.1016/j.autcon.2017.11.003.

[85] T. Cheng, M. Venugopal, J. Teizer, and P. Vela, "Performance evaluation of ultra wideband technology for construction resource location tracking in harsh environments", *Automation in Construction*, vol. 20, no. 8, pp. 1173–1184, 2011. DOI: 10.1016/j.autcon.2011.05.001.

[86] F. Vahdatikhaki and A. Hammad, "Framework for near real-time simulation of earthmoving projects using location tracking technologies", *Automation in Construction*, vol. 42, pp. 50–67, 2014. DOI: 10.1016/j.autcon.2014.02.018.

[87] A. Montaser and O. Moselhi, "RFID+ for tracking earthmoving operations", in *Construction Research Congress 2012: Construction Challenges in a Flat World*, ASCE, 2012, pp. 1011–1020. DOI: 10.1061/9780784412329.102.

[88] C. R. Ahn, S. Lee, and F. Peña-Mora, "Monitoring system for operational efficiency and environmental performance of construction operations using vibration signal analysis", in *Construction Research Congress*, 2012, pp. 1879–1888. DOI: 10.1061/9780784412329.189.

[89] R. Akhavian and A. H. Behzadan, "An integrated data collection and analysis framework for remote monitoring and planning of construction operations", *Advanced Engineering Informatics*, vol. 26, no. 4, pp. 749–761, 2012. DOI: 10.1016/j.aei.2012.04.004.

[90] R. Akhavian and A. H. Behzadan, "Construction equipment activity recognition for simulation input modeling using mobile sensors and machine learning classifiers", *Advanced Engineering Informatics*, vol. 29, no. 4, pp. 867–877, 2015. DOI: h10.1016/j.aei.2015.03.001.

[91] N. Mathur, S. Aria, T. Adams, C. Ahn, and S. Lee, "Automated cycle time measurement and analysis of excavator's loading operation using smart phone-embedded IMU sensors", *Computing in Civil Engineering*, pp. 215–222, 2015. DOI: 10.1061/9780784479247.027.

[92] H. Kim, C. R. Ahn, D. Engelhaupt, and S. Lee, "Application of dynamic time warping to the recognition of mixed equipment activities in cycle time measurement", *Automation in Construction*, vol. 87, pp. 225–234, 2018. DOI: 10.1016/j.autcon.2017.12.014.

[93] J. Bae, K. Kim, and D. Hong, "Automatic identification of excavator activities using joystick signals", *International Journal of Precision Engineering and Manufacturing*, vol. 20, no. 12, pp. 2101–2107, 2019. DOI: 10.1007/s12541-019-00219-5.

[94] C. Hernandez, T. Slaton, V. Balali, and R. Akhavian, "A deep learning framework for construction equipment activity analysis", in *Computing in Civil Engineering 2019: Data, Sensing, and Analytics*, ASCE, 2019, pp. 479–486. DOI: 10.1061/9780784482438.061.

[95] K. M. Rashid and J. Louis, "Times-series data augmentation and deep learning for construction equipment activity recognition", *Advanced Engineering Informatics*, vol. 42, p. 100 944, 2019. DOI: 10.1016/j.aei.2019.100944.

[96] K. M. Rashid and J. Louis, "Automated activity identification for construction equipment using motion data from articulated members", *Frontiers in Built Environment*, vol. 5, 2020. DOI: 10.3389/fbuil.2019.00144.

[97] T. Slaton, C. Hernandez, and R. Akhavian, "Construction activity recognition with convolutional recurrent networks", *Automation in Construction*, vol. 113, p. 103 138, 2020. DOI: 10.1016/j.autcon.2020.103138.

[98] A. K. Langroodi, F. Vahdatikhaki, and A. Doree, "Activity recognition of construction equipment using fractional random forest", *Automation in construction*, vol. 122, p. 103 465, 2021. DOI: 10.1016/j.autcon.2020.103465.

[99] L. Joshua and K. Varghese, "Accelerometer-based activity recognition in construction", *Journal of Computing in Civil Engineering*, vol. 25, no. 5, pp. 370–379, 2011. DOI: 10.1061/(ASCE)CP.1943-5487.0000097.

[100] S. K.Gaikwad, B. W.Gawali, and P. Yannawar, "A review on speech recognition technique", *International Journal of Computer Applications*, vol. 10, no. 3, pp. 16–24, Nov. 2010. DOI: 10.5120/1462-1976.

[101] C.-F. Cheng, A. Rashidi, M. A. Davenport, and D. V. Anderson, "Evaluation of software and hardware settings for audio-based analysis of construction operation", *International Journal of Civil Engineering*, vol. 17, no. 9, pp. 1469–1480, 2019. DOI: 10.1007/s40999-019-00409-2.

[102] C. Sabillon, A. Rashidi, B. Samanta, M. A. Davenport, and D. V. Anderson, "Audio-based bayesian model for productivity estimation of cyclic construction activities", *Journal of Computing in Civil Engineering*, vol. 34, no. 1, p. 04 019 048, 2020. DOI: 10.1061/(ASCE)CP.1943-5487.0000863.

[103] Y. B. Kim, J. Ha, H. Kang, P. Y. Kim, J. Park, and F. Park, "Dynamically optimal trajectories for earthmoving excavators", *Automation in Construction*, vol. 35, pp. 568–578, 2013. DOI: 10.1016/j.autcon.2013.01.007.

[104] B. Sherafat, A. Rashidi, Y.-C. Lee, and C. R. Ahn, "A hybrid kinematic-acoustic system for automated activity detection of construction equipment", *Sensors*, vol. 19, no. 19, p. 4286, 2019. DOI: 10.3390/s19194286.

[105] Y. Shi, Y. Xia, Y. Zhang, and Z. Yao, "Intelligent identification for working-cycle stages of excavator based on main pump pressure", *Automation in Construction*, vol. 109, p. 102 991, 2020. DOI: 10.1016/j.autcon.2019.102991.

[106] Y. Shi, Y. Xia, L. Luo, Z. Xiong, C. Wang, and L. Lin, "Working stage identification of excavators based on control signals of operating handles", *Automation in Construction*, vol. 130, p. 103 873, 2021. DOI: 10.1016/j.autcon.2021.103873.

[107] J. Kim, S. Chi, and C. R. Ahn, "Hybrid kinematic–visual sensing approach for activity recognition of construction equipment", *Journal of Building Engineering*, vol. 44, p. 102 709, 2021. DOI: 10.1016/j.jobe.2021.102709.

[108] M. Kassem, E. Mahamedi, K. Rogage, K. Duffy, and J. Huntingdon, "Measuring and benchmarking the productivity of excavators in infrastructure projects: A deep neural network approach", *Automation in Construction*, vol. 124, p. 103 532, 2021. DOI: 10.1016/j.autcon.2020.103532.

[109] J.-Y. Kim and S.-B. Cho, "Classifying excavator operations with fusion network of multi-modal deep learning models", in *14th International Conference on Soft Computing Models in Industrial and Environmental Applications (SOCO)*, Seville, Spain: Springer International Publishing, 2020, pp. 25–34. DOI: 10.1007/978-3-030-20055-8_3.

[110] J.-Y. Kim and S.-B. Cho, "A deep neural network ensemble of multimodal signals for classifying excavator operations", *Neurocomputing*, vol. 470, pp. 290–299, 2022. DOI: 10.1016/j.neucom.2020.01.127.

[111] O. Moselhi, D. Gong, and K. El-Rayes, "Estimating weather impact on the duration of construction activities", *Canadian Journal of Civil Engineering*, vol. 24, no. 3, pp. 359–366, 1997. DOI: 10.1139/l96-122.

[112] A. Vasenev, T. Hartmann, and A. Dorée, "A distributed data collection and management framework for tracking construction operations", *Advanced Engineering Informatics*, vol. 28, no. 2, pp. 127–137, 2014. DOI: 10.1016/j.aei.2014.01.003.

[113] S. Ashraf, S. Ahmad, and M. Osama, "Fuzzy-based configuration of automated data acquisition systems for earthmoving operations.", *Journal of Information Technology in Construction (ITcon)*, vol. 23, pp. 122–137, 2018. [Online]. Available: http://www.itcon.org/2018/6.

[114] *Technical Handbook – Earthmoving*, Liebherr, Germany, 2003.

[115] *Specification and Application Handbook*, 31st ed., Komatsu Ltd., 2013. [Online]. Available: https://www.directminingservices.com/wp-content/uploads/2011/05/Edition31.pdf.

[116] *Volvo Performance Manual*, Volvo Construction Equipment (Volvo CE), 2015.

[117] *Caterpillar Performance Handbook*, 48th ed., Caterpillar Inc., Peoria, Illinois, USA, 2018.

[118] G. Garbotz, "Die Leistungen von Baumaschinen", *Koln-Braunsfeld Muller*, 1966.

[119] G. Girmscheid, *Leistungsermittlungshandbuch für Baumaschinen und Bauprozesse*, 4th ed. Germany: Springer, 2010.

[120] M. Hoffmann, *Zahlentafeln fur den Baubetrieb*, 7th ed. Germany: Teubner, 2006.

[121] Fachgruppe Erdbau Bundesausschuss Leistungslohn Bau, *Handbuch BML: Daten für die Berechnung von Baumaschinen-Leistunge*, 3rd ed., Zeittechnik, Neu-Isenburg, 1983.

[122] F. Hüster, *Leistungsberechnung der Baumaschinen*. Germany: Shaker Verlag, 2005.

[123] G. Kotte, "Ermittlung der Nutzförderleistung von Hydraulikbaggern", *TIS Tiefbau Ingenieurbau Strassenbau*, vol. 39, no. 9, 1997.

[124] G. Kühn, *Der maschinelle Erdbau*. Germany: Teubner Verlag, 1984.

[125] S. Nunnally, *Construction Methods and Management*, 7th ed. USA: Prentice Hall, 2007.

[126] R. L. Peurifoy, C. J. Schexnayder, R. L. Schmitt, and A. Shapira, *Construction planning, equipment, and methods*, 9th ed. New York: McGraw-Hill Education, 2018.

[127] S. D. Smith, "Earthmoving productivity estimation using linear regression techniques", *Journal of Construction Engineering and Management*, vol. 125, no. 3, pp. 133–141, 1999. DOI: 10.1061/(ASCE)0733-9364(1999)125:3(133).

[128] D. J. Edwards and I. J. Griffiths, "Artificial intelligence approach to calculation of hydraulic excavator cycle time and output", *Mining Technology*, vol. 109, no. 1, pp. 23–29, 2000. DOI: 10.1179/mnt.2000.109.1.23.

[129] D. J. Edwards and G. D. HOLT, "Estivate: A model for calculating excavator productivity and output costs", *Engineering, Construction and Architectural Management*, vol. 7, no. 1, pp. 52–62, 2000. DOI: 10.1108/eb021132.

[130] J. Yang, D. J. Edwards, and P. E. Love, "A computational intelligent fuzzy model approach for excavator cycle time simulation", *Automation in Construction*, vol. 12, no. 6, pp. 725–735, 2003. DOI: 10.1016/S0926-5805(03)00056-6.

[131] C. TAM, T. K. TONG, and S. L. TSE, "Artificial neural networks model for predicting excavator productivity", *Engineering, Construction and Architectural Management*, vol. 9, no. 5/6, pp. 446–452, 2002. DOI: 10.1108/eb021238.

[132] B. Hola and K. Schabowicz, "Estimation of earthworks execution time cost by means of artificial neural networks", *Automation in Construction*, vol. 19, no. 5, pp. 570–579, 2010. DOI: 10.1016/j.autcon.2010.02.004.

[133] J. Yoon, J. Kim, J. Seo, and S. Suh, "Spatial factors affecting the loading efficiency of excavators", *Automation in Construction*, vol. 48, pp. 97–106, 2014. DOI: 10.1016/j.autcon.2014.08.002.

[134] G. D. Holt and D. Edwards, "Analysis of interrelationships among excavator productivity modifying factors", *International Journal of Productivity and Performance Management*, vol. 64, no. 6, pp. 853–869, 2015. DOI: 10.1108/IJPPM-02-2014-0026.

[135] S. V. Manyele, "Investigation of excavator performance factors in an open-pit mine using loading cycle time", *Engineering*, vol. 9, no. 7, pp. 599–624, 2017. DOI: 10.4236/eng.2017.97038.

[136] A. R. ElQasaby, F. K. Alqahtani, and M. Alheyf, "State of the Art of BIM Integration with Sensing Technologies in Construction Progress Monitoring", *Sensors*, vol. 22, no. 9, p. 3497, 2022. DOI: 10.3390/s22093497.

[137] Y. Turkan, F. Bosche, C. T. Haas, and R. Haas, "Automated progress tracking using 4D schedule and 3D sensing technologies", *Automation in Construction*, vol. 22, pp. 414–421, 2012. DOI: 10.1016/j.autcon.2011.10.003.

[138] Y. Wu, H. Kim, C. Kim, and S. H. Han, "Object Recognition in Construction-Site Images Using 3D CAD-Based Filtering", *Journal of Computing in Civil Engineering*, vol. 24, no. 1, pp. 56–64, 2010. DOI: 10.1061/(ASCE)0887-3801(2010)24:1(56).

[139] B. Gledson and D. Greenwood, "Surveying the extent and use of 4D BIM in the UK", *Journal of Information Technology in Construction (ITcon)*, vol. 21, pp. 57–71, 2016. [Online]. Available: http://www.itcon.org/2016/4.

[140] M. Hakkarainen, C. Woodward, and K. Rainio, "Software architecture for mobile mixed reality and 4D BIM interaction", in *Proceedings of 26th International Conference on IT in Construction/Managing Construction for Tomorrow, CIB W78*, Istanbul, Turkey, 2009, pp. 517–524.

[141] K. Mirzaei, M. Arashpour, E. Asadi, H. Masoumi, Y. Bai, and A. Behnood, "3D point cloud data processing with machine learning for construction and infrastructure applications: A comprehensive review", *Advanced Engineering Informatics*, vol. 51, p. 101 501, 2022. DOI: 10.1016/j.aei.2021.101501.

[142] G. S. Cheok, R. R. Lipman, C. Witzgall, J. Bernal, and W. C. Stone, "Field demonstration of laser scanning for excavation measurement", in *Proceedings of the 17th International Symposium on Automation and Robotics in Construction (ISARC)*, Taipei, Taiwan: International Association for Automation and Robotics in Construction (IAARC), Sep. 2000, pp. 1–6. DOI: 10.22260/ISARC2000/0077.

[143] H. Yamamoto, M. Moteki, T. Ootuki, Y. Yanagisawa, A. Nozue, T. Yamaguchi, *et al.*, "Development of the autonomous hydraulic excavator prototype using 3D information for motion planning and control", *Transactions of the Society of Instrument and Control Engineers*, vol. 48, no. 8, pp. 488–497, 2012. DOI: 10.9746/sicetr.48.488.

[144] J. Wang, H. González-Jorge, R. Lindenbergh, P. Arias-Sánchez, and M. Menenti, "Automatic estimation of excavation volume from laser mobile mapping data for mountain road widening", *Remote Sensing*, vol. 5, no. 9, pp. 4629–4651, 2013. DOI: 10.3390/rs5094629.

[145] H. Honda, A. Minami, Y. Takahashi, S. Tajima, T. Ohtsuki, and Y. Shiiba, "Visualization of the progress management of earthwork volume at construction jobsite", in *Proceedings of the 37th International Symposium on Automation and Robotics in Construction (ISARC)*, Kitakyushu, Japan: International Association for Automation and Robotics in Construction (IAARC), Oct. 2020, pp. 1286–1290. DOI: 10.22260/ISARC2020/0176.

[146] W. Y. Amaglo, "Volume Calculation Based on LiDAR Data", M.S. thesis, KTH, Real Estate and Construction Management, 2021.

[147] A. Rasul, J. Seo, and A. Khajepour, "Development of integrative methodologies for effective excavation progress monitoring", *Sensors*, vol. 21, no. 2, p. 364, 2021. DOI: 10.3390/s21020364.

[148] T. Kujundžić, M. Klanfar, T. Korman, and Z. Briševac, "Influence of crushed rock properties on the productivity of a hydraulic excavator", *Applied Sciences*, vol. 11, no. 5, p. 2345, 2021. DOI: 10.3390/app11052345.

[149] E. Bernardes and S. Viollet, "Quaternion to euler angles conversion: A direct, general and computationally efficient method", *PLOS ONE*, vol. 17, no. 11, pp. 1–13, 2022. DOI: 10.1371/journal.pone.0276302.

[150] C. M. Bishop, *Pattern Recognition and Machine Learning*. Singapore: Springer Science+ Business Media, LLC, 2006. [Online]. Available: https://www.microsoft.com/en-us/research/uploads/prod/2006/01/Bishop-Pattern-Recognition-and-Machine-Learning-2006.pdf.

[151] M. Zauner, F. Altenberger, H. Knapp, and M. Kozek, "Phase independent finding and classification of wheel-loader work-cycles", *Automation in Construction*, vol. 109, p. 102 962, 2020. DOI: 10.1016/j.autcon.2019.102962.

[152] A. Panas and J. P. Pantouvakis, "Comparative analysis of operational coefficients' impact on excavation operations", *Engineering, Construction and Architectural Management*, vol. 17, no. 5, pp. 461–475, 2010. DOI: 10.1108/09699981011074565.

[153] J. Xu and H.-S. Yoon, "A review on mechanical and hydraulic system modeling of excavator manipulator system", *Journal of Construction Engineering*, vol. 2016, p. 9 409 370, 2016. DOI: 10.1155/2016/9409370.

[154] N. Tam Lam, I. Howard, and L. Cui, "A review of trajectory planning for autonomous excavator in construction and mining sites", in *ACAM10: the 10th Australasian Congress on Applied Mechanics*, Barton, Australia: Engineers Australia, 2021, pp. 368–382. [Online]. Available: https://search.informit.org/doi/10.3316/informit.323406814564895.

[155] J. E. Schaufelberger and G. C. Migliaccio, *Construction equipment management*, 2nd ed. Routledge, 2019. DOI: 10.1201/9781351117463.

[156] Y. Du, M. C. Dorneich, and B. Steward, "Virtual operator modeling method for excavator trenching", *Automation in construction*, vol. 70, pp. 14–25, 2016. DOI: 10.1016/j.autcon.2016.06.013.

[157] A. Kleiner and C. Dornhege, "Real-time localization and elevation mapping within urban search and rescue scenarios", *Journal of Field Robotics*, vol. 24, no. 8-9, pp. 723–745, 2007. DOI: 10.1002/rob.20208.

[158] J. Z. Kolter, Y. Kim, and A. Y. Ng, "Stereo vision and terrain modeling for quadruped robots", in *2009 IEEE International Conference on Robotics and Automation (ICRA)*, IEEE, 2009, pp. 1557–1564. DOI: 10.1109/ROBOT.2009.5152795.

[159] A. Kolu, M. Lauri, M. Hyvönen, R. Ghabcheloo, and K. Huhtala, "A mapping method tolerant to calibration and localization errors based on tilting 2D laser scanner", in *2015 European Control Conference (ECC)*, IEEE, Linz, Austria, 2015, pp. 2348–2353. DOI: 10.1109/ECC.2015.7330889.

[160] J. Kümmerle, T. Kühner, and M. Lauer, "Automatic calibration of multiple cameras and depth sensors with a spherical target", in *2018 IEEE/RSJ International Conference on Intelligent Robots and Systems (IROS)*, IEEE, 2018, pp. 1–8. DOI: 10.1109/IROS.2018.8593955.

[161] A. Kaczmarek, W. Rohm, L. Klingbeil, and J. Tchórzewski, "Experimental 2D extended Kalman filter sensor fusion for low-cost GNSS/IMU/Odometers precise positioning system", *Measurement*, vol. 193, p. 110 963, 2022. DOI: 10.1016/j.measurement.2022.110963.

[162] R. Heikkiläa, T. Kolli, and T. Rauhala, "Benefits of Open Infra BIM - Finland Experience", in *39th International Symposium on Automation and Robotics in Construction (ISARC)*, Bogota, Columbia: International Association for Automation and Robotics in Construction (IAARC), Jul. 2022, pp. 253–260. DOI: 10.22260/ISARC2022/0036.

[163] M. Quigley, K. Conley, B. Gerkey, *et al.*, "ROS: an open-source Robot Operating System", in *ICRA workshop on open source software*, vol. 3, Kobe, Japan, 2009, p. 5. [Online]. Available: http://lars.mec.ua.pt/public/LAR%20Projects/BinPicking/2016_RodrigoSalgueiro/LIB/ROS/icraoss09-ROS.pdf.

Internet Sources

[164] L. Bryer. "Construction Industry Training Board (CITB), UK Industry Performance Report". (2018), [Online]. Available: https://constructingexcellence.org.uk/wp-content/uploads/2018/11/UK-Industry-Performance-Report-2017.pdf (visited on 01/08/2022).

[165] Building SMART Finland (Infra-toimialaryhmä). "Yleiset inframallivaatimukset yiv". (2021), [Online]. Available: https://drive.buildingsmart.fi/s/AAELrj83NbrHae2 (visited on 01/08/2023).

[166] K. Ltd. "Komatsu's proprietary intelligent machine control 2.0 promotes significant productivity gains for excavators". (2022), [Online]. Available: https://www.komatsu.com/en/newsroom/2022/komatsu-intelligent-machine-control/ (visited on 01/03/2024).

[167] Novatron Ltd. "G2 inclination sensor". (2018), [Online]. Available: https://novatron.fi/en/components/ (visited on 01/03/2024).

[168] Leica Geosystems Ltd. "Leica iCON iXE3 - 3D System: Advanced 3D excavator machine control solution". (2023), [Online]. Available: https://leica-geosystems.com/products/machine-control-systems/excavator/leica-icon-ixe3---3d-system (visited on 01/03/2024).

[169] Caterpillar Inc. “Cat grade assist for excavators”. (2022), [Online]. Available: https://www.cat.com/en_US/products/new/technology/assist/assist/153921756853575 (visited on 01/08/2022).

[170] M. Marandola. “How much does it cost to dig a trench?” (2022), [Online]. Available: https://www.angi.com/articles/trenching-cost.htm (visited on 01/12/2022).

[171] “Spherical coordinates system (Spherical polar coordinates)”. (2018), [Online]. Available: https://physicscatalyst.com/graduation/spherical-coordinates-system/ (visited on 01/10/2022).

[172] Rakennustieto. “InfraRYL (General quality requirements for infrastructure construction)”. (2024), [Online]. Available: https://www.rakennustieto.fi/palvelut/tietoa-rakentamiseen/ryl/infraryl (visited on 01/04/2024).

[173] Novatron Ltd. “Novatron (Earthmoving Automation)”. (2018), [Online]. Available: https://novatron.fi/en/ (visited on 01/02/2022).

Own Publications

[174] A. Molaei, A. Kolu, K. Lahtinen, and M. Geimer, “Automatic estimation of excavator actual and relative cycle times in loading operations”, *Automation in Construction*, vol. 156, p. 105 080, 2023. DOI: 10.1016/j.autcon.2023.105080.

[175] A. Molaei, A. Kolu, N. Haaraniemi, and M. Geimer, “Automatic estimation of excavator’s actual productivity in trenching and grading operations using Building Information Modeling (BIM)”, *Actuators*, vol. 12, no. 11, p. 423, 2023. DOI: 10.3390/act12110423.

[176] A. Molaei, M. Geimer, and A. Kolu, “An approach for estimation of swing angle and digging depth during excavation operation”, in *Proceedings of the 39th International Symposium on Automation and Robotics in Construction (ISARC)*, Bogotá, Colombia: International Association for Automation and Robotics in Construction (IAARC), Jul. 2022, pp. 622–629. DOI: 10.22260/ISARC2022/0087.

[177] A. Molaei, A. Kolu, K. Lahtinen, and M. Geimer, “Automatic recognition of excavator working cycles using supervised learning and motion data obtained from inertial measurement units (IMUs)”, *Construction Robotics*, vol. 8, no. 14, 2024. DOI: 10.1007/s41693-024-00130-0.

[178] A. Molaei, M. Geimer, and A. Kolu, “Evaluation of deterministic models for the excavator’s theoretical productivity estimation in the digging and trenching operations”, in *Proceedings of the 2023 European Conference on Computing in Construction*, vol. 4, Heraklion, Greece: European Council on Computing in Construction, Jul. 2023. DOI: 10.35490/EC3.2023.191.

[179] A. Molaei, M. Geimer, and A. Kolu, "A novel framework for the estimation of excavator's actual productivity in the grading operation using Building Information Modeling (BIM)", in *Proceedings of the 18th Scandinavian International Conference on Fluid Power (SICFP'23)*, Tampere, Finland: Tampere University, Jun. 2023, pp. 251–263.

[180] T. Machado, D. Fassbender, A. Taheri, *et al.*, "Autonomous heavy-duty mobile machinery: A multidisciplinary collaborative challenge", in *2021 IEEE International Conference on Technology and Entrepreneurship (ICTE)*, 2021, pp. 1–8. DOI: 10.1109/ICTE51655.2021.9584498.